The Influence of Topography and Vegetation Canopy on the Deposition of Atmospheric Particulates Studied with ^{210}Pb and ^{137}Cs Soil Inventory Measurements

This Thesis is Submitted by

Alfred Sello Likuku

for the degree of

Doctor of Philosophy

School of Physics

University of Edinburgh

2003

Abstract

Naturally occurring radioactive isotopes of ^{210}Pb and ^{7}Be in the atmosphere, plant material and soil have been used to investigate the transport and removal of atmospheric aerosols from the atmosphere by precipitation and turbulent deposition to natural surfaces.

Concentrations of ^{210}Pb and ^{7}Be contained in aerosols in surface air were measured using a high volume sampler at the King's Buildings site of the University of Edinburgh (55.9°N, 03.2°W) over a 12 month period (July 2002-June 2003). The log-normally distributed concentrations of ^{210}Pb, with a median of 0.141 mBq m^{-3} over the monitoring period, indicated a surface source and dispersion by wind. The concentrations were largest in air with trajectories over terrestrial surfaces, consistent with soil as the source, and smallest in air with marine trajectories and also air masses subject to precipitation, the main removal process for aerosol bound ^{210}Pb. Concentrations of ^{7}Be were largest during spring which is consistent with a stratospheric origin and, like ^{210}Pb, concentrations were smaller in air masses subject to precipitation.

Measurements of ^{210}Pb and ^{7}Be in tree foliage, precipitation and throughfall water beneath tree canopies were used to investigate the transport pathway of these isotopes from the atmosphere to soil. The measurements showed that the ^{210}Pb aerosols attach and bind effectively to foliar surfaces, so that deposition to soil relies mainly on leaf fall. In open parkland trees, the distribution of the falling leaves determines the deposition of the ^{210}Pb. Foliar surfaces effectively filter ^{7}Be from precipitation as it passes through the woodland canopy.

Studies of soil inventories of ^{210}Pb beneath woodland and grassland, undisturbed for several half-lives of the isotope, were used to deduce annual average fluxes, wet deposition, cloud droplet deposition and dry deposition of aerosols onto these surfaces. The measurements showed dry deposition velocities of ^{210}Pb containing aerosols of 7.4 $\pm$ 1.8 mm s^{-1} on mature mixed deciduous woodland, and 2.6 $\pm$ 1.3 mm s^{-1} on grassland, substantially larger than current theoretical values but consistent with much recent work by a range of methods.

A transect of ^{210}Pb and ^{137}Cs inventories was measured in soil beneath woodland and moorland between the coast of Wales and the summit of Plynlimon (∼700 m asl). Along the transect, precipitation increased by a factor of ∼1.8, whereas ^{210}Pb inventories in moorland soils increased by a factor of 2.4 ± 0.4, consistent with the seeder-feeder scavenging of orographic cloud containing ^{210}Pb concentrations larger than those in seeder precipitation by a factor of 1.3 ± 0.4.

Declaration

No part of this thesis has been submitted for any other degree or professional qualification. In accordance with the University of Edinburgh regulation 3.8.7, I here state that:

- This thesis has been composed by myself.
- For the purpose of this study, the soil, vegetation, air and precipitation samples were collected from Edinburgh and Wales, UK. I played a major role in all the sampling expeditions. The work involved in the data analysis and interpretation reported here is my own.

.....

A. S. Likuku

Acknowledgements

The author would like to acknowledge the Botswana College of Agriculture for funding this PhD research.

I will always be gratefull to my supervisors: Prof. Derek Branford, Prof. David Fowler and Dr. Keith Weston for their assistance and guidance during the course of this study.

I would like to thank the British Atmospheric Data Center for the letting me use their ECMWF Trajectory Models for part of my data analysis.

Thanks are also due to the various people at Edinburgh who assisted with experimental, technical and computing, in particular: Dr. Ute Skiba, Dr. Tom Davinson and Dr. Klaus Föhl.

This work is dedicated to Tumi and Laone for their moral support and patience.

Contents

List of Figures

List of Tables

Chapter 1

Introduction

1.1 Overview

With increased concern over air pollution problems, research has been in progress for the last six decades to quantify the input of airborne substances to aquatic and terrestrial ecosystems. In the past, smoke from domestic fires and sulphur dioxide (SO_2) emissions from industries were considered to be the main damaging agents of the ecosystem but gradually, it became apparent that the polluted atmosphere contains mixtures of pollutants.

Research on the chemical composition of rain on the regional scale began with the Scandinavian studies in the 1950s and 1960s. Understanding of the processes involved in environmental acidification expanded dramatically with the years since Swedish scientists first demonstrated the relationship of SO_2 emissions outside Sweden and the acidification of Swedish lakes [1]. Although this research and development has been going on for several decades, there are still major difficulties estimating the deposition of air pollutants. With the development of techniques for measuring different types of deposition, wet deposition has been successfully measured with a reasonable degree of accuracy in simple terrain, whereas, dry, cloud and fog deposition are still measured with great difficulty. Particles responsible for the bulk of long range transport of sulphur and nitrogen consist of: sulphates (SO_4^{2-}), nitrates (NO_3^-), chlorides (Cl^-) and ammonium (NH_4^+); base cations such as calcium (Ca^{2+}), magnesium (Mg^{2+}), sodium (Na^+) and potassium (K^+). The deposition of particles containing SO_4^{2-},

NO_3^-, Cl^- and NH_4^+ contribute to the acidification and eutrophication of ecosystems and those of base cations are important sources of the nutrients cycle in soil and ecosystems and also in neutralisation of acid input. The deposition of heavy metals such as lead (Pb), cadmium (Cd), and zinc (Zn). may lead to possible toxic effects in a range of species [2] [3].

Emission of pollutant gases such as NO_x[1] from a variety of biogenic and anthropogenic sources and the volatile organic compounds (VOCs) into the atmosphere may present a health risk directly, or as a result of their oxidation [4]. The secondary oxidised products include photochemical oxidants such as ozone (O_3), the chemistry of which is considered in detail elsewhere [5]. Since the late 1800s, surface ozone measurements in Europe have doubled over the period, from the annual mean of 10-15 ppb to 20-30 ppb [6], reaching levels that are potentially harmful to human health, vegetation and materials. In the UK, ground level ozone concentrations defining areas most at risk are given in the Third Report of the UK Photochemical Oxidants Review Group [7].

Tropospheric aerosols derived from oxidation of the primary pollutants (SO_2, NO_2 and NH_3) increase the albedo directly by scattering and indirectly by modifying the cloud microstructure. Studies by numerous workers, for example: Poet *et al.* [8], Moore *et al.*[9], Moore *et al.* [10], Lambert *et al.* [11], Wieland *et al.* [12] and Tokieda [13], have shown that the residence times of tropospheric aerosols range from about 4 to 60 days. The lower range of the scale reflect aerosols confined to regions of their origin while the upper end indicates that these aerosols may be transported on a hemispheric scale.

In this chapter, a general outline of the emission, chemical composition and deposition of the acid precursors is presented. Also discussed are sources of radioactivity to the environment, with particular attention given to radionuclides of concern to this study, including their origin and geographical distributions, based on figures obtained from previous studies. Chapter 2 describes the equipment used together with the γ-ray analysis procedures employed in this work. Surface air concentration mea-

[1] NO_x = NO and NO_2.

surement techniques, results, discussion and conclusions are given in chapter 3, while investigations on the effect of vegetation and topography on the aerosol depositional fluxes are reported in chapters 4 and 5, respectively. A summary of the main results obtained in this study and suggestions for further work are given in chapter 6.

1.2 Atmospheric Aerosols

An aerosol is defined as a suspension of liquid or solid particles in gas [14]. Atmospheric aerosols vary in size from $\sim 10^{-3}$ μm (smallest clusters of molecules detectable by condensation nuclei counters) up to $\sim$20 μm. Particles greater than 10 μm in diameter tend to settle very quickly close to the source. Aerosols of size range $\sim 10^{-3}$ to 1 μm in diameter are known as *Aitken nuclei* and are usualy formed either by condensation of hot vapours (*e.g.* of metals) or following oxidation of substances like SO_2 to form involatile products. The Aitken nuclei may then coagulate together to form relatively larger and stable particles of size range $\sim$0.1 to 1 μm in diameter. These particles can act as nuclei for the condensation of water to form clouds and are removed by the two major processes that introduce contaminants to wet deposition: *rainout*[2] and *washout*[3] [15] [16].

Emissions of SO_2, NO_x and NH_3 may contribute to the atmospheric particulates: SO_4^{2-}, NO_3^- and NH_4^+. Both SO_2 and NO_x are subject to chemical transformation processes by oxidants including H_2O_2, O_3 and OH radicals. These transformation processes are referred to as the gas-to-particle conversions and may lead to the formation of the sulphuric acid (H_2SO_4)-containing aerosol and gaseous nitric acid HNO_3, *i.e.*, secondary pollutants. Secondary aerosols formed from non-precipitating clouds result from a process called droplet-to-particle conversion: a process whereby the chemistry taking place in cloud water involving conversion of SO_2, NO_x, NH_3 and other compounds produce aerosols that are left when the droplets evaporate. Junge [17] reported that about 90% of cloud droplets existing at any instant time will evaporate. The droplet-to-particle conversion for SO_2 and NH_3 produce a stable $(NH_4)_2SO_4$-

[2]The process that occurs in clouds, such as nucleation, condensation or gas dissolution.

[3]The process that scavenges the airborne particulates between the cloud base and the Earth's surface.

containing aerosol which will remain in the atmosphere until removal by wet and dry deposition processes. The NH_4NO_3-containing aerosols are unstable and may dissociate again when the equilibrium shifts in favour of the gasous NH_3 and HNO_3 constituents. The air over Europe and North America generally contains H_2SO_4, NH_4HSO_4, $(NH_4)_2SO_4$ and NH_4NO_3 and these are very effective cloud condensation nuclei [18].

Studies on the size distribution of aerosols of anthropogenic origin have indicated a mass peak at the size range of 0.1-1 μm in diameter. For example, Whitby [19] reported that a mass median distribution function of anthropogenic SO_4^{2-} aerosol exhibit a log-normal distribution characterised by a mass median diameter (MMD) of 0.48 ± 0.01 μm.

1.2.1 Emission

The main man-made acidity precursors are emissions of SO_2 and NO_x. Natural sources such as volcanoes can also emit aerosols as well as gaseous precursors. Global anthropogenic emissions of SO_2 have increased steadily since the pre-industrial times and are currently between 60-80 Mtonnes S yr^{-1} [20]. Emissions in Europe are mainly due to the burning of sulphur-containing fossil fuels. Europe was responsible for producing about 44% of the world's total SO_2 emissions in 1979 [21]. There has been marked reductions of emissions over most of Europe between the 1970s and 1990s. In the UK alone, emissions declined from a peak of more than 3 Mtonnes S yr^{-1} in 1963 to 1.3 Mtonnes S y^{-1} in 1994 [20], and 0.5 Mtonnes S y^{-1} in 2001 [22].

Emissions of NO_x from the anthropogenic sources have been estimated by Müller [23] and Benkovitz *et al.* [24] to be 21 and 21.9 Mtonnes N yr^{-1} respectively. These emissions are due to a number of sources including aircraft, soil, lightning, biomass combustion and NH_3 oxidation. Emissions from lightning and biomass burning are estimated at 5.7 and 8 Mtonnes N yr^{-1} respectively [25]. Emissions of NO_x are more geographically dispersed than those of SO_2 since motor vehicles are the major sources and are continuing to grow in large numbers worldwide. The UK emissions of NO_x are between 0.7 and 0.8 Mtonnes N yr^{-1} [20]. Ammonia emissions are less well de-

fined because of the complexity and number of sources. Europe NH_3 emissions are estimated to be ~6.4 Mtonnes N yr^{-1} of which 0.26 Mtonnes N yr^{-1} are due to the UK contributions [20]. The oxidation of NH_4^+ in soil results in NO_3 and therefore NH_3 has an acidifying effect in soil.

Figure 1.1 gives the estimated total UK emission of SO_2 and NO_2 between 1970 and 1999, and that of NH_3 between 1990 and 1999, based on data reported by the National Expert Group on Transboundary Air Pollution (NEGTAP) [22]. The total UK emissions of SO_2 and NO_2 have declined substantially from 1970 to 1990 by approximately 80% and 35%, respectively. Although the UK emmisions of NH_3 are less certain, they are, however, expected to decline by 11%, relative to 1990, by 2010 [22].

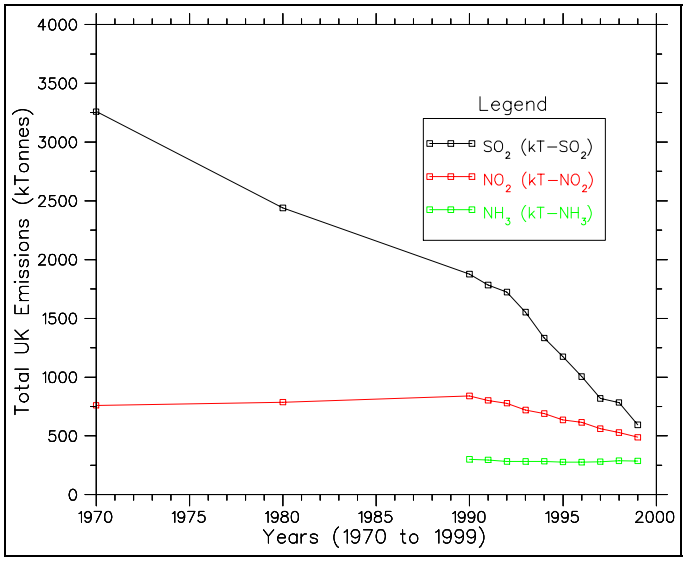

Figure 1.1: *The estimated total UK emissions of SO_2, NO_2 and NH_3 (expressed as kTonnes-SO_2, KTonnes-NO_2 and kTonnes-NH_3, respectively).*

1.2.2 Transformation and Transport

The formation of SO_4^{2-}, NO_3^- and NH_4^+ occurs during atmospheric transport of their gaseous precursors. Many of the anthropogenic pollutants that are emitted to the atmosphere are transported over thousands of kilometres from their sources. The lifetime, spatial distribution and concentration variations are determined by the meteorological conditions. For example, sulphur deposition, particularly in rainfall, was

implicated in the acidification of lakes with the long-range transport of sulphur compounds in the atmosphere over Europe [1]. Emission data for nearly all European countries participating in the European Monitoring and Evaluation Programme (EMEP) employed in the calculations of sulphur and nitrogen transport as part of the 1983 Convention on Long Range Trans-Boundary Air Pollution is available elsewhere [26].

Sulphur emitted into the atmosphere is oxidised during transport with the air masses and subsequently removed by dry and wet deposition and finally come to sulphate aerosol, mainly in the form of ammonium sulphate. Anthropogenic emission of NO_x mainly occurs in the form of NO, but a fast chemical reaction, strongly dependent on NO concentration, with participation of ozone and VOCs, results in a dynamic equilibrium between the two gases. Other chemical transformations of NO_x lead to a variety of inorganic and organic nitrogen compounds, described in detail by Jenkin and Clemitshaw [4].

1.2.3 Deposition

Both dry and wet deposition are the ultimate pathways by which airborne substances are removed from the atmosphere to the aquatic and terrestrial ecosystems. There are very few internationally established methodologies for the routine observation of dry deposition. Moreover, research on dry deposition is still limited in comparison with the many research projects and ongoing measurements of wet deposition.

1.2.3.1 Dry Deposition

Dry deposition is defined as the transport of gaseous and particulate species from the atmosphere to the ground in the absence of precipitation. Dry deposition flux Φ, is directly proportional to the local concentration of the depositing species at some reference height above the ground, $\chi(z)$.

$$\Phi = v_{dd} \times \chi(z) \tag{1.1}$$

The constant of proportionality, v_{dd} has the units of length per unit time and is therefore termed the *deposition velocity*.

Calculations for aerosol deposition velocities have been attempted by several researchers using ^{210}Pb and ^{7}Be carrier aerosols. Turekian *et al.* [27] reports a total deposition velocity (v_d) of ∼8.5 mm s^{-1} (with a range of 13.3 to 4.3 mm s^{-1}) for ^{210}Pb data obtained from Australia, England and New York-Connecticut. Calculations for dry deposition velocity (v_{dd}) using ^{210}Pb from the Rothamsted soil inventory measurements (UK) are 4.6 ± 0.6 mm s^{-1} for grassland field and an average of 8.9 ± 0.8 mm s^{-1} for the forest canopies [28]. Aerosol deposition velocities on the Pacific and Atlantic oceans using ^{7}Be were calculated to be 0.80 mm s^{-1}, although this value may be argued to be about 10 to 50% too small since calculations were based on atmospheric ^{7}Be concentrations measured at continental sampling stations. Atmospheric ^{7}Be concentrations measured over continental stations averaged 10-50% higher than the concentrations over the ocean [29].

1.2.3.2 Wet Deposition

Wet deposition refers to the natural processes by which atmospheric pollutants are scavenged by atmospheric hydrometeors (cloud and fog drops, rain and snow) and subsequently delivered to the Earth's surface. The amount of the deposited material is measured as the amount of the compound received per unit area of the receiving surface. Wet deposition rate is independent of the nature of the receiving surfaces, and depends on the rate of precipitation R (mm) and the rainout or washout ratios (α), obtained by taking the ratio of the concentration in the rain, c_r (washout) or in cloud, c_c (rainout), both measured in g m^{-3}, to the ambient air concentration, c_a (g m^{-3}):

$$\alpha = c_r/c_a \tag{1.2}$$

Wet deposition D_w (g m^{-2}) from the rain, and when the concentrations are measured in g l^{-1}, can now be obtained from the following [30]:

$$D_w = c_r R = \alpha c_a R \tag{1.3}$$

The major wet deposition process begins with the removal of the particles by nucle-

ation scavenging. The $(NH_4)_2SO_4$, H_2SO_4-containing aerosols are deliquescent and provide ideal condensation nuclei for the production of cloud droplets [31]. For particles of size range $\sim$ 0.01 to 0.1 μm in diameter, scavenging of aerosol particles within clouds by collision of atmospheric gas molecules with particles (*i.e.*, Brownian Motion) is significant. For aerosol particles which can not follow streamlines of airflow around hydrometeors, wet deposition operates via impaction scavenging. This mechanism is only efficient for particles larger than $\sim$5 μm in diameter and increases with particle size [31].

In the 1960's and 1980's, the method that was most commonly used to measure wet deposition was the open or bulk sampler, which included dry deposition to the collector during periods of no precipitation. This has led to overestimates of wet deposition of particles such as SO_4^{2-} and NO_3^- due to sorption of SO_2 and HNO_3 onto the collecting material during dry periods. Bulk precipitation of SO_4, NO_3 and NH_4 is found to be between 4% and 34% higher than wet only precipitation fluxes. For base cations like Na, Ca, Mg and K, large differences of 7 to 75% have also been reported [32]. Contributions of the dry deposited SO_2 to the SO_4^{2-} measurements have been investigated by Fowler and Cape [33]. It is recommended that wet only samplers be used and also that shorter collecting periods be made to minimise bacterial or chemical reactions that may occur during periods of exposure to the atmosphere. Other sources of error during collection of rainfall in funnels are due to the rain adhering to the funnel walls, evaporation, residual amount adhering to the container walls during emptying (wetting loss) and deflecting of precipitation by streamlines of airflow (aerodynamic error). Beier and Rasmussen [34] have reported that errors due to wetting loss are $\sim$3 to 6% and that the aerodynamic errors for water collection on unsheltered funnels are $\sim$10 to 18%.

Another kind of wet deposition, sometimes known as cloud droplet interception, is occult deposition and this occurs when an area is immersed in a fog or low cloud. The typical size of a cloud drop is 4 to 20 μm in diameter. The collection efficiency by impaction, increases with increasing wind speed. The efficiency also increases rapidly with the increase in the diameter of the cloud droplet size. Fine needled conifers

are particularly efficient collectors of cloud drops because of their fine structure and increased turbulence over forests than over shorter vegetation. A review of work on occult deposition rates and suggestions for estimating occult deposition on forests is given by Unsworth and Wilshaw [35].

1.3 Deposition to Complex Topography

Early work carried out by the Review Group on Acid Rain (RGAR) between 1981 and 1985 [20] to map deposition of pollutants by rain was based on the assumption that the ionic concentration in precipitation were independent of altitude and calculated deposition on hills to be linearly related with the amount of rainfall. This has provided an underestimate on the deposition of the pollutants on mountainous areas.

1.3.1 Deposition on Mountainous Terrain

Deposition over hills is commonly enhanced by the *seeder-feeder* mechanism: a model first conceptualised by Bergeron in 1965 [36]. In this process, hill cap clouds are formed when low-level moist air is forced to ascend over hills and this results in cooling and condensation. The low-level cloud associated with the hill (*i.e.*, the feeder cloud) is efficiently scavenged of its liquid content and deposited to the ground by precipitation from the upper level (seeder) cloud. This process is responsible for the enhancement of the rainfall that is commonly found over elevated areas. Figure 1.2 illustrates the process of the seeder-feeder effect on rainfall concentrations of major ions in rain (adapted from Fowler [31]).

Measurements of the ionic composition of rainfall at different elevations at Great Dun Fell (UK) provide some detailed information on the influence of topography on the deposition of major ions: SO_4^{2-}, NO_3^-, NH_4^+, H^+, Cl^- and Na^+ [37]. The concentrations of the ions in orographic cloud at altitude 847 m asl. were found to be higher than concentrations in rain by factors of 2.0 to 3.9. A sharp decrease in concentrations of these ions with increase in altitude from cloud base was observed in orographic clouds. This change is due to the dilution of solutes by the increase of cloud water content with increasing height.

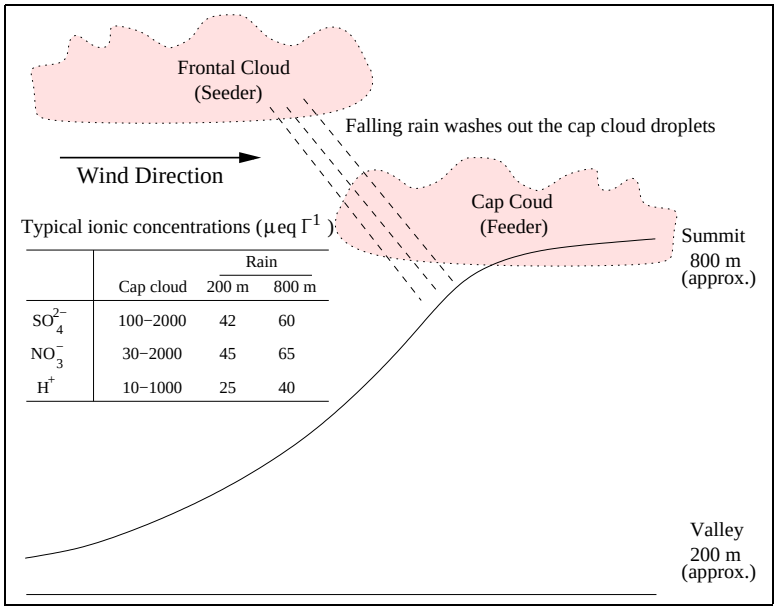

Figure 1.2: *The process of the seeder-feeder mechanism for enhanced rainfall concentrations of major ions over hills.*

A model of the seeder-feeder process for the orographic rainfall enhancement in the areas of more complex terrain was developed by Jones and Choularton [38]. The results of the model show that the rainfall enhancement and deposition are a function of both the topography and the spatial scales. This model could be of much use in improving the wet deposition map of the UK. In the UK, the seeder-feeder process is responsible for a large fraction of wet deposition over the Pennines, the Lake District and Snowdonia [39].

1.3.2 Deposition on Forests

Forests possess surface structures that promote interception of atmospheric pollutants. The enhancement of the deposition of the pollutants is due, in part, to the turbulence of air above and within the forest canopies. The processes of deposition of atmospheric particles, cloud droplets and major gaseous pollutants onto forest canopies and the properties of forests as sinks for the atmospheric pollutants have been examined by Fowler *et al.* (1989) [18]. For gaseous species such as SO_2, NO, NO_2, HNO_3, HCl, and NH_3, the rate of uptake by forests is controlled by turbulent and molecular diffusion to surfaces with reaction or dissolution at the surface.

Although tall trees are more efficient in intercepting aerosols and cloud droplets, the efficiency is also determined by the size of the particles. For example, both modelling and experimental results show the dependence of deposition velocity, v_d on particle size of the various compounds studied to increase with increase in mass median diameter of the size distribution of the compounds as illustrated by the ranking: $v_d(^{214}\mathrm{Pb}) < v_d(\mathrm{SO_4}) < v_d(\mathrm{NO_3}) < v_d(\text{base cations}) < v_d(\text{fog})$ [40]. Impaction is the most efficient deposition mechanisms for cloud droplets in the radius size of 4 or 5 μm [41]. The inputs of pollutants from rain falling under gravity are the same for both lower and higher vegetation.

1.4 Total UK Deposition

The combined inputs of wet, dry and cloud water deposition for sulphur in the UK during the period of 1992 to 1994 amount to 0.35 Mtonnes S yr^{-1} with maximum values occurring over the Pennines and the minimum values in the drier parts of northern Scotland. The total nitrogen deposition is estimated to be 0.38 Mtonnes N yr^{-1} (equivalent to an average deposition of approximately 1.4 g N m^{-2} yr^{-1} throughout the UK). The sources of sulphate and nitrate are principally due to combustion while ammonium sources are from agriculture. Man-made SO_2 emissions are due to fossil fuel combustion, with motor vehicles being accountable for $\sim$50% of NO_x emissions [42]. Livestock wastes and, to a less extent, fertiliser applications are responsible for the emission of NH_3.

Although most of the pollutants deposited in the UK are from national sources, studies from the long-range transport models have shown that airborne substances can be transported up to thousands of kilometres [26]. For example, the modelling results by third report of the RGAR [42] used to estimate the sulphur budget for the UK in 1987 show that of the total $\sim$0.5 Mtonnes deposited, about 32% originated from outside the UK. Dry deposition accounted for approximately 60% of this total. In the UK, a large proportion of the total sulphate concentration in rainfall is naturally occurring and derived from sea spray. This accounts for up to 60% of sulphur deposition in the western coast of England but generally decreases to $<$20% in east-

ern England [43]. Deposition of base cations (calcium, magnesium and potassium) influence the critical loads of acid deposition to soil. From the non-sea salt annual deposition of base cations of 0.1 Mtonnes, ∼84% comes from Ca^{2+}, 16% from Mg^{2+} while K^{+} deposition is neglegible [20].

1.5 Radioactivity in the Environment

In the environment, radioactivity may be categorised into three main groups, based on their origin: (1) primordial (those present during the formation of the earth and are still present due to their long half-lives ($t_{1/2} > 10^8$ years): (2) cosmic-ray produced (both in the atmosphere and lithosphere) as a result of cosmic radiation and: (3) anthropogenic (introduced into the earth's environment due to nuclear weapons testing and nuclear accidents) [17].

Radionuclides present in the environment have been widely used as tracers in a number of investigations pertaining to the earth sciences. In this study, we used ^{210}Pb (from category 1), ^{7}Be (from category 2) and ^{137}Cs (from category 3) as tracers in the study of submicron aerosol deposition using air, precipitation, vegetation and soil inventory measurements.

1.5.1 ^{210}Pb in the Environment

The naturally occurring atmospheric ^{210}Pb ($t_{1/2}$ = 22.3 years) is a daughter of a radioactive water insoluble inert gas, ^{222}Rn ($t_{1/2}$ = 3.8 days) belonging to a ^{238}U decay series. Since ^{238}U and ^{226}Ra are ubiquitous in rock and soil, ^{222}Rn is constantly being produced. Because ^{222}Rn is not chemically bound or attached to other materials, its atoms can outgas from the earth's continental crust to the atmosphere and decay through a series of short-lived daughters to ^{210}Pb metal atoms in the atmosphere. Once produced, the ^{210}Pb ions instantaneously (∼30 s) and irreversibly attach to aerosol particles, and are distributed by the general atmospheric circulation [44] [45].

The main source of ^{210}Pb is the ^{222}Rn, a noble gas which escapes from the ice-free earth's continental crust at an emission rate that varies with location, depending on the geological structure (*i.e.*, the abundance of the ^{226}Ra in soil), the soil type, soil

moisture and freezing conditions [46]. Jaworowski *et al.* [47] estimated that, with the mean ^{222}Rn exhalation rate of 14.8 mBq m^{-2} y^{-1} from 112×10^{12} m^2 of the ice-free surface land, ∼25.53×10^{15}Bq ^{210}Pb y^{-1} is introduced in the atmosphere. Robbins (as quoted from reference [47]) estimated that ∼0.925×10^{15} Bq ^{210}Pb y^{-1} comes from the ^{222}Rn exhalation from the oceans with negligible amounts coming from other natural sources such as volcanic dust, atmospheric meteoric matter and wind transfer of soil and sea water. Anthropogenic ^{210}Pb sources such as coal combustion, uranium mining and phosphate fertilisers are minute when compared to ∼10^3 times greater natural contribution from ^{222}Rn emanated from both land and sea. The significant alternative source of ^{210}Pb is from nuclear explosions, although amounts are limited to single geographical regions and are of short-term duration [48]. Figure 1.3 illustrates the principal members of the ^{238}U series.

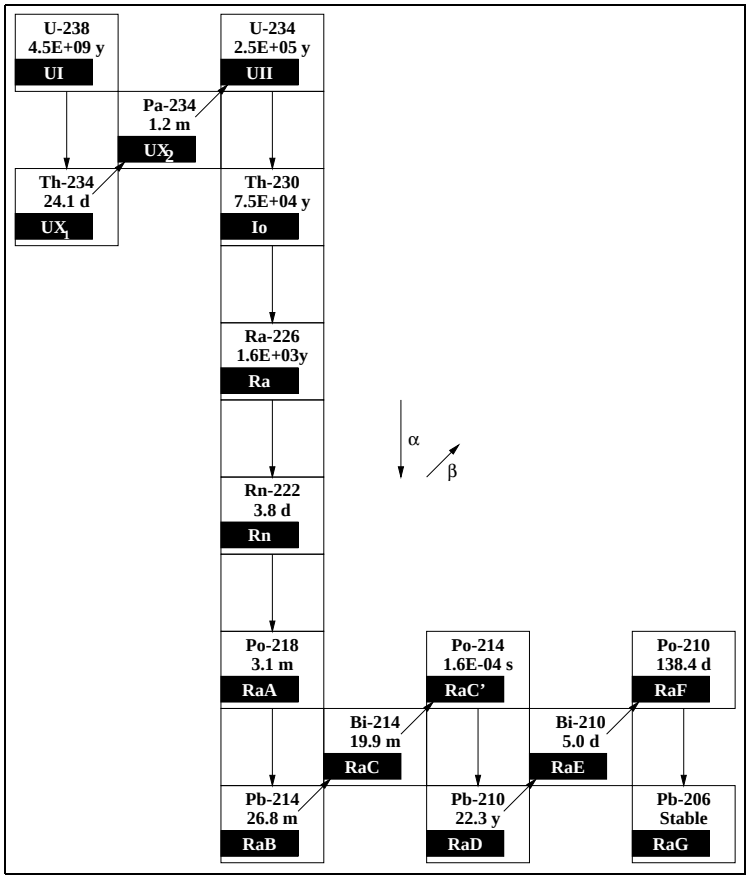

Figure 1.3: *Principal members of the ^{238}U Decay Series.* Letters in black background are historical symbols.

1.5.1.1 ^{222}Rn Production in Soils

^{222}Rn is a daughter of a long lived ^{226}Ra present within mineral grains and rocks in the ground. On average, the ^{226}Ra concentration in soils is in the order of 1×10^{-12} kg/kg of dry soil, and a fraction of this produces ^{222}Rn which is free to migrate in the pore spaces of the soil by molecular diffusion and or flow of interstitial fluid [49]. Assuming that the escape of ^{222}Rn into the atmosphere is by diffusion alone, the fraction of ^{222}Rn that escapes from the soil will decrease exponentially with increasing depth. Modelled results show that ^{222}Rn concentrations in soil have a minimum value close to the earth's surface and increase sharply with depth until a constant value is reached at a certain depth, commonly referred to as the relaxation depth [17] [49] [50] [51] [52] [53] [54]. A schematic diagram showing a typical ^{222}Rn concentration distribution with depth is given in figure 1.4.

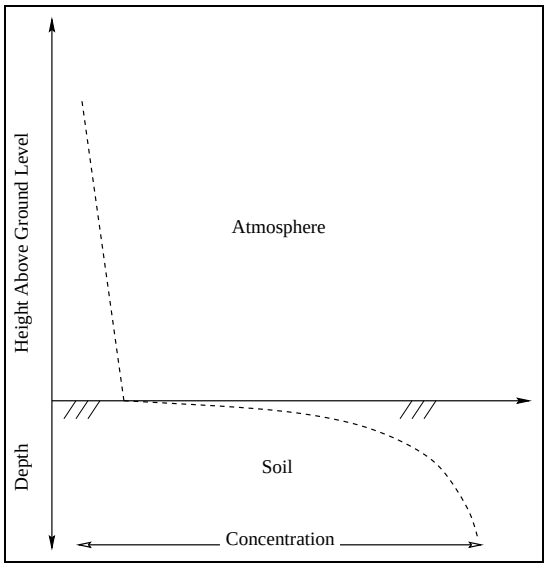

Figure 1.4: *A schematic diagram of ^{222}Rn concentrations in soil air and in the atmosphere, as a function of depth and height above ground level, respectively, as described by Israël's model (adapted from Junge). Deep in undisturbed soil and at ground surface, the typical values are 4.8×10^{-3} Bq cm^{-3} and 4.8×10^{-6} Bq cm^{-3}, respectively.*

1.5.1.2 Release of ^{222}Rn from Soils

The fraction of ^{222}Rn which escapes in the pore space of the soil depends upon the surface volume ratio of the mineral grains and the weathering processes. Barretto *et*

al. [55] reports that rocks in general, with the exception of granitic types, are poor emanators of ^{222}Rn. Balkamens [56] estimates that between 74 and 93% of radon in the New Zealand soils is retained in soil grains, while Kurata and Tsunogai [50] estimates that 20 to 50% of ^{222}Rn escapes in soil profiles from Japan. The ^{222}Rn release for a given terrain is affected by meteorological conditions and soil characteristics such as the amount of parent ^{226}Ra present, the porosity and permeability of the soil and the degree of water saturation. Dueñas *et al.* [54], using diverse soils from a region surrounding Málaga (Spain) found that, the presence of water in soils retards the ^{222}Rn release and increases its concentration in the top layer near the soil-atmosphere interface. Junge [17] reported that a decrease of up to 70% of the exhalation rate of ^{222}Rn was observed during rainfall.

Both experimental observations [54] and modelled results [49] have indicated that ^{222}Rn release decreases with increase in atmospheric pressure. This effect, referred to as atmospheric pumping[4] has been reported by Clements and Wilkening [49] who quoted ∼20-60% of ^{222}Rn flux change associated with the atmospheric pressure change of 1-2% during a passage of a frontal system. However, Dörr and Münnich [51] did not find any correlation between ^{222}Rn release and meteorological variations and soil characteristics in wet climate. Tidjani [57] also found no systematic variations of ^{222}Rn concentrations with changes in barometric pressure in Dakar, Senegal. However, this was (according to the author) attributed to weak variations of atmospheric pressure at the site.

Turekian *et al.* [27] discussed the two most common methods used for measuring ^{222}Rn flux from earth's surface to the atmosphere, namely: (1) the direct method whereby the ^{222}Rn emitted during a known time is collected into a vessel covering a known area of the soil and: (2) the indirect method based on an understanding of the vertical profile of the ^{222}Rn present in the soil in the first few metres below ground surface. He concluded that both methods underestimate the true continental ^{222}Rn flux. For example, in terrain covered by large vegetation, significant amounts of ^{222}Rn

[4]Cyclic variations in barometric pressure resulting in gases being drawn out of permeable geologic media during periods of low atmospheric pressure and air being forced into the same media during periods of high atmospheric pressure.

may be delivered into the atmosphere through transpiration by vegetation. Pearson and Jones [58] reported that the ^{222}Rn emanation per unit area from leaves of a field corn was a factor of 2.6 higher than that from the adjacent soil. The indirect methods employed in ^{222}Rn flux measurements was also criticised by Moore *et al.* [9].

The most commonly quoted values for ^{222}Rn flux are 0.7 atoms cm^{-2} s^{-1} [59] or 0.75 atoms cm^{-2} s^{-1} [60]. Turekian and others [27] however, in their global model of ^{222}Rn from the earth's surface and ^{210}Pb flux to the earth's surface used a ^{222}Rn continental emission rate of 1.2 atoms cm^{-2} s^{-1}.

1.5.1.3 Global Distribution of Atmospheric ^{210}Pb

Many types of environments such as soils, vegetation and snow receive ^{210}Pb mainly through wet deposition. The distribution of ^{210}Pb concentration is governed mainly by two factors: (1) the ^{210}Pb source and: (2) the meteorological conditions such as transport and deposition mechanisms. The ^{210}Pb distribution in the atmosphere varies according to the proportion of the ice-free continental areas as compared to the oceanic and polar (ice-covered) areas, resulting in air enrichment in ^{210}Pb in the former as opposed to the latter. When annual averages are considered, the zonal circulation in the temperate latitude bands (30° - 60°) is from west to east (westerlies) and vice-versa (trade winds) in the tropical bands (10° - 30°). Therefore, the ^{210}Pb concentrations vary between areas where the dominant air mass is of continental (^{210}Pb enriched) or oceanic (^{210}Pb depleted) origin. Thus, an asymmetry in ^{210}Pb concentrations is observed between the east and the west of the continent, and also a reversed asymmetry between the temperate and the tropical latitudes.

The vertical atmospheric exchange of air between the ice-free continental planetary boundary layer and the free troposphere also determines the ^{210}Pb concentrations in that: (1) the ^{210}Pb-rich air over the planetary boundary layer is transported to the free troposphere, hence lowering the ^{210}Pb concentration in the surface air and: (2) when the air mass is more stable, ^{222}Rn and its daughters accumulate in the planetary boundary layer, elevating the ^{210}Pb concentration. Therefore, continental areas experiencing frequent anticyclonic conditions generally have higher ^{210}Pb concentrations

as opposed to areas of frequent cyclonic conditions. High ^{210}Pb concentrations in areas of negligible ^{222}Rn emanations such as oceans and polar regions are due to long-range transport of continental air through the free troposphere. Lambert *et al.* [61], on his study of the atmospheric transport of the trace elements towards Antarctica (at Dumont d′Urville), found that there is a rapid transport of ^{222}Rn and ^{210}Pb from remote continental sources through the higher layers of the troposphere to Dumont d′Urville.

1.5.1.4 The Residence Times of ^{210}Pb Aerosols

The degree of disequilibrium between the long-lived radon-222 daughters provides a measure of the survival times of the aerosols in the air column relative to removal to the surface [27]. The mean residence time of tropospheric aerosols have been determined by means of the ^{210}Bi/^{210}Pb and ^{210}Po/^{210}Pb ratios in rain and in air samples. However, both these ratios overestimate the actual residence times, with the Polonium-210 ratio to a greater degree than the Bismuth-210 ratio. Poet *et al.* [8] have estimated the ground level tropospheric residence times from measurements of long-lived ^{222}Rn decay products in air and precipitation. They found different values; 6 days when using the ^{210}Bi/^{210}Pb ratio and 24 days for the ^{210}Po/^{210}Pb ratio. Based on these findings, Marenco and Fontana [62] argued that the mean residence times calculated from the ^{210}Bi/^{210}Pb and ^{210}Po/^{210}Pb cannot be concordant if the radon daughters found in the rain samples come from more than one air mass type.

Literature estimates for mean residence times of tropospheric aerosols range from 4 to 60 days [63] depending, in part, on the origin of the aerosol, its size distribution, the regional frequency of precipitation and the rate of dry deposition. In the UK for example, several workers have reported the ^{210}Pb mean residence time ranging from 9 days to a few weeks [48]. Moore *et al.* [9] estimated the residence time of aerosols in the lower troposphere over the continental USA to be $\leq$4 days, and increased with altitude within the troposphere by a factor of 3 or less. Balkanski *et al.* [64] used modelled results and estimated the mean residence time of ^{210}Pb aerosols in the tropospheric column to be 20 days over the Antarctica, 5 days at the southern midlatitudes, 10-20

days in the tropics and between 5 days (in winter) and 10 days (in summer) at the northern midlatitudes. They attributed the long residence times in the midlatitudes in summer and in the tropics to the frequent convective pumping of ^{222}Rn to the high altitudes. Lambert *et al.* [11] used a model based on the assumption that the the northern and southern tropospheres are separated form each other and obtained mean residence time values of 5.88 days and 8.79 days respectively.

1.5.2 ^{7}Be in the Environment

^{7}Be is a cosmogenic gamma-emitting radionuclide with a radioactive half-life of 53.3 days. It is produced by the cosmic spallation reactions with nitrogen and oxygen with about 2/3 of the ^{7}Be source being located in the stratosphere and the rest being mainly produced in the upper troposphere [65] [66]. The relatively high production rate in the upper troposphere and the transport of ^{7}Be from the lower stratosphere to the upper troposphere maintains a steep vertical concentration gradient between the upper and lower troposhere [67]. Soon after production, the ^{7}Be atoms rapidly and irreversibly attach themselves primarily to submicron-sized aerosol particles. The fate of ^{7}Be is determined by mechanisms governing the removal and transport of atmospheric aerosols, since the mean residence time of tropospheric aerosols is ∼10 days *i.e.*, much shorter than the ^{7}Be decay lifetime ($\tau_{Be} = 77$ days).

Typical ^{7}Be activity concentrations at the lower stratosphere and tropopause level in the northern midlatitudes are 155 mBq m^{-3} and 18 mBq m^{-3} respectively [68]. UNSCEAR, 2000, as quoted from Gerasopoulos *et al.* [69], reported the average tropospheric production rate and the concentrations of ^{7}Be to be 810 atoms m^{-2} s^{-1} and 12.5 mBq m^{-3}, respectively. On the other hand, surface level concentrations normally fluctuate around 3.5 mBq m^{-3} [66] [68]. Thus, air coming from the upper troposphere and especially the stratosphere, can be identified by its enhanced ^{7}Be levels. Table 1.1 gives some measurements of the ^{7}Be mean concentrations.

Table 1.1: *Measurements of ^{7}Be mean air concentrations at various locations in the world.*

Reference	Dates	Altitude (m)	Location	^{7}Be (mBq m^{-3})
Peirson [70]	1959-1961	1219	42-65°N (UK)	5.18
Peirson [70]	1959-1961	0	42-65°N (UK)	2.22
Shapiro *et al.* [71]	1973-1975	-	33.9°N (USA)	7.99
Crecelius [72]	1976-1977	50	46°N (USA)	4.15
Hötzl and Winkler [73]	1983-1985	490	48.1°N (Germany)	3.63
Choubedar [28]	1996-1999	-	55.6°N (UK)	2.71

Surface level concentrations are typically a factor of magnitude smaller than the tropospheric mean due to the incomplete mixing [74]. High ^{7}Be surface air concentrations are normally associated with places of relatively infrequent precipitation events, since ^{7}Be is allowed to accumulated in the lower troposphere. For example, Shapiro *et al.* [71] reports about 8 mBq m^{-3} of ^{7}Be air concentration in California (USA), where the average rainfall recorded for the years 1974 and 1977 were 37.1 cm and 36 cm respectively. Table 1.2 gives measured average ^{7}Be concentrations in rainfall and the depositional flux to the ground.

Table 1.2: *Measurements of ^{7}Be mean rainfall concentrations at various locations in the world.*

	Rainfall			^{7}Be Concentration and Flux	
Reference	Dates	(mm)	Location	mBq l^{-1}	Bq m^{-2} y^{-1}
Peirson [70]	1959-1960	820	51°N (UK)	1345	913
Peirson [70]	1959-1960	1330	51°N (UK)	1379	863
Todd *et al.* [75]	1983	1340	36.9°N (USA)	1494	1992
Todd *et al.* [75]	1984	1290	36.9°N (USA)	1660	2141
Baskaran *et al.* [76]	1989	1030	29.3°N (USA)	1438	1479
Baskaran *et al.* [76]	1990	1970	29.3°N (USA)	2057	1992
Baskaran *et al.* [76]	1991	1500	29.3°N (USA)	2570	3851
Choubedar [28]	1997-1999	930	55.6°N (UK)	732	787

The rainfall concentrations may be slight overestimates due to contributions from dry deposition. Olsen *et al.* [77] and Todd *et al.* [75] compared wet only and bulk samples and concluded that dry deposition contributes to less than 10% of the total deposition.

According to Koch and Mann [78], ^{7}Be concentrations follow a certain time variation: the 11-years cycle of solar radiation and the annual cycle. In the northern midlatitudes, studies have shown maximum ^{7}Be concentrations in late summer [79]. Feely *et al.* [67] suggested that there are at least four processes that control the seasonal variability of ^{7}Be surface concentrations. The first one is that of the stratosphere-to-troposphere air exchange associated with the tropopause folding near the polar front and the subtropical jet-streams (a process most common in the midlatitudes). Other studies using ^{7}Be as a tracer of stratosphere-troposphere exchange have also been carried out by several researchers [68] [80] [81] [82].

Another process which influences the ^{7}Be surface concentration is the vertical transport within the troposphere. High ^{7}Be concentrations in many stations in both the north and south hemisphere have been observed during warm seasons, and lower concentrations during the cold seasons. The difference in air surface concentrations of this radionuclide can be attributed to more increased vertical mixing in summer, enhanced by solar heating, that transports the ^{7}Be air produced in the upper troposphere (or transported from the lower stratosphere to the upper troposphere) down to the lower troposphere. Graustein and Turekian [83], using data sampled from the eastern North Atlantic, have shown that high positive correlation of summertime ^{7}Be and ozone concentrations are more likely to indicate the upper tropospheric source of ^{7}Be than the direct stratospheric intrusions for elevated ozone. Another study showing an enhanced ^{7}Be concentration due to vertical mixing in the troposphere rather that the stratosphere is one by Dibb and others [81] conducted at Alert, Canada.

The third process important in the ^{7}Be concentration is the effect of washout. From both the ^{7}Be measurements and modelled results, wet scavenging accounts for more that 90% of the total deposition [66] [76] [84]. The last process is the horizontal transport (advection) of ^{7}Be from the midlatitudes to the lower and higher latitudes. Both the Arctic and Antarctica polar air masses are stable, inhibiting vertical transport of air even during summer, preventing the polar stratospheric ^{7}Be from directly reaching the lower layers of the troposphere. Thus, the most likely source region of the ^{7}Be that reaches the polar regions is the midlatitudes areas [67]. Different annual

cycles of ^{7}Be concentrations are observed depending on geographical locations, driven by the relative contributions of all the four processes of the ^{7}Be budget.

In the stratosphere, the ^{7}Be activity concentrations do not exhibit an annual cycle. This is due to the steady state production and removal by radioactive decay, since the mean stratospheric residence time is more than a year, which is much longer than the lifetime of ^{7}Be [68]. However, there is an inter-annual variability of ^{7}Be activity concentrations due to the 11-year solar cycle. The amplitude of this variation increases with geomagnetic latitude and height, details of which are described elswhere [66].

1.5.3 ^{137}Cs in the Environment

^{137}Cs ($t_{1/2}$ = 30.2 years) is an anthropogenic radionuclide derived from two principal sources: testing of nuclear weapons and the 1986 Chernobyl nuclear-reactor accident. There is also a possibility of localised inputs at sites near nuclear power plants. Global fallout in the northern hemisphere due to nuclear weapon testing commenced around 1954, peaked in 1963, the year of most intensive weapon testing, and had fallen to very small concentrations by 1986. An additional ^{137}Cs input in some parts of Europe and adjacent regions was received in April 1986 from the reactor at the Chernobyl nuclear power plant in the Ukraine. Figure 1.5 depicts the global ^{137}Cs depositional fluxes (southern and northern hemispheres) from 1954 (pre-Chernobyl) to 1988, based on data reported by Cambray and others [85].

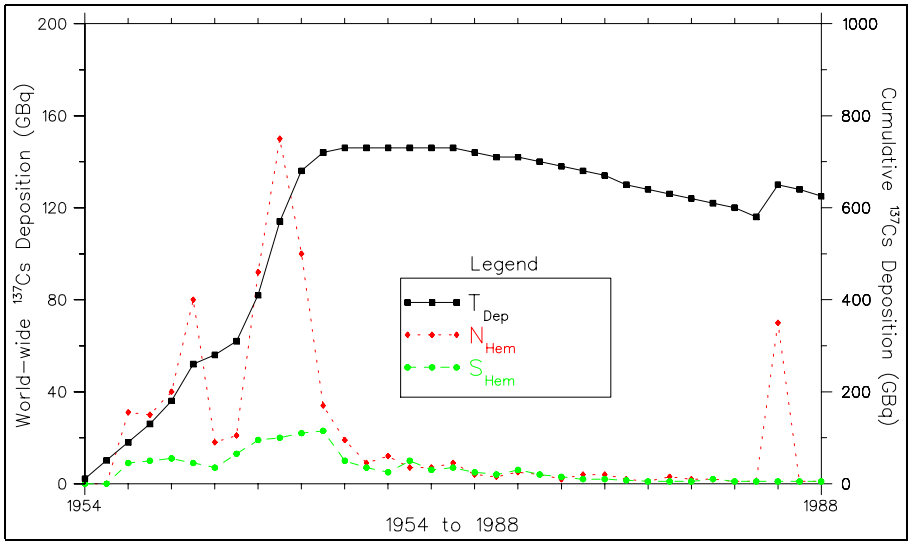

Figure 1.5: *^{137}Cs depositional fluxes from 1954 (pre-Chernobyl) to 1988, based on data reported by Cambray and others (1983). N_{Hem} = Northern Hemisphere; S_{Hem} = Southern Hemisphere and T_{Dep} = Total Cumulative Deposition.*

Air concentrations of ^{137}Cs, measured at several stations operated by Harwell in the southern hemisphere (Botswana, Australia, New Zealand and Singapore) have shown no activity concentrations attributed to the Chernobyl plume, *i.e.*, <0.01 mBq m^{-3} throughout the period of interest [86].

Like ^{210}Pb and ^{7}Be, ^{137}Cs associates itself with submicron sized particles in the environment and it reaches the earth's surface mainly through wet deposition. Thus, higher ^{137}Cs inventory values will be associated with areas receiving heavy rainfall [87]. For example, following the 1986 accident at the Chernobyl, one of the three major parts of the plume reached Britain on a generally fine dry weather [88]. Over North Wales, Cumbria, North Ireland and Scotland, heavy convective rain fell, causing substantial deposition in these areas. The ^{137}Cs soil inventory measurements attributable to the Chernobyl accident indicated <10% that of the present weapon test fallout at Suffolk, whereas in Cumbria, the ^{137}Cs soil inventory measurements were about 3 times that estimated for weapons fall-out [86].

1.6 Aims of this Study

Naturally occurring radioisotopes provide useful information on the deposition of aerosols from the atmosphere. Isotopes of ^{210}Pb and ^{7}Be have been extensively used by a number of workers, for example: as tracers of deposition of submicrometre aerosols; Graustein and Turekian [89] [90]: in determining the rate of sediment mixing as well as dating of sediments; Clifton [91] and Eakins [92]: as heavy metal tracers in river-estuarine system; Benninger *et al.* [93] and Lewis [94]: in determining aerosol residence times; Moore *et al.* [9], Lambert *et al.* [11], Wieland *et al.* [12] and Tokieda [13]: and in determining aerosol deposition velocities; Crecelius [72] and Young and Silker [29]. The following are the aims of this study:

- To investigate factors influencing concentrations of ^{210}Pb and ^{7}Be in surface level air (chapter 3).
- To investigate the effect of vegetation on (^{210}Pb and ^{137}Cs) aerosol deposition and the pathways of ^{210}Pb deposition to woodland canopy soils (chapter 4).
- To investigate the influence of topography on the deposition of ^{210}Pb and ^{137}Cs (chapter 5).

Soils were sampled from the open grassland and woodland areas from areas of relatively simple topography (in Edinburgh) and extended to areas of moderately high altitudes (in Wales) to gain insight into both the woodland and orographic effects on the deposition of the nuclide-bearing aerosols. The ^{210}Pb and ^{7}Be intercepted and retained by trees was estimated by means of rain and throughfall techniques conducted with Sitka Spruce (*Pecea Sitchensis*), as well as by direct concentration measurements of the tree leaf needles. Furthermore, monthly measurements of ^{210}Pb and ^{7}Be concentrations on foliage harvested from selected deciduous tree species from the Edinburgh sites (see chapter 4) were made to determine any possible rate of accumulation of the ^{210}Pb and ^{7}Be species. Collection of air samples were made continuously for 12 months at an Edinburgh site, in order to determine factors influencing the concentrations of ^{210}Pb and ^{7}Be in surface-level air. Treatment of the soils and vegetation samples was done at the Scottish Agricultural College (SAC) Analytical Services Department, (at

the Bush Estate) and at the Centre for Ecology and Hydrology (CEH-Edinburgh), respectively. Rain and throughfall samples were treated at the University of Edinburgh, School of Physics. Finally, γ-ray analyses of all the samples were conducted at the University of Edinburgh, Nuclear Physics Group Laboratories using High Purity Germanium detectors.

Chapter 2

Gamma-ray Analysis Procedure

2.1 Interaction of γ-rays

When an atomic nucleus disintegrates, the resulting daughter product left at an excited state may possibly reach its ground state through the emission of γ-rays. For example, ^{137}Cs nucleus results in the formation of a ^{137m}Ba and a β particle. The resulting ^{137m}Ba left in an excited state de-excites to ground state by emission of 661.7 keV γ-rays. Thus, samples exhibiting a peak at a 661.7 keV line on a multi-channel analyser (MCA) when counted, may indicate the presence of ^{137}Cs nuclei.

Gamma (γ)-rays (and X-rays) can be treated as photons and are detected by means of the electrons they produce when they interact in the material of which the detector is made. In the energy range (10 keV$<E_\gamma<$ 2000 keV) of interest for γ-ray studies in this work, three interaction mechanisms for γ-rays with matter play a major role: (1) *photoelectric effect*, (2) *Compton scattering* and (3) *pair production*. In this section, these mechanisms, as well as their contributions to the energy spectrum of γ-rays, are discussed. Radionuclides of interest, measured to determine their concentrations and inventories in environmental samples collected in the course of this study, are listed in table 2.1.

Table 2.1: *Details of radionuclides measured in environmental samples collected during the course of this study.*

Radionuclide	Half-life $t_{1/2}$	γ-ray used (keV)	†Branching ratio (%) P_γ
^{210}Pb	22.3 years	46.5	4.25
^{214}Pb	26.8 minutes	351.9	37.1
^{7}Be	53.3 days	477.6	10.5
^{137}Cs	30.0 years	661.7	85.1

†The Branching ratio (P_γ), is the absolute probability by γ decay through the selected energy.

2.1.1 Photoelectric effect

A gamma ray may interact with a bound atomic electron in such a way that it disappears completely, ejecting an energetic photoelectron from one of its bound shells. Some of the γ-ray is used to overcome the electron binding energy, the bulk is transferred to the freed electron as kinetic energy, while a small amount of recoil energy remains in the atom to conserve momentum. This photoelectric process is very important for γ-ray detection because the gamma ray gives up all its energy, resulting in a *photopeak*, the height of which is proportional to the photon energy. The probability of the photoelectric absorption depends on the γ-ray energy, $h\nu$ and the atomic number, Z. Thus, the K-shell electrons are mostly affected, provided $h\nu > E_b$, where E_b is the binding energy. The kinetic energy, T_{e^-} given to the electron (independent of the scattering angle, θ) is the difference between the γ-ray and electron binding energy. The photoelectron is stopped quickly in the active volume of most detectors, which emits a small output pulse, the height of which is proportional to the energy of the deposited photelectron, and the electron binding energy appears as characteristic X-rays emitted in coincidence with the photoelectron. The X-rays are absorbed in coincidence with the photoelectron, resulting in an output pulse proportional to the total energy of the incident gamma-ray.

2.1.2 Compton scattering

The Compton effect is the inelastic scattering of a photon with an electron of the absorbing material. The photon loses only part of its energy to this electron. The scat-

tered photon can either escape or undergo a new interaction with the same medium. Unless the detector is infinite in size, there is always a chance that the scattered photon may escape, in which case a pulse will be formed with height proportional to an energy, which is always less than the incident photon. The scattered γ-ray energy $h\nu'$, in terms of the scattering angle θ, is given by:

$$h\nu' = \frac{h\nu}{1 + (h\nu/m_0c^2)(1 - cos\theta)} \tag{2.1}$$

where m_0c^2 is the rest mass energy of the electron (0.511 MeV). The kinetic energy, T_{e^-} of the recoil electron is therefore given by the difference between the incident γ-ray energy ($h\nu$) and the scattered γ-ray energy ($h\nu'$). Features of the Compton effect are illustrated in figure 2.1.

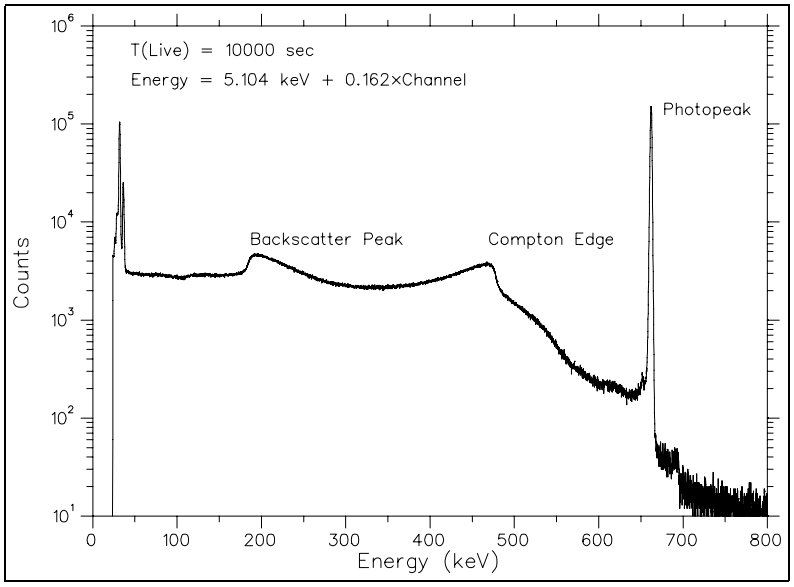

Figure 2.1: *The ^{137}Cs spectrum obtained with a HPGe detector (Det01), illustrating features of the Compton effect.*

The full-energy peak at 662 keV is formed by interactions where the γ-ray loses all of its energy in a detector by either a single photoelectric absorption or a series of Compton scattering, followed by photoelectric absorption. The spectrum of events just below the photopeak is formed by Compton scattering where the gamma ray loses only part of its energy in the detector. The step near 470 keV (the Compton edge) corresponds to the maximum energy that can be transferred to an electron by a

662-keV γ-ray in a single Compton scattering. The backscatter peak is formed when the gamma ray undergoes a large-angle scattering ($\approxeq$180°) in the material surrounding the detector and then absorbed in the detector.

2.1.3 Pair production

If $h\nu > 2m_0c^2$, an $e^- - e^+$ pair (pair production) can be produced in the field of a nucleus. The probability for this creation depends on $\sim Z^2$ (where Z is the atomic number of the absorber material) and increases with the energy of the incident γ-ray. The total kinetic energy of the electron-positron pair is given by:

$$T_{e^-} + T_{e^+} = h\nu - 2m_0c^2 \tag{2.2}$$

The total kinetic energy of the pair contributes to a pulse formation (the arguments are the same as for photoelectrons or Compton electrons). The electron and positron lose energy through collisions and eventually come to rest. The positron then annihilates with the neighbouring electron and emits the characteristic annihilation radiation, a pair of γ-rays each of energy m_0c^2. Several possibilities for the fate of these gammas occur: (1) if the energy of both annihilation gammas is deposited in the detector, a pulse proportional to energy $h\nu$ is produced; (2) if both annihilation photons escape, a pulse height proportional to energy $E - 2m_0c^2$ is formed; and (3) if one annihilation photon escapes, a pulse height proportional to energy $E - m_0c^2$ is formed. At low energies, below a few keV, the photoelectric effect dominates, the Compton effect is small, and pair production is energetically impossible.

2.1.4 Gamma-ray Attenuation

The linear attenuation coefficient, μ, which is the probability per unit length for removal of a photon, is the sum of the respective probabilities for photoelectric absorption (τ), the Compton scattering (σ), and pair production (κ). The number of transmitted photons, I, given in terms of the number without the absorber, I_0, is given by the fundamental law:

$$I = I_0 e^{-\mu\rho x} \tag{2.3}$$

where μ is the total attenuation coefficient (cm^{-2} g), ρ is the density of the absorber

material (g cm^{-3}) and x is the photon path length (cm).

Many gamma spectrometric studies involving environmental samples are concerned with low energy photons, for example, in ^{210}Pb determination at 46.5 keV in soil samples. Furthermore, the low activity of environmental materials encourages the use of thick samples to maximise the counting rate, therefore self-absorption corrections can be relevant to photon energies of a few keV. Cutshall *et al.* [95] derived the self absorption correction factor by combining equation 2.3 with the self-absorption equation:

$$O = A\frac{1 - e^{-\mu\rho x}}{I/I_0 - 1} \tag{2.4}$$

where O is the attenuation sample output and A is the sample photon emission rate. A detailed procedure for determining the self-absorption correction factors for soils sampled in this work is given in chapter 4.

2.2 Gamma Spectrometry System

As detailed understanding of radioisotope-bearing (^{210}Pb, ^{137}Cs and ^{7}Be) aerosol behaviour and fate in the environment is the main subject of concern in this study, it is necessary to measure each of them directly to provide the most accurate predictions. This involves measurement of large numbers of environmental samples, some of which contain complex mixtures of radionuclides whose concentrations may vary by orders of magnitude. Thus, it is crucial that the detectors used for this work are of high enough resolving power and the spectrometric system is set to its optimum performance.

2.2.1 Detectors and Electronics Used

In this study, ^{210}Pb, ^{137}Cs and ^{7}Be concentrations in the collected samples were determined by use of two high-purity germanium (HPGe) detectors belonging to the nuclear physics group, University of Edinburgh. A reversed-electrode coaxial HPGe detector, manufactured by Canberra™ (referred to here as Det01) with a volume of 65 cm^3 (4.4 cm diameter 4.3 cm long) and a 0.5 mm Be-window was selected for use primarily in soils and vegetation activity measurements. The detector efficiency at 1332 keV measured 25 cm from the detector relative to a 7.62 cm diameter by 7.62

cm long NaI(Tl) detector was 12.9% and its resolution at 122 keV and 1332 keV was 0.8 keV and 1.8 keV respectively. The other HPGe detector (Det02), manufactured by Detector Systems GmbH (DSG): 4.4 cm in diameter and 3.8 cm long (58 cm^3), was used for rainfall and air sample analysis. Its efficiency at 1332 keV measured 25 cm from the detector relative to a 7.62 cm diameter by 7.62 cm long NaI(Tl) detector was 10.2%, and its resolution at 122 keV and 1332 keV was also 0.8 keV and 1.8 keV, respectively. To maximise the performance of detector systems, charge-sensitive preamplifiers were located very near each detector in order to take advantage of the cooling which is necessary for the detectors, and which also aids the preamplifiers to operate with low noise. The preamplifiers were supplied as integral parts of both detector units.

A Canberra™ high-voltage power supply (HVPS) was used to supply a negative 3 kV bias voltage supply to Det01, while an EG&G (ORTEC)™ Model 572 HVPS was used for supplying Det02 HPGe with (-ve) 2.4 kV bias voltage needed for operation of each of the detectors. Amplification of output signals from preamplifiers of both detectors were obtained by means of linear amplifiers manufactured by ORTEC™. The coarse gains of the amplifiers were set at 100 (and 1.4, for the fine gain) and 50 (9.0, for the fine gain) for Det01 and Det02 respectively. The pulses produced by the output of the detectors were shaped for better performance of the counting system by setting the time constant at 2 μs for both detector systems. Spectra were stored through Canberra AccuSpec/A interface card multi-channel analysers (MCAs), which consisted of 8 k channels analog-to-digital converters (ADCs), installed in DELL 486/P33 computers.

2.2.2 Background Reduction

Each detector was shielded by an approximately 10 cm thick containment of low-background lead. It is established that the optimal lead shield thickness is 10 cm to 15 cm. Less thickness may not provide enough shielding and more thickness produces more background due to cosmic interactions with the shield [96]. The lead shield was lined with approximately 1 cm-thick copper to minimise the lead X-ray interference at the lower energy γ-rays of interest in this study.

One of the HPGe detectors (Det01), was fitted with an annular NaI(Tl) anti-Compton shield detector, set to run with the HPGe detector in anti-coincidence mode. In a germanium detector, if a γ-ray undergoes a Compton scattering and then the scattered photon interacts with a NaI(Tl) detector crystal, a coincident detection of the escaping photon serves as means to reject pulses that lead to Compton continuum generation without affecting the full-energy peak events. This process is achieved by an electronic gate that is closed if a coincident pulse is detected from the surrounding detector. The NaI(Tl) detector well also provides the insertion of the HPGe detector's end cap along with the sample, as well as to provide a greatly reduced natural background from the surroundings.

2.2.3 Detector Calibration

In order to be able to identify the principal radionuclides within the sample, by matching the principal γ-rays observed in the spectrum to the energies of the γ-rays emitted by known radionuclides, and to be able to quantify radionuclides present in a sample, it is essential that both the energy and the efficiency calibrations of the detector system are accurately performed. Each of these calibrations are simple to accomplish, however, there are potential sources of errors such as: efficiency changes due to variable source matrix, effect of source/detector distance, effect of sample density, *etc.*, that must be taken into consideration. Ideally, such calibrations are performed by use of a mixture of γ emitters consisting of known energy peaks that encompass the entire energy region over which the spectrometer is to be used. However, both energy and efficiency calibrations reported in this work were accomplished by use of standard sealed radioactive point sources, listed in table 2.2.

Table 2.2: *The standard sealed radioactive sources used for both the energy and efficiency calibrations of the detector systems used in this study.*

Source	Half-life $t_{1/2}$	γ-ray used (keV)	†Activity (kBq)	Branching ratio (%) P_γ
^{210}Pb	22.3 years	46.5	203	4.25
^{241}Am	432.2 years	59.4	38	36.0
^{133}Ba	10.5 years	81.0	29	34.1
^{133}Ba	10.5 years	276.4	29	7.1
^{133}Ba	10.5 years	302.6	29	18.3
^{133}Ba	10.5 years	356.0	29	61.9
^{137}Cs	30.0 years	661.7	35	85.1

†The activities were decay corrected for loss of activity from the reference date stated in the certificates supplied with the standards to the date the calibration was performed.

2.2.3.1 Energy Calibration

The energy calibration sources were placed onto empty standard containers (used as sample holders, described in the next section) and were counted for 20 minutes *i.e.*, long enough to produce well defined photopeaks. The channel number that corresponds to the centroid of the full energy peak (FEP) were recorded and a first order equation that uses a least square fit to multiple data points was automatically performed by the Accuspec, Genie-PC, model S400 spectroscopy software during the calibration routine. Thus, the energy *versus* channel number could be directly read out from the MCA.

2.2.3.2 Efficiency Calibration

The efficiency of a detector is dependent on the sample geometry (*i.e.*, size, density and source/detector distance). It is therefore important that the sample counting configuration is reproducible. In order to achieve this, two sets of polythene containers: 70.6 mm dia., 26 mm in height (used to hold soil samples) and 48 mm dia., 9 mm in height (used to hold air and rain filter samples) were designed to suit the dimensions of the detectors and the lead housing (and the size of the NaI(Tl) annulus for Det01). For Det01, 17 fixed positions, distributed to cover the face of the detector, were marked on the lid of one of the containers used. Each of the point sources (listed in table 2.2)

was positioned on each of the marks for 20 minutes to measure the count rate for the energies selected for this procedure. The measurements were obtained using an empty container and the procedure was repeated with the sources placed at ∼0 mm, 15 mm and then at 26 mm from the detector face. Thus, for each source (and/or each energy emitted by the source) the count rate were measured for 17×3 different geometries. The counts were weighted to the distance of the marked positions relative to the centre of the detector end cap, and then averaged to obtain a single value. For Det02, the measurements were carried out with the sources at 9 different fixed positions at a distances ∼9 mm from the detector but with the container filled with a blank filter paper to mimic the sample matrix. This efficiency calibration procedure was adapted from the procedure by Choubedar [28] using the same detectors described in this work.

When the γ-ray count rate C_γ under a full-energy peak of energy (E), emitted in the decay of a given source has been determined, the full energy peak efficiency, ϵ_γ at that energy for the given counting configuration was obtained from the following:

$$(\epsilon_\gamma)_E = \frac{(C_\gamma)_E}{(A_N) \times (P_\gamma)_E} \tag{2.5}$$

where A_N is the activity of the radionuclide used (decay corrected as described in the previous section) in Becquerels (Bq) and P_γ is the probability per decay of that transition. Least squares fitting procedures were used to fit the efficiency data to analytical expressions for both the detectors. The efficiency curves for Det01 and Det02 are given in figure 2.2.

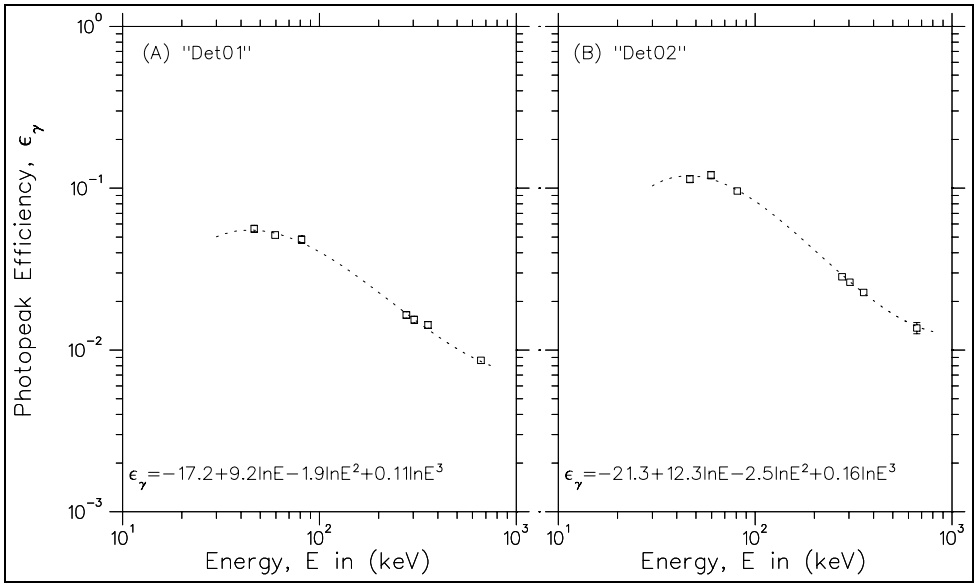

Figure 2.2: *The efficiency curves for the two germanium detectors: (A) Det01, used for soil samples and (B) Det02, used for rain and air samples showing the analytical expressions obtained from the least squares fitting to the efficiency data determined from equation 2.5.*

2.2.4 Counting Considerations

Samples were counted using containers used to acquire the counting efficiencies, to ensure that the counting geometry is maintained. Background counts for both detectors were determined prior to counting of the samples. Although both detectors were shielded for background reduction, the measured background spectra always showed peaks, mostly due to the X-rays and some from the natural radionuclides present in the shielding materials, at energies, in keV: 26.3 (^{241}Am), 46.5 (^{210}Pb), 63.3 (^{234}Th), 93.3 (X-rays, from ^{228}Ac) and 186.1 (^{226}Ra). The background measurements were made with empty sample holders and with blank filters compressed into the holders. No contribution was detected from the blank filters, particularly for ^{210}Pb which is important in this study. Background count rates for ^{210}Pb were subtracted from the measured sample count rates for soils, precipitation and air samples accordingly. For soil samples, it was necessary for an adjustment to be made to the background count rate, as described in chapter 4. An estimate of the standard deviation (σ) of the net counting rate was given using the rule:

$$\sigma = \sqrt{\sigma_T^2 + \sigma_B^2} \tag{2.6}$$

where the subscripts T and B refer to the counting of samples plus background (total) and the counting of the background, respectively. Although the spectral evaluation for peak area determination together with the errors associated with the peak reported here were automatically performed by the software used for analysis, manual calculations in the initial set up of regions of interest were performed, to check the validity of output data, as reported in literature [96] [97] [98].

2.2.5 γ-ray Analysis of Samples

Samples were presented to HPGe detectors (after treatment, where applicable) for counting, typically, for 24 hours or when the counting errors were $\leq$10%. The activity (A_N) of the specific nuclide in the counted sample was obtained from the following equation:

$$A_N = \frac{(C_\gamma)_E}{(\epsilon_\gamma P_\gamma)_E} \times f(c) \tag{2.7}$$

(see equation 2.5 for description of terms). The correction factor $f(c)$, is introduced here to compensate for self-absorption within samples; more important for the low energy ^{210}Pb γ-rays.

Since sample counting times t, were short compared to the half-lives of the radionuclides concerned in this study, the decrease in disintegration rates during counting were assumed constant, and no corrections were applied to the measurements. The total errors (exclusive of sampling errors) in the determination of radionuclides reported are the combination of the nuclide counting efficiency and the statistical counting error, governed by Poisson statistics. Other methods employed for treatment of errors reported in this study are discussed under relevant sections in this thesis.

Chapter 3

^{210}Pb and ^{7}Be Concentrations in Surface-Level Air

3.1 Introduction

The long-term measurements of the naturally occurring radionuclides: ^{210}Pb and ^{7}Be provide useful data in the study of atmospheric processes and as tracers of aerosol species. For example, the two radionuclides have been found to be particularly useful since they are associated with the same class of submicron aerosols as that which carries pollutant species such as $SO_4^=$ [89] [99]. These radionuclides have been measured routinely in many places of the world in order to study the description of environmental processes such as aerosol transit and residence times in the troposphere, aerosol deposition velocities and aerosol trapping by ground vegetation [29] [100].

The activities of ^{210}Pb and ^{7}Be in air are expected to vary with time and location. For most sampling sites, data have revealed seasonal variations in the ^{7}Be concentrations which have often been attributed to the influence of variations in the rate of exchange of air between the stratosphere and the troposphere. Other factors responsible for the variabilities in the ^{7}Be concentrations in air are the rate of vertical mixing within the troposphere, the rate of poleward transportation of air masses from midlatitudes to high latitudes and the rainfall rates. The latter being important since washout of the atmospheric aerosols is the most effective removal mechanism. On the other hand, ^{210}Pb provides information on continental aerosols in the lower troposphere. Recently, a world database providing information on global atmospheric distribution of ^{210}Pb concentrations in air has been established [44]. It is found that

the ^{210}Pb concentration is dominated by the tropospheric distribution with occasional stratospheric injection. High values of surface air ^{210}Pb concentrations are found at midlatitudes with rapid decrease towards higher latitudes due to reasons outlined in chapter 1. This chapter reports the annual average concentrations of ^{210}Pb and ^{7}Be surface-level air in Edinburgh. The concentration measurements were carried out for the following reasons:

- To determine the factors influencing both ^{210}Pb and ^{7}Be concentrations in surface level air.
- To determine whether the ^{210}Pb and ^{7}Be concentrations are affected in a similar way.
- To estimate the annual average concentrations of ^{210}Pb and ^{7}Be in air.
- To provide input data in estimating deposition velocities of both isotopes using flux measurements reported in chapter 4.

3.2 Sampling Procedure

The monitoring programme was started on 28$^{\text{th}}$ June, 2002 and continued until 29$^{\text{th}}$ June, 2003. Aerosol samples were collected over 3 day periods (occasionally 4 days) throughout the year, to obtain sufficient ^{210}Pb and ^{7}Be for the counting system. The sampling station was located at the Kings Buildings, University of Edinburgh (55.9°N, 03.2°W; 50 m asl.): national grid reference NT 267 705. The roof of the James Clerk Maxwell Building (30 m above ground level) was chosen, to minimise the number of dust particles entering the sampler, which could lead to blockage of the filters. Samples were collected on filter papers (Gelman Sciences, Type A/E Glass Fibre Filter; 20.3 cm $\times$ 25.4 cm) using a sampler with an average air flow rate of 65 m^3 h^{-1}. The filters were then pressed into pellets and placed in polythene holders for γ-ray spectrometry.

Precipitation data at site for each sampling period were obtained from the Institute for Meteorology; School of GeoSciences (University of Edinburgh). The rainfall records were obtained by using a tipping-bucket rain gauge. The rainfall data for the sampling period were registered on a recording chart. On a few occasions when rainfall data

were not available due to technical problems, hourly rainfall averages for Edinburgh stations: Blackford Hill (NT 258 706); Blinkbonny (NT 227 741) or Hillview (NT 194 734), obtained through the Meteorological Office, were used. The hourly atmospheric pressure data were recorded on a barometer available at the Institute for Meteorology (Univeristy of Edinburgh). The origins of air masses arriving at the sampling site were ascertained with the help of back-trajectories calculated using the British Atmospheric Data Centre (BADC) online trajectory service (http://www.badc.rl.ac.uk).

3.2.1 Concentration Measurements of ^{210}Pb and ^{7}Be

The activities of ^{210}Pb and ^{7}Be were determined using a 10.2% relative efficiency HPGe detector (det02) from the 46.5 keV and 447.7 keV γ-lines, respectively. The evaluation was based on equation 2.7: with the attenuation factor $f(c)$ set to 1. The procedures for energy calibration and geometric efficiency determination are outlined in chapter 2. The counting intervals ranged from 172800 to 259200 seconds. The air flow rate was determined using an air velocity meter (model 1650) to measure the rate of air passing through the filter. The measurements were carried out on different positions across the area of the filter and then averaged to represent the mean speed of air flow over the whole filter. Knowing the area of the filter paper, the air flow rate and the total sampling time, the volume of air (in m^3) passing through the area was determined. The ^{210}Pb and ^{7}Be concentrations in mBq m^{-3} were then calculated.

3.2.2 Trajectory Analysis

To determine the origins of air masses for the sampling periods, back-trajectories ending over the sampling station (55.6°N, 03.2°W; 50 m asl.) were determined using wind fields from the global weather prediction model of the European Centre for Medium-Range Weather Forecasts (ECMWF). The trajectories are three-dimensional. These winds are held online at the BADC. At present, the BADC trajectory model uses 6 hourly (0000, 0600, 1200 and 1800 GMT) pressure level data from the ECMWF. The three components of the wind (u, v, and ω) are held on a 2.5°×2.5° latitude-longitude grid and a vertical domain extending from 1000 up to 1 hPa.

For the purpose of this study, 3 day (72 hours), back-trajectories, starting at local noon, were determined. Each trajectory is given with points indicating 6-hour intervals. Thus, 12 six-hourly x-y co-ordinates (*i.e.*, end points of the trajectory location at every sixth hour) were taken as input variables. The ω levels of the air parcel position for the trajectory integration was chosen to be 950 (the model's lowest pressure level), 900 and 850 hPa (corresponding approximately to 500, 1000 and 1500 metres above ground level, respectively), on the reasonable assumption that the pressure levels are within the mixing layer of the atmosphere. Only the 950 hPa pressure level was, however, considered for analysis. The other two levels (900 and 850 hPa) were only included to give an indication of the possible wind shear uncertainties. If all three trajectories showed similar transport pathways for one time period, then the trajectory was accepted on the basis that the wind field is reasonably consistent along the transport pathway. Conversely, in cases where trajectories show a divergence of flow, and/or cases showing complex trajectories, probably due to missing archived meteorological data, the trajectories were discounted because they introduced more uncertainties in the air transport. From a total of 366 trajectories, only 3% could not be analysed due to missing archived data and <1% due to divergence of flow. Figure 3.1 shows an example of a trajectory obtained with the BADC.

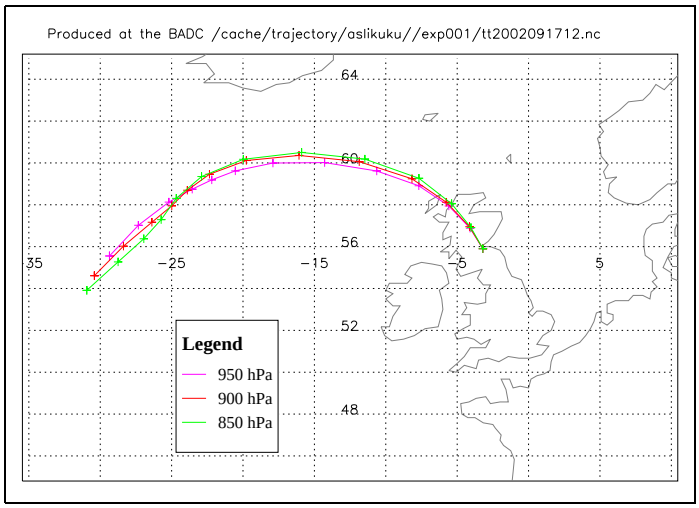

Figure 3.1: *An example of a 3-day back trajectory obtained with BADC, for the period 17-September-2002, starting at 12 noon, for 950, 900 and 850 hPa pressure levels.*

In order to identify source regions with episodes of relatively high and/or low ^{210}Pb and ^{7}Be concentrations, the start points of each trajectories were labelled as oceanic (O), or continental (C) depending on whether they originated from the ocean or the continent, respectively. This provided a rough idea about the potential source responsible for relatively high or low concentrations of the isotopes. For each trajectory, the time (in hours) it spends over the land, relative to the ocean was calculated based on the assumption that the air may pick up characteristics from those regions where it stays for a long time. The relative residence time statistics (hereafter referred to as residence time index) showing the portion of hours the air spends over the land relative to the ocean, before it reaches the measuring site, was computed by dividing the sum of hours the trajectories resided over the continent by the total number of hours for all trajectories associated with the measured isotope concentrations for that particular exposure period.

3.3 Results and Discussion

Results for ^{210}Pb and ^{7}Be concentrations in surface air at Edinburgh sampling station are reported in this section. The concentrations of both species were correlated with short-term (weather-related) meteorological variables. Data for the concentrations of both ^{210}Pb and ^{7}Be and rainfall amount recorded over the collection period are presented in appendix A.

3.3.1 Variation in ^{210}Pb and ^{7}Be with Precipitation

Figures 3.2 (a) and (b) show variations in ^{210}Pb and ^{7}Be concentrations in air with precipitation, respectively.

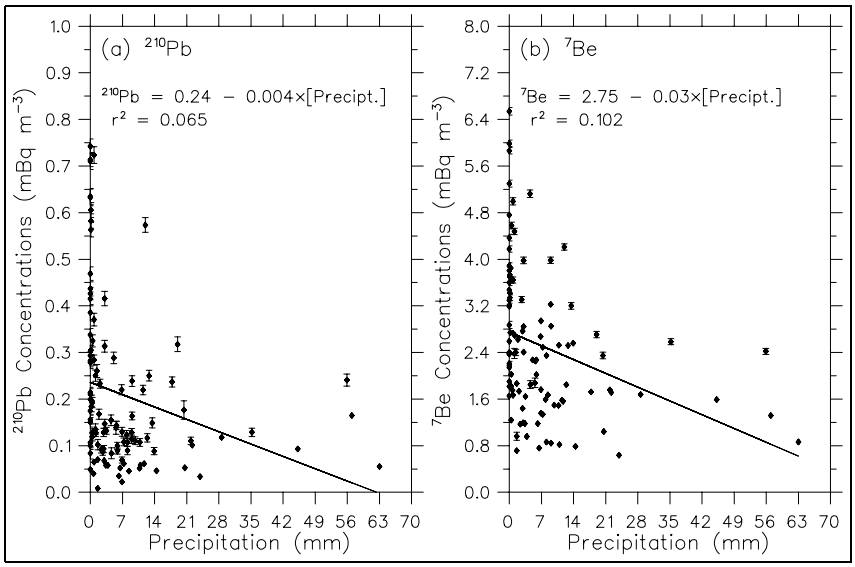

Figure 3.2: *Variation in: (a) ^{210}Pb and (b) ^{7}Be concentrations in air with precipitation.*

Clearly, there is a significant decrease (P = 0.05) in the concentrations of both ^{210}Pb and ^{7}Be in air with increase in rainfall. This is due to the 'cleansing of the ambient air' during the rainy periods, leading to lower concentrations of both species in air compared to periods of no and/or very little rainfall. Similar observations have been reported by numerous authors, for example: Hötzl and Winkler [73] reported marked troughs in the concentrations of ^{226}Ra, ^{228}Ra, ^{210}Pb, ^{40}K and ^{7}Be coinciding with periods of stronger rainfall; Monaghan [101] also reports a dramatic decrease in ^{210}Pb

concentrations in the California (USA) surface air during or immediately following precipitation events and frontal system or cyclonic storm passage. Model studies by Koch *et al.* [84], on the vertical transport of the tropospheric aerosols indicated that removal of ^{210}Pb and ^{7}Be from the troposphere is dominated by rainfall scavenging processes: approximately 88% of ^{210}Pb is removed by rainfall and 12% by dry deposition; whereas 68% of ^{7}Be is removed by precipitation and 3% by dry deposition. The remaining 29% is accountable to radioactive loss, due to its short (53-day) half life.

The weak r^2 values depicted in figure 3.2, however, suggest that rainfall alone is not the only variable controlling the concentrations of the isotopes in air, as will be discussed in the following sections.

3.3.2 Variation in ^{210}Pb and ^{7}Be with Pressure

In general, concentrations of both ^{210}Pb and ^{7}Be exhibit troughs coinciding with periods of low atmospheric pressure and *vice versa*, as shown in figures 3.3 (a) and (b), respectively. This was not unexpected because low pressure (cyclonic) conditions are associated with episodes of heavy rainfall, and consequently, the washout effect of the lower atmosphere.

Although the atmospheric pressure during the summer months (July/August, 2002) was persistently high during the sampling period, both the ^{210}Pb and ^{7}Be concentrations were relatively low. With respect to ^{210}Pb, the relatively lower concentrations may be ascribed to increased convective pumping of ^{222}Rn and its daughters upwards when the ground receives the highest flux of solar radiation. This process is, however, expected to result in high ^{7}Be concentrations due to the vertical (downward) transport of the upper tropospheric air. Because both the ^{210}Pb and ^{7}Be concentrations were relatively lower over this period, it seems reasonable to ascribe the low activity measurements to the dominant effect of washout processes by rainfall, as can be seen from the data presented in appendix A. Similarly, a sharp drop in both ^{210}Pb and ^{7}Be concentrations during high pressure periods observed in late March-early April of 2003 was also due to the rainfall recorded over the sampling period ending 02/04/03. On the other hand, periods of high pressure in the wintertime associated

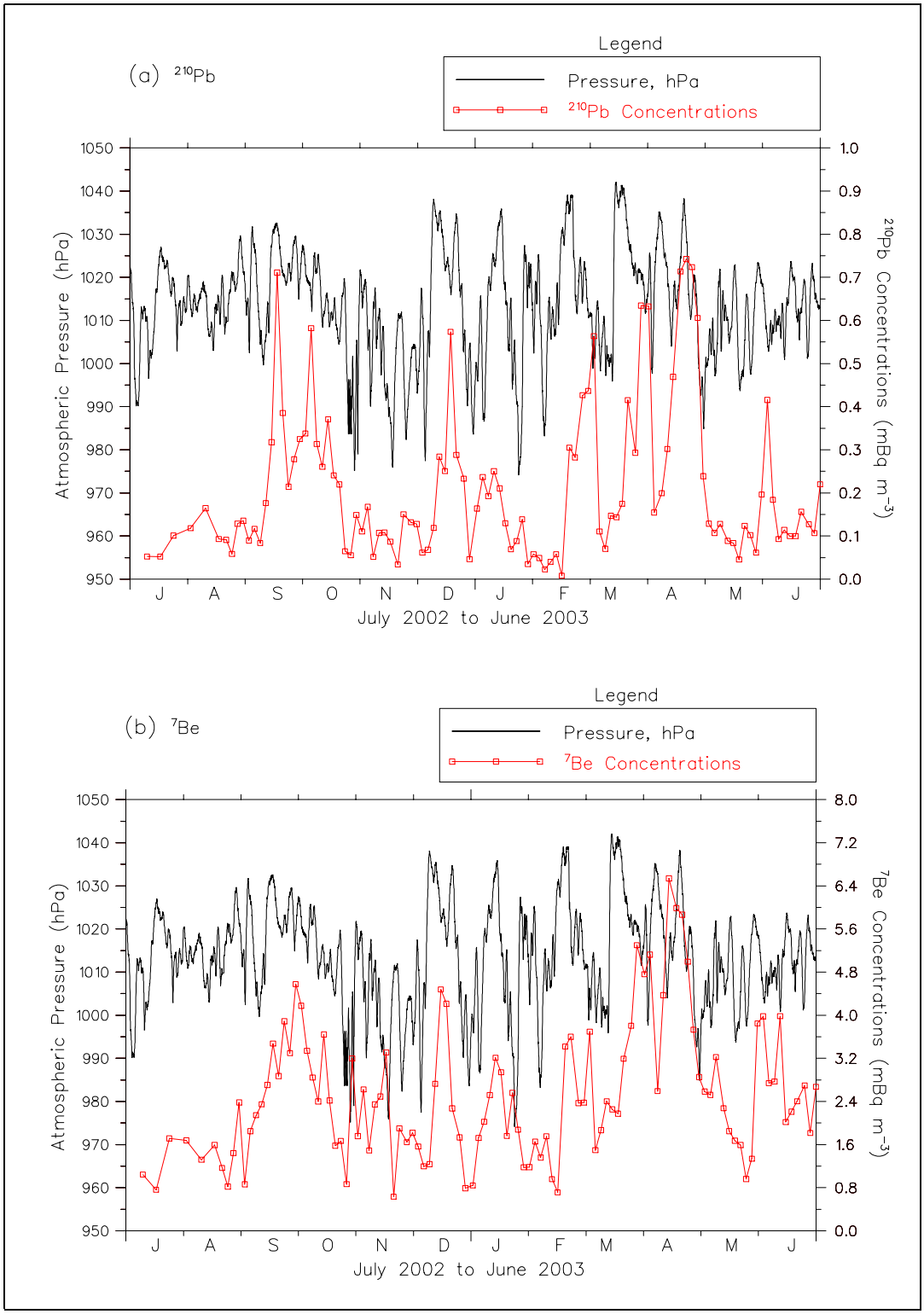

Figure 3.3: *Variations in ^{210}Pb and ^{7}Be concentrations in air with atmospheric pressure.*

with high ^{210}Pb concentrations may be due to the build-up of ^{222}Rn and ^{210}Pb in ground-level air. However, relatively high ^{7}Be concentrations during these periods may be ascribed to lower removal rates.

3.3.3 Influence of Air-mass Type on ^{210}Pb and ^{7}Be Concentrations

The origins of the air masses were determined by analysing 3-day back trajectories arriving at the sampling station. The trajectories were broadly categorised as either continental or oceanic, depending on whether they arrived to the sampling station coming from the continent or the ocean, respectively. This was achieved by means of an arbitrary line drawn 20° from the true north, passing through Edinburgh. The percentages of the total air masses originating from the ocean and the continent were 66% and 34%, respectively. Figure 3.4 gives the percentage contributions of the air masses arriving at the Edinburgh site during the sampling period.

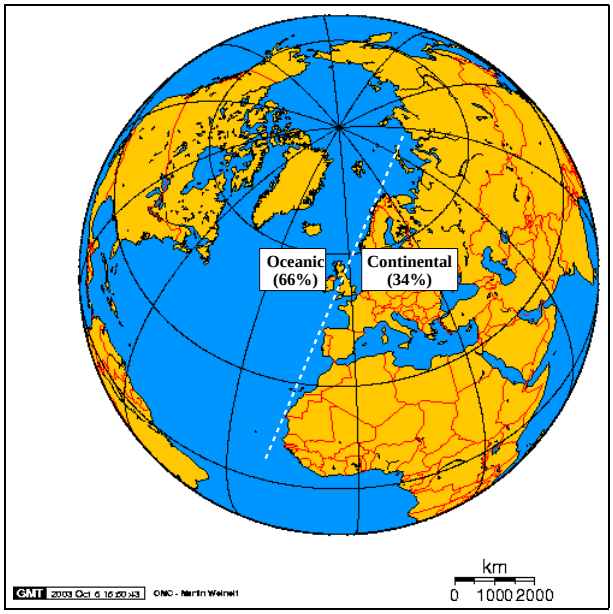

Figure 3.4: *The world map showing percentage contributions of the air mass origins arriving at the Edinburgh site during the sampling period. The white dotted line seperates the two different air mass classes.*

3.3.3.1 Air-mass Type

A plot of ^{7}Be *versus* ^{210}Pb concentrations in air (figure 3.5) shows that data can be classified into two groups: one for air originating from the continent and the other for air coming in from the ocean. Both groups of data give good correlations. The

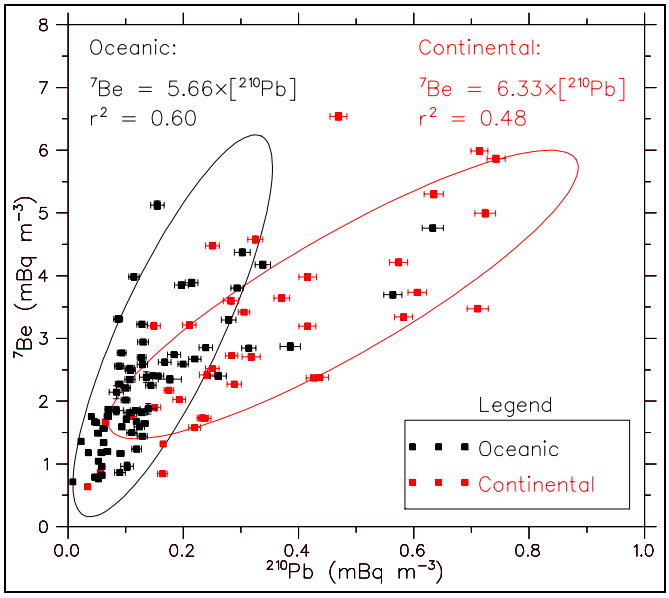

Figure 3.5: *The influence of air mass origin on ^{210}Pb and ^{7}Be concentrations in air. The rings are just a guide to the eye.*

(^{7}Be/^{210}Pb)$_{oceanic}$ to (^{7}Be/^{210}Pb)$_{continental}$ activity ratio was 1.12. Although this difference is moderate, it gives an indication that air originating from the continent is rich in ^{210}Pb relative to that originating from the ocean.

3.3.3.2 Residence Time Analysis

The strong evidence in the correlation (at P = 0.003) between the ^{210}Pb concentrations and the residence time index (r^2 = 0.51) compared to that of ^{7}Be (r^2 = 0.21) suggest that air parcels that spend most of their times over the continent are enriched with ^{210}Pb compared with those which spend most of their times over the ocean, as presented in figure 3.6 (a) and (b) for ^{210}Pb and ^{7}Be concentrations, respectively.

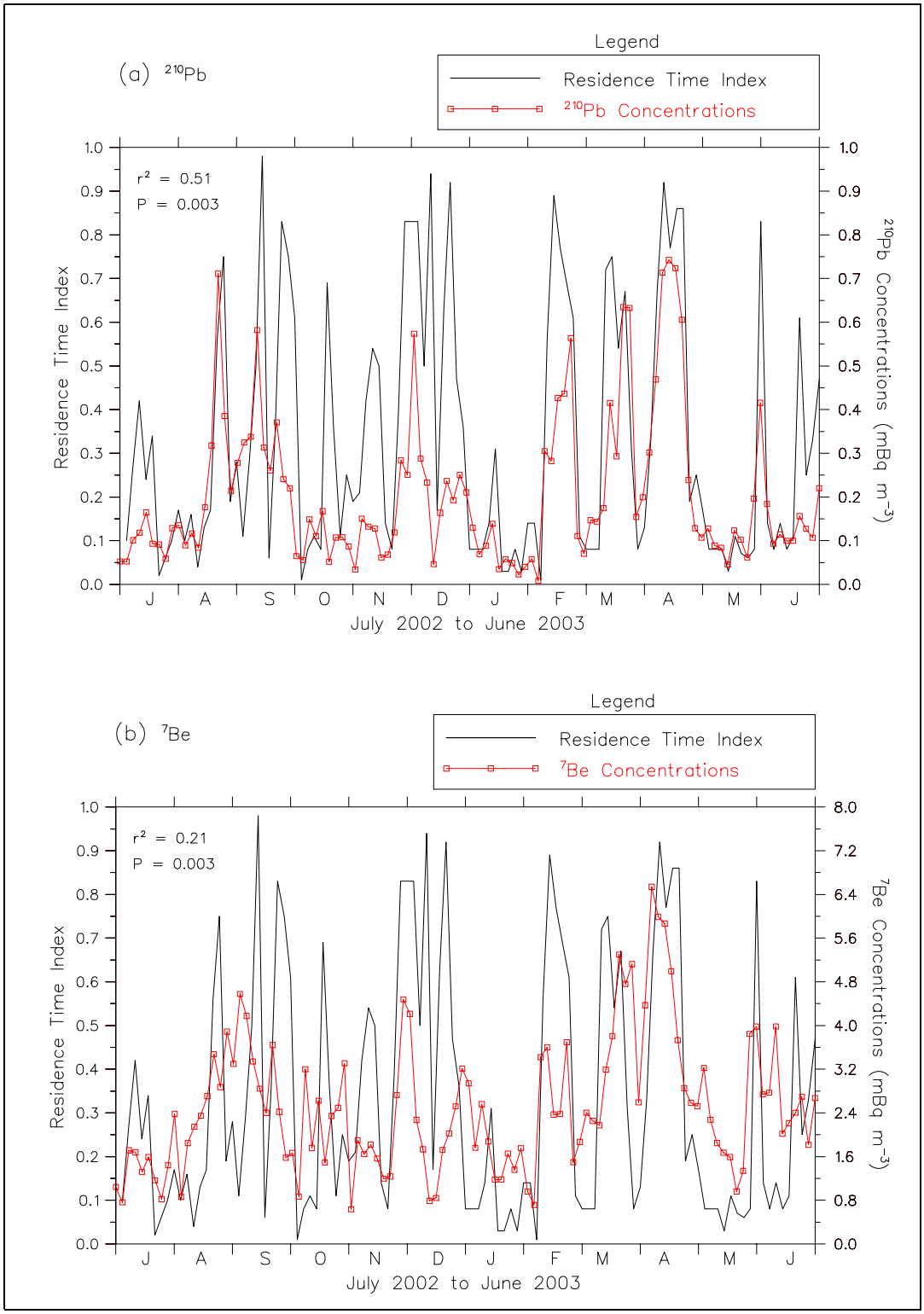

Figure 3.6: *Variations in ^{210}Pb and ^{7}Be concentrations in air with residence time index.*

This is not unexpected because ^{210}Pb is a daughter of ^{222}Rn, which predominantly emanates from the continent, as opposed to the ocean surfaces. A closer look at figure 3.6 (a) shows that there was a negative correlation in the ^{210}Pb concentrations with the residence time of air over the continent for the period of October and November. However, this may be due to the effect of washout by rain falling over that period, (data is presented are appendix A). On the other hand, the concentrations ^{7}Be in air are not expected to vary with the air-mass types due to its cosmogenic origin. However, the observed positive correlation between ^{7}Be and ^{210}Pb concentrations is due to other meteorological parameters, especially washout of air masses.

3.3.4 Seasonal Variations in ^{210}Pb and ^{7}Be Concentrations

The seasonal behaviour of both ^{210}Pb and ^{7}Be concentrations are quite similar to each other. Figures 3.7 and 3.8 show monthly variations in ^{210}Pb and ^{7}Be concentrations, respectively.

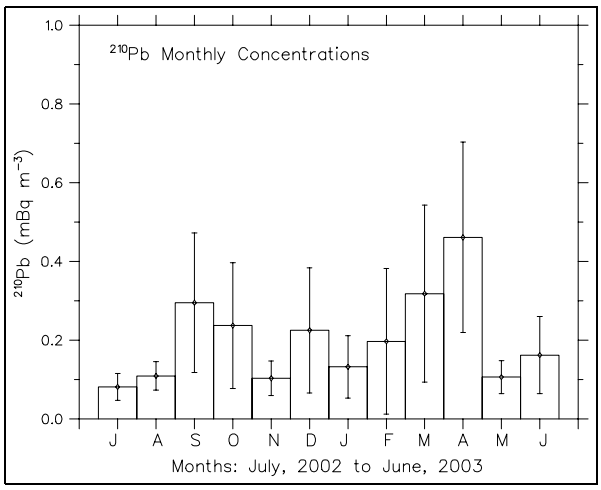

Figure 3.7: *Monthly variations in ^{210}Pb concentrations in air.*

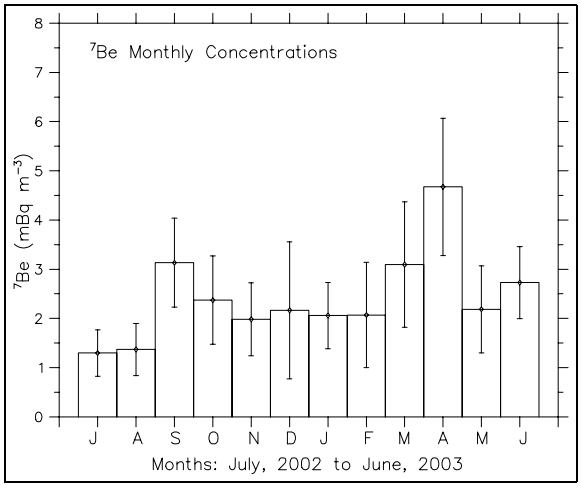

Figure 3.8: *Monthly variations in ^{7}Be concentrations in air.*

Both ^{210}Pb and ^{7}Be nuclides exhibit marked peaks in the early spring (March and April) months. The spring peak in ^{7}Be concentrations may be ascribed to: (1) increased stratosphere-troposphere exchange; (2) increased downward transport such as that associated with the convective subsidence; (3) low removal rates due to low rainfall over that period; and (4) a combination of all the three processes. Processes (1) and (2) are expected to result in anticorrelations in ^{210}Pb and ^{7}Be concentrations. Thus, the observed positive monthly correlations between the two radionuclides of different origins are most likely due to washout of air masses in the lower atmosphere as pointed out earlier.

The results presented suggest that to effectively determine the seasonal variabilities of ^{210}Pb and ^{7}Be, data should cover a period of several years, presumably 3 or more, in order to apply correlation tests which would detect whether or not there exists a relationship between the ground level concentrations of the isotopes and the long-term (climate), rather than the short-term (weather) related meteorological parameters.

3.3.5 Frequency Distributions of ^{210}Pb and ^{7}Be Concentrations

The frequency distributions in figures 3.9 and 3.10 demonstrate that the modes of ^{210}Pb and ^{7}Be concentrations in air were between 0.05-0.14 and 1.5-1.9 mBq m^{-3}, respectively.

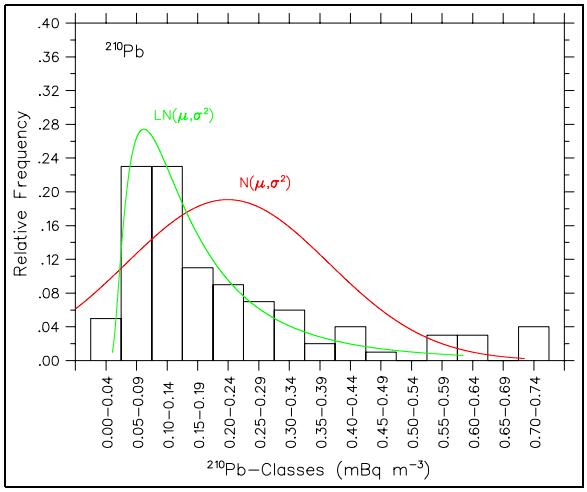

Figure 3.9: *Histogram of ^{210}Pb air concentration frequency distribution.*

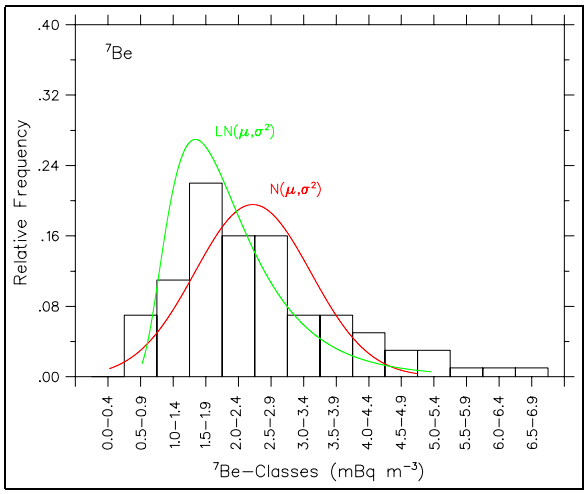

Figure 3.10: *Histogram of ^{7}Be air concentration frequency distribution.*

The class intervals for the ^{210}Pb and ^{7}Be concentrations were set to 0.05 and 0.5 mBq m^{-3}, respectively. The histograms for both ^{210}Pb and ^{7}Be concentrations appear to follow positively skewed probability distributions and further suggest a possibility of

interpreting the distributions as unimodal. The possible explanations of the unimodal distributions of the two isotope concentrations in air are given later in this section.

It can be clearly seen that both the ^{210}Pb and ^{7}Be concentrations are log-normally distributed. The histograms have been fitted with the normal N(μ, σ^2) and the log-normal LN(μ, σ^2) distribution functions, where the μ and variance σ^2 are the mean and variance of the log-transformed ^{210}Pb and ^{7}Be concentrations. The geometric means of ^{210}Pb and ^{7}Be concentrations were 0.151 and 2.212 mBq m^{-3}, respectively. The basic statistics on the ^{210}Pb and ^{7}Be concentrations in surface level air for the 108 observations recorded in this study are presented in table 3.1.

Table 3.1: *Basic statistics of ^{210}Pb and ^{7}Be concentrations in surface level air.*

	Quartiles					Mean	Variance
Isotope	Minimum	1st	Median	3rd	Maximum	(μ_1)	(σ_1^2)
^{210}Pb	0.008	0.091	0.141	0.279	0.742	0.208	0.031
^{7}Be	0.634	1.653	2.358	3.215	6.539	2.504	1.550

The mean and variance, μ_1 and σ_1^2, respectively, are in original units.

For the investigation of the modes of distribution given in figures 3.9 and 3.10, both ^{210}Pb and ^{7}Be concentration data were sorted into two distinct classes with regard to the rainfall (R). One class was associated with the rainfall, $R \leq R_m$ and the other class with $R > R_m$, where R_m represents the median of the total rainfall recorded over the sampling period. The second class ($R > R_m$) with relatively low ^{210}Pb activity concentrations (median = 0.11 mBq m^{-3}) represents the influence of wet scavenging and is centred around the observed mode of ^{210}Pb distribution (0.05-0.14 mBq m^{-3}). Similarly, the low ^{7}Be activity concentrations (median = 1.80 mBq m^{-3}) are associated with wet scavenging, and is also centred within the mode of ^{7}Be activity frequency distributions.

The mean ^{210}Pb and ^{7}Be concentrations in air over the whole period of measurements were 0.21 $\pm$ 0.17 and 2.50 $\pm$ 1.24 mBq m^{-3}, respectively. The mean ^{210}Pb and ^{7}Be concentrations compare well with the 0.23 mBq m^{-3} for coastal air measurements in Europe (52.5°N, 02.5°W) reported by Preiss and Genthon [102] and the 2.2 mBq m^{-3}, for ground-level air at Chilton (51°N), reported by Peirson [70], respectively.

3.4 Conclusions

Surface level air concentrations of ^{210}Pb and ^{7}Be were measured. The activity concentrations were correlated with the meteorological variables: rainfall and atmospheric pressure. Back trajectories were used to determine the effect of air-mass type and residence times of the air parcels over the continent or ocean on the concentrations of both isotopes. The following were the main results:

- Both ^{210}Pb and ^{7}Be concentrations decrease with increasing precipitation, indicating that the effect of washout by rainfall partly controls the surface level air concentrations of the two isotopes to a similar degree.

- Both isotopes generally exhibited relatively low values with periods of low atmospheric pressure, and relatively high values during high pressure periods. The ^{210}Pb, high concentration values obtained during periods of wintertime high pressure may be due to the stagnation of the ^{222}Rn daughters associated with lack of mixing and relatively low wind speeds associated with eposides of high pressure . However, the dominant washout processes resulted in lower concentrations of both radionuclides during summertime high pressure periods.

- Higher ^{210}Pb activities were recorded with air parcels coming from the continent than that from the oceans and/or whenever the air parcels had spent most of their times over the continent.

- The correlation in monthly variabilities between ^{210}Pb and ^{7}Be concentrations may be attributed to the strong effect of washout processes of aerosols by rainfall. The short record of ^{210}Pb and ^{7}Be measurements does not provide enough data for correlation tests to be applied in order to separate the short-term from the long-term meteorological variables.

- The distributions of both ^{210}Pb and ^{7}Be concentrations in air are log-normal, with the modes of distributions centred at lower concentration representing the influence of wet scavenging.

Chapter 4

Effects of Vegetation on ^{210}Pb, ^{137}Cs and ^{7}Be Deposition

4.1 Introduction

The deposition flux of aerosols to terrestrial surfaces are regulated, in part, by the aerodynamic roughness of the surface. It is to this effect that focuses this chapter. In addition, a proportion of the deposited aerosols are intercepted and retained by vegetation for a period of time. The capture efficiency for particles partly depends on the wind speed, leaf orientation (which may partly be determined by the wind), leaf surface structure such as stickiness and the wetness of the surface. The main factors affecting the efficiency of the mechanisms of deposition are discussed in chapter one, while the physical processes governing deposition on surfaces and the applications to deposition on vegetation are discussed elsewhere [103] [104].

The determination of the rate at which radioactivity-bearing aerosols are intercepted and retained by foliar surfaces is challenging in that, one must distinguish between soil derived and atmospherically-deposited radionuclides. Furthermore, both the morphological and physiological processes may play some role in the distribution of superficially deposited isotopes in the whole tree. However, the effects of forest vegetation on the deposition of radioactive materials have been successfully demonstrated using ^{210}Pb soil inventory measurements by Olsen [77] and by Graustein and Turekian [90]. More recently, the same technique was employed, using ^{210}Pb and ^{137}Cs, in the Highlands of Scotland, by Moghaddam [105] and by Choubedar [28], using soils from Rothamsted experimental station in Hertfordshire, England. All these authors

report a similar degree of enhancement in the deposition of radioactive material under forest canopies relative to the adjacent open grassland areas.

Another method which has been successfully employed in estimating the increase of airborne pollutants (not necessarily radionuclides) due to the presence of forest vegetation is the throughfall technique. Several authors have found an increased deposition of aerosols in canopy throughfall relative to open fields, for example: Beier *et al.* [106], Beier and Gunderson [107], Bobbink *et al.* [108] and Kolka [109].

This chapter reports the long-term average ^{210}Pb and ^{137}Cs deposition in soils at open grassland relative to woodland canopy soils. ^{210}Pb and ^{7}Be measurements in foliage, precipitation (bulk and throughfall samples) and litterfall were also measured, to investigate the influence of foliage on the pollutant inputs to catchment. Measurements were conducted at several selected sites in Edinburgh (55.6°N, 03.2°W) and the Scottish Borders. The following questions are addressed:

- Whether the presence of woodland vegetation significantly influences the long-term annual deposition flux of ^{210}Pb and ^{137}Cs in soils.
- Whether the main pathway responsible for delivering aerosols to woodland soils are through precipitation or leaf fall.

4.2 Sampling Locations and Site Description

Soil samples were collected from five different lowland locations, four of which were golf courses: (1) Centre for Ecology and Hydrology (CEH) [*referred to here as* (CE)], sampled on January, 31st 2001; grid reference number NT 245 637, (2) Bruntsfield Links golf course situated in Cramond (CR), sampled on July, 9th 2001; grid ref. no. NT 194 760, (3) Lothianburn golf course situated to the southwest of Edinburgh on the NE slopes of the Pentland Hills (PE), sampled on July, 9th 2001; grid ref. no. NT 241 668, (4) West Linton golf course (WL), sampled on July, 11th 2001; grid ref. no. NT 138 525, and (5) Prestonfield golf course (PR), sampled on February, 11th 2002; grid ref. no. NT 378 721.

Bulk precipitation and throughfall samples were collected at a Sitka spruce (*Picea Sitchensis*) forest plantation (at Deepsyke forest), in south central Scotland: 290 m asl. (NT 185 540). The trees were planted in 1986 on an acid drained basin peat in a commercial plantation and are used for various experimental studies [110] [111]. Sitka spruce foliage and litterfall were also collected at the forest plantation. Further foliage sampling was done at the Bush Estate (CEH), on three different types of deciduous tree species. Figure 4.1 gives a map of Scotland showing the position of Edinburgh location.

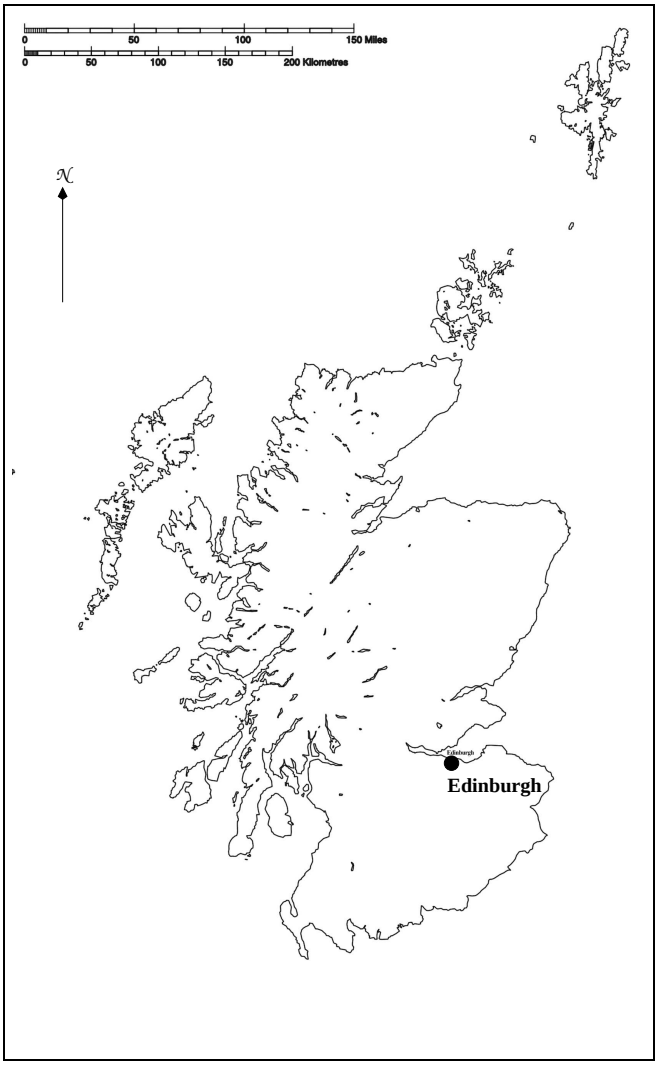

Figure 4.1: *Map of Scotland showing Edinburgh location.*

4.2.1 Soils Samples

Soils were obtained from areas of open grassland and under the woodland canopy at each site in order to investigate the effect of vegetation canopy on the deposition of atmospheric ^{210}Pb and ^{137}Cs using inventory measurements. The reasons for site selection were that: (1) the history of the sites were known, to avoid sites which may have been physically disturbed; (2) the sites were situated at relatively low altitudes, in order to eliminate the effects of topography; (3) the mean annual rainall at the sites was similar; and (4) the sites were confined to a small region to eleminate the effect of regional changes in ambient ^{210}Pb concentrations.

4.2.1.1 Centre for Ecology and Hydrology Edinburgh site

Six samples were taken under an approximately 5 m tall, ∼50 year old single oak (*Quercus robur*) tree. Samples were taken at 1, 2 and 3 m from tree trunk, making an east-west transect on both sides of tree canopy. Three more samples were taken approximately 80 m east of the tree on an open grassland area. Samples were obtained using a (small) 5.2 cm diameter corer, therefore two samples were taken from each sampling point[1], subdivided into four equivalent depth intervals of 5 cm and were then bulked to form one sample. The bulking procedure was meant to ensure that enough material was collected for analysis.

4.2.1.2 Bruntsfield Links (Cramond) Site

A total of 9 samples (four from the open grassland area and five under the woodland canopy) were taken from the Bruntsfield Links golf course, situated about 6 kilometres from the Edinburgh city centre, off the A90 Queensferry road. The golf course is 102 years old and was built on Branton (housing) Estate. The layout of the course (according to the information gathered from the green keepers) has changed three times since, the last having occurred in the 1970s. Within the golf course, samples were taken under a small patch of woodland canopy, consisting of approximately 6 m tall sycamore trees (*Acer pseudoplatanus*), alder (*Alnus glutinosa*) and ∼10 cm tall

[1] A position within a site at which a single or bulked core is extruded.

grass. The canopy size was about 15 m in diameter. Samples from the open grassland 'the rough' area were obtained approximately 20 m away from the woodland area. The soil from the rough was extremely dense to sample, making it difficult for the corer to go through. Samples were obtained using a 5.2 cm dia. corer and bulked according to 0-5 cm, 5-10 cm and 10-20 cm depth intervals. Figure 4.2 shows both open and woodland canopy site at Cramond.

Figure 4.2: *Cramond site, showing sampled areas. CRW and CRO are woodland and open grassland areas, respectively.* (The picture was taken at 340° with respect to the North).

4.2.1.3 Lothianburn (Pentlands) Golf Course Site

Samples were collected from Lothianburn golf course, situated to the southwest of the city of Edinburgh on the slopes of the Pentland Hills. The final layout of the golf course was completed in 1929. Five samples were collected from a closed 'T-shaped' woodland canopy of beech (*Fagus sylvatica*) and sycamore woodland (approx. 15 m tall) with some undergrowth cover of grass. The soil was composed mainly of reddish brown mineral matter, with a top cover (∼1 cm) of decaying litter. The grassland area consisted of dry moorland and mosses, and lay on a very gentle slope. Four samples were collected from this area. In each case, samples were obtained using a 5.2 cm

dia. corer and bulked according to 0-5 cm, 5-10 cm and 10-20 cm depth intervals. Figure 4.3 shows the Pentland golf course sampling site.

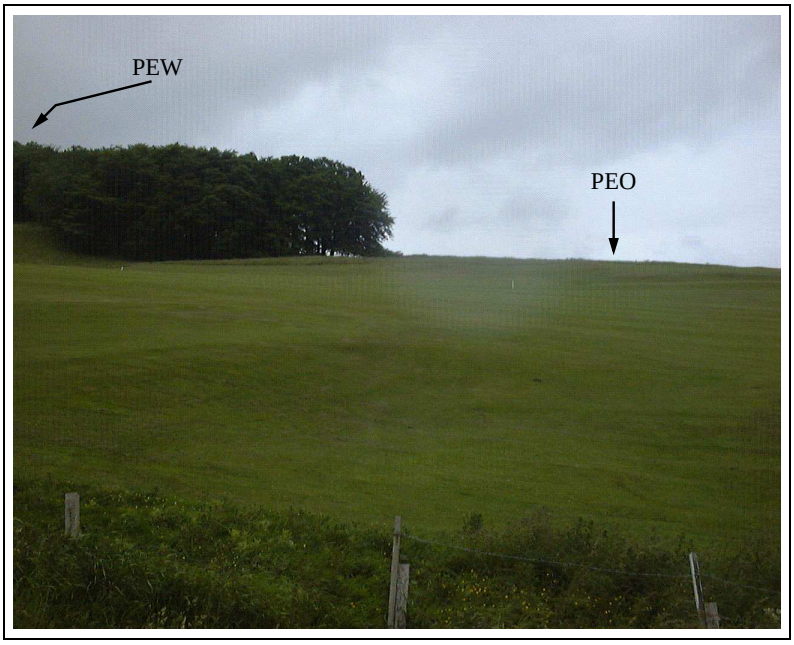

Figure 4.3: *The Pentland hill-end, showing sampled areas. PEW and PEO are woodland and open grassland areas, respectively.* (The picture was taken at 290° with respect to the North).

4.2.1.4 West Linton Golf Course Site

The West Linton golf course if situated approximately 24 kilometres southwest of the Edinburgh city centre, off the A702. Five samples were obtained from a narrow strip of deciduous woodland between the access road and the golf course premises. The woodland was mainly of sycamore and lime (*Tilia cordata*), approximately 15 m tall, and some undergrowth of grass and ferns. The soil was dark brown, organic rich and relatively soft to sample. Samples were taken on an approximately 15×15 m area inside the woodland. Four samples were taken from a wet moorland with some sphagnum, and bilberry on an open area about 60 m from the woodland. The first 5 cm of the cores taken from this area were composed mostly of grass, decomposing sphagnum and some roots. Samples were obtained using a 5.2 cm dia. corer and bulked according to 0-5 cm, 5-10 cm and 10-20 cm depth intervals. Figure 4.4 shows the West Linton site.

Figure 4.4: *West Linton site, showing sampled areas. WLW and WLO are woodland and open grassland areas, respectively.* (The picture, showing 'WLO' was taken at 10° with respect to the North).

4.2.1.5 Prestonfield Golf Course Site

The golf course is situated about 3 kilometres southeast of the Edinburgh city centre, off the A68 Dalkeith Road. There was little canopy-forming woodland at this site. Four samples were obtained under a single (about 4 m tall) sycamore tree and another set of four samples was taken about 10 m away from the tree. Samples were obtained using a 10 cm diameter corer, therefore no bulking was necessary. Each sample was subdivided into four-5 cm thick subsamples. Detailed information about the sampling sites at Edinburgh location is presented in table 4.1.

Table 4.1: *Details of sampling sites at Edinburgh. All samples were taken to a depth of 20 cm (unless otherwise stated) using corers.*

Site	Grid No. (NT)	Elevation (m) asl.	Rainfall (mm/y)	Notes
CE	245 637	180	900	9 samples, single tree canopy, bulked.
CR	194 760	50	700	9 samples, bulked.
PE	241 668	230	850	9 samples, bulked.
WL	138 525	260	1000	9 samples, bulked.
PR	378 721	40	700	10 samples, single tree canopy, not bulked.
Total number of samples obtained = 46				

4.2.2 Bulk Precipitation and Foliage Samples

Bulk precipitation and the throughfall technique were employed on a forest plantation. ^{210}Pb and ^{7}Be concentrations in the collected precipitation and on the age-graded Sitka needles were measured. Leaf samples were also collected from three different types of deciduous vegetation for ^{210}Pb and ^{7}Be activity measurements.

4.2.2.1 Deepsyke Site

Bulk precipitation and throughfall samples were simultaneously collected from 18th of May, 2001 through to 10th May, 2002. The total rainfall for the collection period at this site was 1184 mm. Bulk precipitation was collected in three funnels (each, 0.20 m in diameter) mounted about 1.5 m above ground level and exposed continuously to obtain both wet and dry deposition. The funnels were located within the plantation in an open field, to minimise the aerodynamic error caused by the funnel influencing the air flow. The funnels were placed about 10 m apart and average values of the amount of precipitation collected were calculated to take into account the spatial variability in precipitation at site. Throughfall was collected by means of a system of open gutters, 0.3 m above the ground running under the trees. Four sites, each covering an area of 1 m^2, were selected for this experiment. This strategy relies on the assumption that the spatial variations are randomly distributed, and that the increased number of a system of gutters will sample this variability [34]. In total, 14 rain and throughfall collections were made during the sampling period. Emptying and redeployment of both rain and throughfall collectors was done at irregular time intervals, depending on the amount of rainfall accumulated. Litter that has accumulated in the gutters for the sampling period was also collected in August 2001 and again in May 2002.

Both bulk precipitation and throughfall samples were transferred into separate beakers for treatment using methods described by Clifton [91] and Choubedar [28] as follows: about 30 cm^3 of lead nitrate [$Pb(NO_3)_2$] and aluminium nitrate [$Al(NO_3)_3$] (both at concentrations of 1000 mg/l) were added to the samples to precipitate the ^{210}Pb. The pHs of the whole samples were then adjusted to pH 11 using 0.88 specific gravity ammonia solution. The pHs of the solutions were determined by an Amphel

gel-fitted pH electrode meter, which was calibrated using three pH buffers, at pH 4.0, 7.0 and 9.0 before each measurement. Samples were then left for a minimum of 7 days for ^{210}Pb and ^{7}Be aerosols to precipitate. The resulting precipitates were filtered on 15 cm diameter Whatman Fibre Glass filter papers (type GF/C). The filters were left to dry at room temperature before being pressed into pellets and sealed into polythene holders for ^{210}Pb and ^{7}Be counting. Whatman glass micro-fibre (GF/C) type filters are widely used as standard for the determination of suspended particles in water. The filter papers retain 98% of about 1 micron of particle size in aqueous suspension [112].

Four sets of Sitka spruce leaf needles, well exposed to the atmosphere were collected using a cutting pole in July 2001 and again in July 2002 (when the current year shoots had fully emerged). The needles were separated according to age of growth as follows: the current year's growth (cr.) aged about 3 months; the previous year's needles (1 yr.) aged about 15 months; the 2-year needles (2 yr.) aged about 27 months and the 3-year needles (3 yr.) aged about 39 months. The needles were oven dried at 80°C for three days before being crushed through a 0.5 mm mesh sieve. The needle powders were then sealed into 103 cm^3 polythene containers and their weights recorded to determine the specific activities of the radioactive isotopes measured.

4.2.2.2 The CEH Edinburgh site

Three deciduous tree species: oak (*Quercus robur*), lime (*Tilia platyphyllos*) and sycamore (*Acer pseudoplatanus*) were selected for this experiment. The tree ages were in the range 30-50 years and their heights ranged from about 5 to 10 metres. The trees were isolated from each other and other tree colonies (about 20 m to 80 m apart). The choice for a single site was important in that the trees were all subjected to the same atmospheric conditions at the site. Leaf harvesting commenced in June 2002 when the shoots had fully emerged, and this continued at about a 30-day interval until November when the leaves had started to shed. In each case, shoots were taken from around the whole tree with the help of a cutting pole. A known number of leaves collected from each tree species was weighed immediately after harvesting. Leaves were oven dried at 80°C for about three days before being re-weighed to determine

the dry weights and were then ground through a 0.5 mm mesh sieve and sealed into 103 cm^3 polythene containers before being presented to a HPGe detector for γ-analysis. Twenty sets of leaf samples for the July through to September sampling periods were selected at random from each species to determine the area to dry weight ratios *i.e.*, specific leaf area (SLA) in $m^2\ kg^{-1}$. Leaf areas were determined by photocopying fresh leaves and multiplying their weights by corresponding area/weight ratios determined from photocopies to give single leaf surface areas. The areas were then divided by the dry weights of the leaves and an average value was determined to represent the SLA of the leaves for each tree species. Weights were determined by means of sensitive electronic balances at CEH laboratories. Sub-sample weights in polythene containers were also determined for reasons discussed earlier in section 4.2.2.1.

4.2.3 Sample Collection and Analytical Methods

The procedures for the selection of sampling sites was based on lack of evidence indicating that physical disturbance of soils had not occured for at least 100 years (approximately 5 ^{210}Pb half-lives). Areas with obvious signs of animal burrowing, recent ploughing, steep slopes and possibilities of flooding were avoided. In order to compensate for small cross-sectional areas given by corers relative to the total area of each selected site sampled, several core samples were obtained. This also provided an indication of intra-site variability for the inventories of each radionuclide at each site.

Extruded soil cores were sectioned (on site with a sharp knife) into sub-samples according to 0-5, 5-10, 10-20 cm (in some cases 10-15 and 15-20 cm) depth intervals and were then labelled *a, b, c* and *d* respectively. Where necessary, the equivalent depth intervals from each of the two cores were bulked to form one sub-sample. From most sites, a depth of at least 20 cm was maintained. It has been established that most of the atmospherically-derived ^{210}Pb in undisturbed soils is trapped and retained with a residence time of thousands of years in the organic-rich top soil and very little or no excess ^{210}Pb has been detected beyond this depth [50] [52] [53] [56] [63] [113] [114].

Prior to γ-ray analysis, all samples were processed using large ovens and mills at the CEH Edinburgh and Scottish Agricultural College soils laboratory, University

of Edinburgh. Samples were weighed, air-dried at 30°C for 2-3 days and re-weighed to obtain the dry weights. Any rock material greater than 2 mm were excluded on the assumption that they are closed systems that do not contain any atmospherically derived ^{137}Cs and in which ^{226}Ra and ^{210}Pb are in radioactive equilibrium. Thus, they would only serve to dilute the counted samples [63]. The remaining samples were homogenised using a crusher and hermetically sealed in a 103 cm^3 polythene containers and kept for at least 14 days prior to assay, in order for equilibrium between ^{226}Ra and its daughter ^{222}Rn to be achieved.

Samples were presented to the HPGe detector (Det01, as described in chapter 2) coupled to a multichannel analyser. The activities of ^{210}Pb and ^{137}Cs were determined by their γ emissions at 46.5 and 661.7 keV, respectively. The ^{226}Ra activity was determined from the ^{214}Pb γ emission at 351.9 keV. Typical counting times were 24 hours per sample, though some samples, particularly at depths beyond 10 cm, were counted longer (∼36 hours) to give improved statistics on the measured count rates. Figure 4.5 shows γ-ray spectra of soil sample and background counts obtained from the HPGe detector.

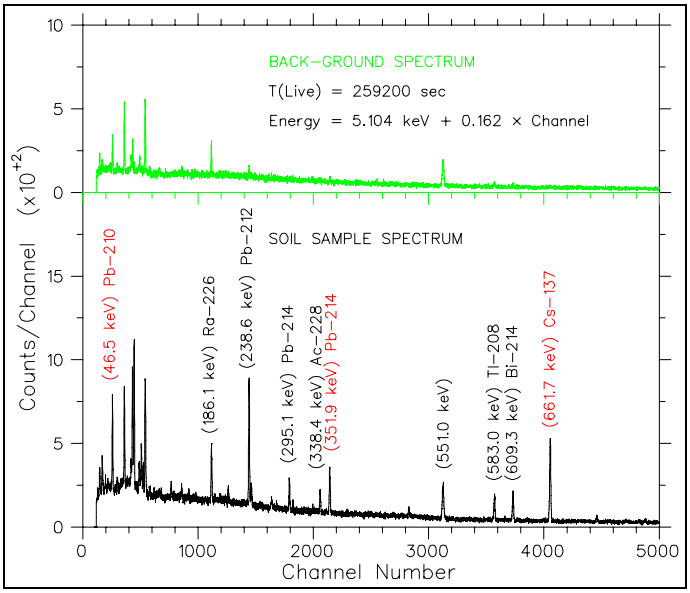

Figure 4.5: *Gamma-ray spectra of background (green) and soil sample (black). The background spectrum was obtained from counting an empty standard sample container. The sample was collected from Prestonfield golf course, sample PRW01a representing a 0-5 cm depth interval. Counting times for both spectra were 36 hrs. Photopeaks labelled in red are of importance in this study.*

The activities in each sub-sample were obtained by applying equation 2.7. Self-absorption correction factors, $f(c)$, were determined by applying a technique outline by Cutshall *et al.* [95] as follows: photopeak areas of ^{210}Pb, ^{133}Ba (at 356.0 keV-line to take the place of the ^{214}Pb at 351.9 keV) and ^{137}Cs were determined by counting sealed sources placed on standard sample holders, with and then without samples. The attenuated count rates $(C_\gamma)_E$ and the unattenuated count rates $(C_{0,\gamma})_E$ were noted, and self absorption correction factors were determined from the following equation:

$$f(c) = \frac{(A_N)_z}{O} = \frac{ln(C_\gamma/C_{0,\gamma})_E}{(C_\gamma/C_{0,\gamma})_E - 1} \tag{4.1}$$

where O is the attenuated sample output and $(A_N)_z$ is the activity of the isotope for depth z. The mass of the measured material in the holder varied between 20 g and 120 g (*i.e.*, a density variation of a factor of about 6) depending on whether the sample was mainly composed of vegetation or mineral matter. Figure 4.6 gives the correction factors, $f(c)$ as functions of the densities of some of the samples analysed.

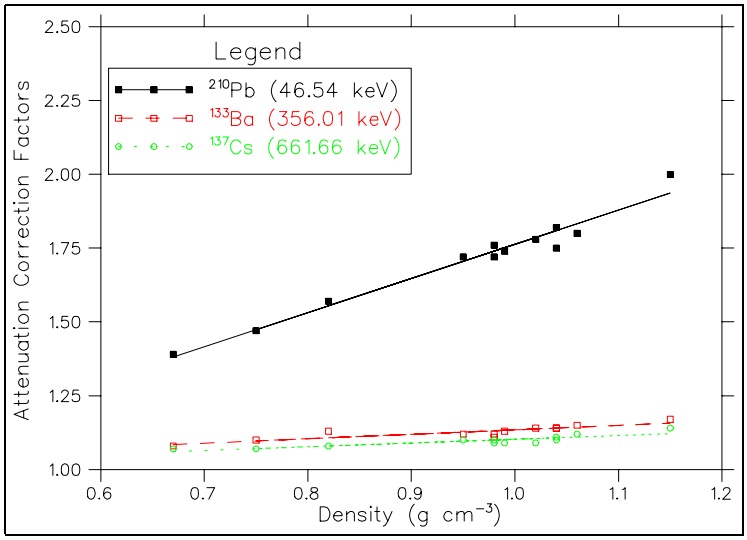

Figure 4.6: *Attenuation correction factors $f(c)$ versus sample density for some of the soil samples obtained from Prestonfield golf course.*

The values of $f(c)$ for ^{210}Pb (E_γ = 46.54 keV) varied greatly with density whereas those for ^{133}Ba (E_γ = 356.01 keV) and ^{137}Cs (E_γ = 661.66 keV) were almost constant.

The specific activity (Bq kg^{-1}) of the counted sample was obtained by dividing the activity obtained from equation 2.7 by the mass of the counted sample. The atmospherically derived (or unsupported) ^{210}Pb component was distinguished from the ^{210}Pb due to *in situ* decay of ^{226}Ra (termed, the supported ^{210}Pb). The supported fraction was estimated from measuring the 351.9 keV γ line of ^{214}Pb under an assumption that the two (supported ^{210}Pb and ^{214}Pb) are in equilibrium. The fallout component was then obtained by subtracting the supported component from the total measured ^{210}Pb specific activity. The supported ^{210}Pb from the *in situ* decay of ^{226}Ra could not be measured directly from the 186.1 keV γ-ray it produces because of its proximity to the 185.7 keV γ-ray due to ^{235}U.

The ratio of the mass of the material sampled from the field (*i.e.*, each sub-sample) to the surface area of the sample (kg m^{-2}) was then multiplied by the specific activity of the sample to obtain the inventory, I (in Bq m^{-2}) in the field. This is the best way of expressing the atmospheric deposition results, as long as the total inventory has been collected, in that it is independent of soil density, which varies from place to place and/or within sites. Inventories of sub-samples in each core were integrated to give a total inventory of the excess ^{210}Pb and ^{137}Cs. Since more than one core was taken from each site, an average value was calculated to estimate the radionuclide inventories at site. To determine the atmospheric ^{210}Pb flux (Φ), the following equation was used:

$$\Phi = \lambda(^{210}Pb) \times I \tag{4.2}$$

where the flux Φ is in Bq m^{-2} y^{-1} and λ is the ^{210}Pb decay constant (0.0311 y^{-1}). Equation 4.2 was used based on the assumption than the soils have not been disturbed for at least 100 years and that the ^{210}Pb inventory is in a steady state, with the decay rate of ^{210}Pb atoms equalling the mean deposition rate [89] [93] [63] [114]. Like ^{210}Pb, ^{137}Cs is carried as sub-micron aerosols and gets delivered to the surface of the earth through wet and dry deposition processes. However, equation 4.2 does not hold for ^{137}Cs inventories in soils since they are not in steady state due to ^{137}Cs activity in air varying with time.

4.2.4 Quality Control and Uncertainty Measurement

Most of the soil samples were obtained by use of a corer. This has an advantage over the use of a spade (*eg.*, at Ynys Hir site, see chapter 5) in that the cross-sectional area sampled is precisely fixed. Great care was taken to make sure that each sub-sample was assigned to the correct depth. This was achieved by means of a ruler and sections were obtained using a sharp knife. The only problems encountered when using a corer were: (1) compaction of the soil during excavation and (2) mixing of the top layer of soil with that at the bottom of the samples on the outermost surfaces of the soil cores as the corer makes its way down into the ground. Although the latter would introduce slightly higher concentration values (specific activities) to the deeper subsections, it was not a problem since the inventories reported reflect an integrated value of all subsections of each soil sample. However, the outer rim ($\sim$2 mm) of each soil core was trimmed to minimise contamination between layers. Other sources of uncertainties were those associated with the counting systems during γ-ray analysis.

The uncertainty in the activity of a specific nuclide counted, $\Delta(A_N)_z$, is a combination of the uncertainties in the number of counts in the full energy peak, the counting time, t, the full energy peak efficiency, ϵ_γ, the probability per decay of the transition, P_γ, and the correction factor introduced to compensate for self-absorption, $f(c)$ (most important for ^{210}Pb). Although contributions of the uncertainties due to t and P_γ are insignificant compared to the uncertainties in ϵ_γ and $f(c)$, the counting period was optimised to accommodate the operating conditions of the detector system so as to minimise the statistical counting errors. For example, all samples were counted for approximately 24 hours, and in each case, and average counting error of 3%, 5% and <10% was obtained for soil sample intervals of a, b and c (and d, where applicable) respectively. In this study, the uncertainties quoted when presenting the specific activity and inventory results in each counted sub-sample were derived from the counting errors obtained from the γ-ray spectrometer system. Uncertainties in average inventories for each site, were obtained from the standard deviation of the reported inventories from each sample core at the site. At all sites sampled in this work, multiple soil cores were taken to measure the intra-site variability, achieved by means

of measuring the Coefficient of Variation[2], (CoV). The inventories reported here may be underestimated by a factor of about 10% due to soil loss during the sieving process.

4.3 Results and Discussion

The specific activities of ^{210}Pb and ^{137}Cs (in Bq kg^{-1}) and inventories (in Bq m^{-2}) in soils are presented in this section. The ^{210}Pb data presented here are atmospherically derived *i.e.*, unsupported, or the excess Lead-210 ($^{210}Pb_{exs}$), determined by subtracting the ^{214}Pb activity (or the supported Lead-210, $^{210}Pb_{sup}$) from the total Lead-210 ($^{210}Pb_{tot}$). Data are tabulated in appendix B. For each sampled site, the ^{210}Pb and ^{137}Cs specific activities results are plotted against soil depth intervals indicated by *a*, *b*, *c* (and *d*, where applicable) as described in section 4.2.3. Each sampled point (or bulked sample) is indicated by a core number, preceded by letters unique to each site, for example: the first two cores sampled from the CEH Edinburgh site are labelled as CEO01 and CEO02 for open grassland, and CEW01 and CEW02 for woodland canopy respectively.

Inventories in each individual core are given together with the average inventories calculated for both open grassland and woodland canopy soils. To compare the differences in the ^{210}Pb and ^{137}Cs soil inventories at open grassland relative to woodland canopies within sites, an unpaired student *t*-test for independent samples was used to determine whether the two sets of samples were drawn from populations with different means.

4.3.1 Variation in ^{210}Pb and ^{137}Cs Activities with Soil Depth

Figures 4.7 to 4.11 present ^{210}Pb and ^{137}Cs distributions in soils as functions of soil depth. The shapes of the profiles for both radionuclide activities have one distinct common feature: higher concentrations at the topmost 0-5 cm of the soil, decreasing with increasing depth suggesting that both unsupported ^{210}Pb and ^{137}Cs activities redistribute in the soil profile after deposition. This feature was however less pro-

[2]The coefficient of variation is a measure of relative dispersion and is given by: 100×(Standard Deviation)/(mean value of set).

nounced in soils obtained from Cramond and Prestonfield golf courses, figures 4.8 (a) & (c) and 4.11 (a) & (b), respectively. At Cramond, the ^{210}Pb activities for core identities CRO (01 & 03) and CRW01 obtained from the open grassland and under the woodland canopy areas, respectively, showed a decrease in concentrations down to a depth of 5-10 cm and a slight increase at 10-20 cm. Furthermore, CRW05 shows a subsurface maxima in ^{210}Pb concentration a depth of 5-10 cm. Although experimental errors could not be ruled out for these anomalies, such features in the ^{210}Pb distribution with soil depth are attributed to some form of physical disturbance at site, possibly when the layout of the golf course was being changed (see section 4.2.1.2). Similarly, core number PRO01 in figure 4.11 also shows subsurface maxima in radionuclide concentrations in soil profile, however, it is difficult to relate this to any form of soil disturbance at this site since the history of Prestonfield golf course was unknown. Subsurface maxima in ^{210}Pb concentrations associated with cores sampled from cultivated soils have been observed for soils receiving continuous fallout at Devon, UK by He and Walling [115].

The following hypothesis explains the excess ^{210}Pb depth profiles in soils, particularly under woodland canopies: the atmospheric ^{210}Pb is efficiently retained ($\sim$90%) by organic-rich topmost layer of the soil [94]. During subsequent years, the fresh organic matter covers previous years depositions, isolating ^{210}Pb specific activities from the atmosphere. Thus, exponential decrease in ^{210}Pb specific activities with increase in depth in most undisturbed soils are due a radioactive decay process. Although microbial processes may play a role in reducing the annual thickness of organic matter of each layer with time, the actual sedimentation processes remains unaffected. This process has been investigated by Dörr and Münnich who confirmed that the downward movement of ^{210}Pb in soils is due to sedimentation of soil organic material [116].

The ^{137}Cs activity distribution with soil depths also follows the same trend as that for ^{210}Pb. Independent investigations involving vertical migrations of both atmospherically derived ^{210}Pb and ^{137}Cs have been made, and ^{137}Cs was reported to show a maximum concentrations in soils at a few centimetres below the ground surface by Dörr and Münnich [116], and by He and Walling [115]. In general, the con-

sensus is such that ^{137}Cs has a higher mobility in more peaty soils than in mineral soils [117] [118]. However, such conclusions can not be drawn based on the results reported here since soil geology were not taken into consideration, for the purpose of this study. Furthermore, one must take into consideration the fact that the ^{137}Cs input is not constant with time (*i.e.*, must separate the bomb and Chernobyl components of ^{137}Cs) and the history of the past climatological conditions at the time of release and subsequent deposition on soils.

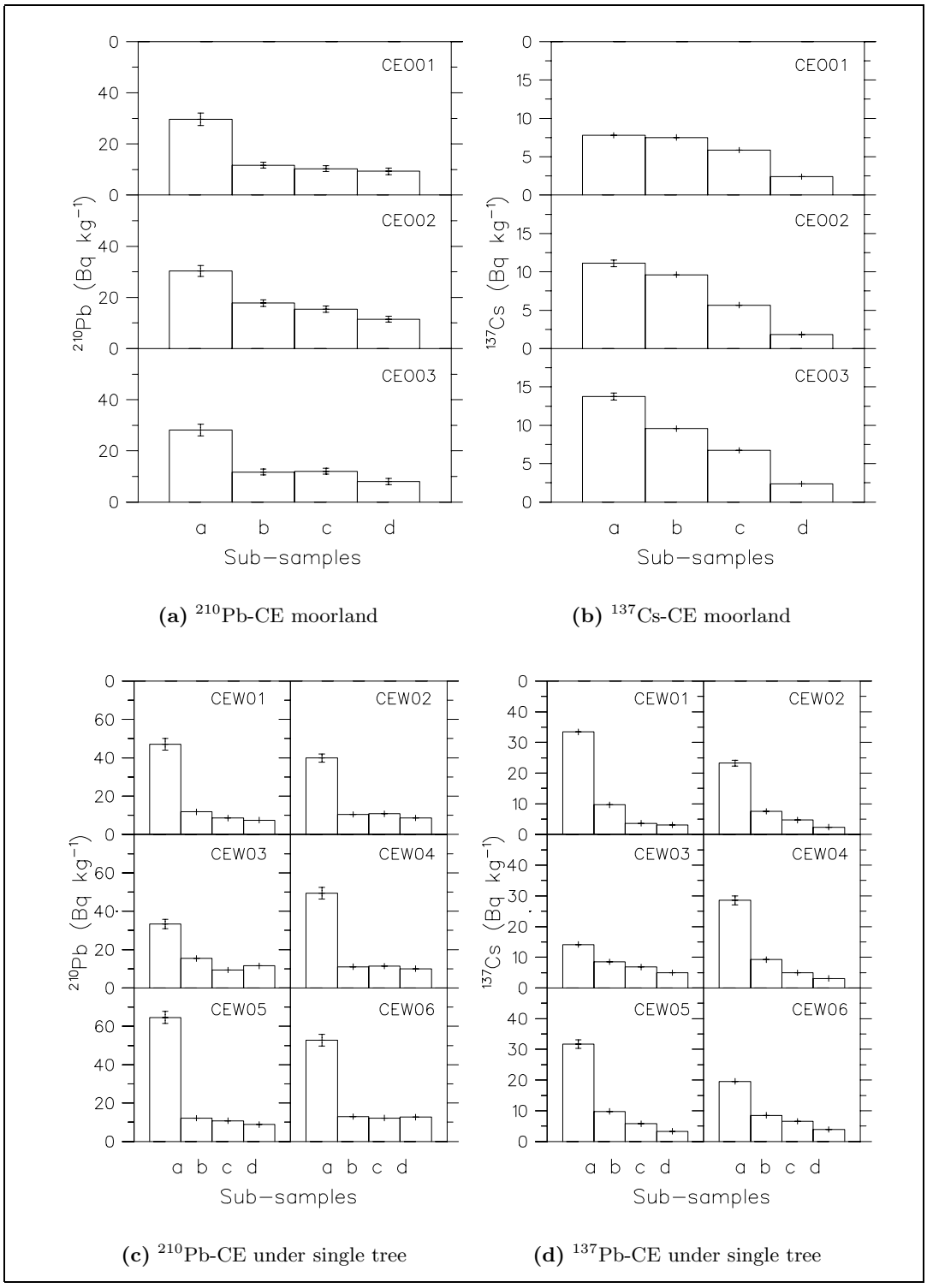

(a) ^{210}Pb-CE moorland

(b) ^{137}Cs-CE moorland

(c) ^{210}Pb-CE under single tree

(d) ^{137}Pb-CE under single tree

Figure 4.7: *Distribution of ^{210}Pb and ^{137}Cs specific activities with soil depth at CEH Edinburgh site: (a) and (b) show the ^{210}Pb and ^{137}Cs activities in the open grassland soil, respectively: (c) and (d) show ^{210}Pb and ^{137}Cs activities in soil under the oak tree, respecticely.*

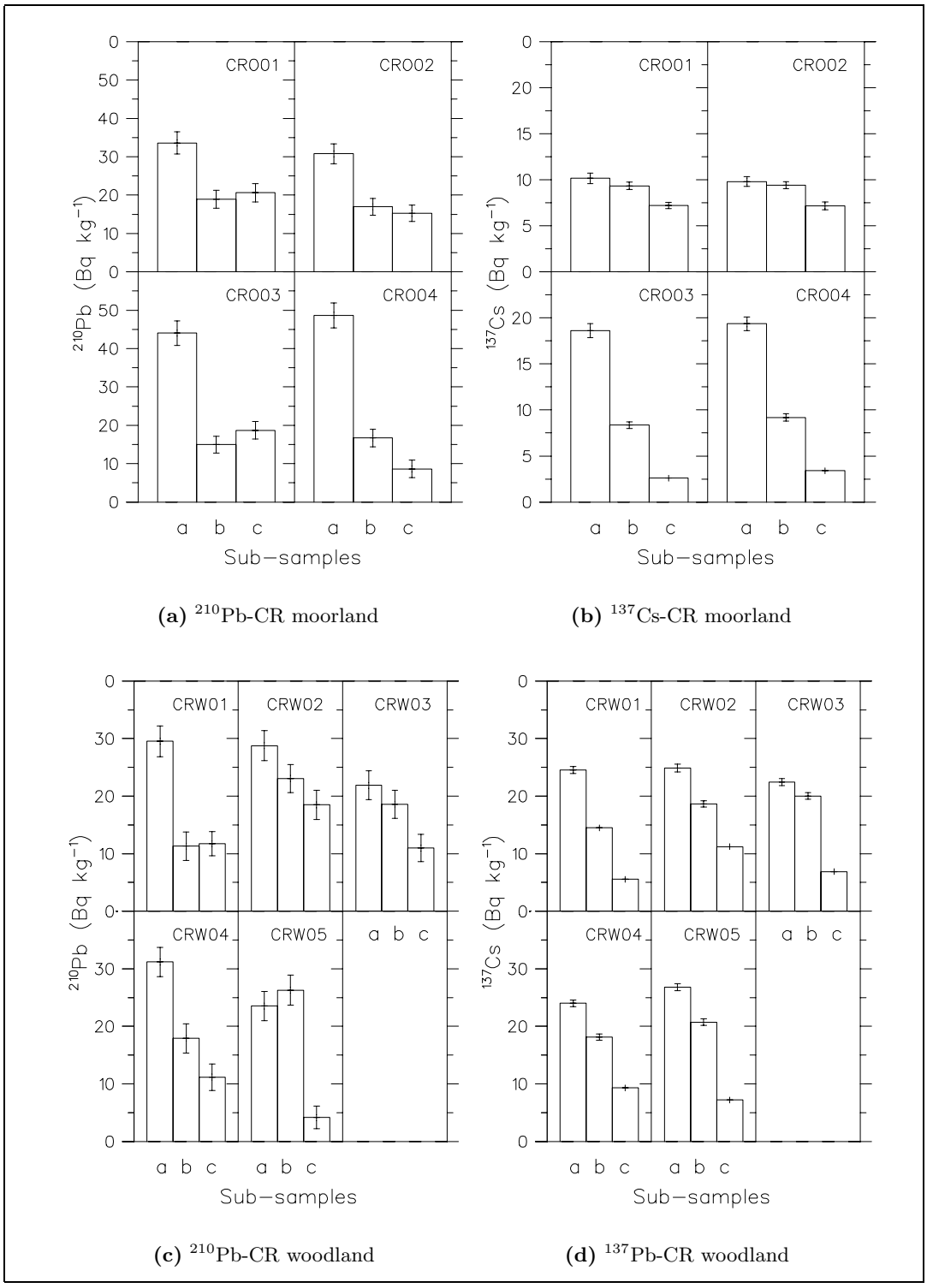

(a) ^{210}Pb-CR moorland **(b)** ^{137}Cs-CR moorland

(c) ^{210}Pb-CR woodland **(d)** ^{137}Pb-CR woodland

Figure 4.8: *Distribution of ^{210}Pb and ^{137}Cs specific activities with soil depth at the Cramond site: (a) and (b) show the ^{210}Pb and ^{137}Cs activities in the open grassland soil, respectively: (c) and (d) show ^{210}Pb and ^{137}Cs activities in soil under the woodland canopy, respecticely.*

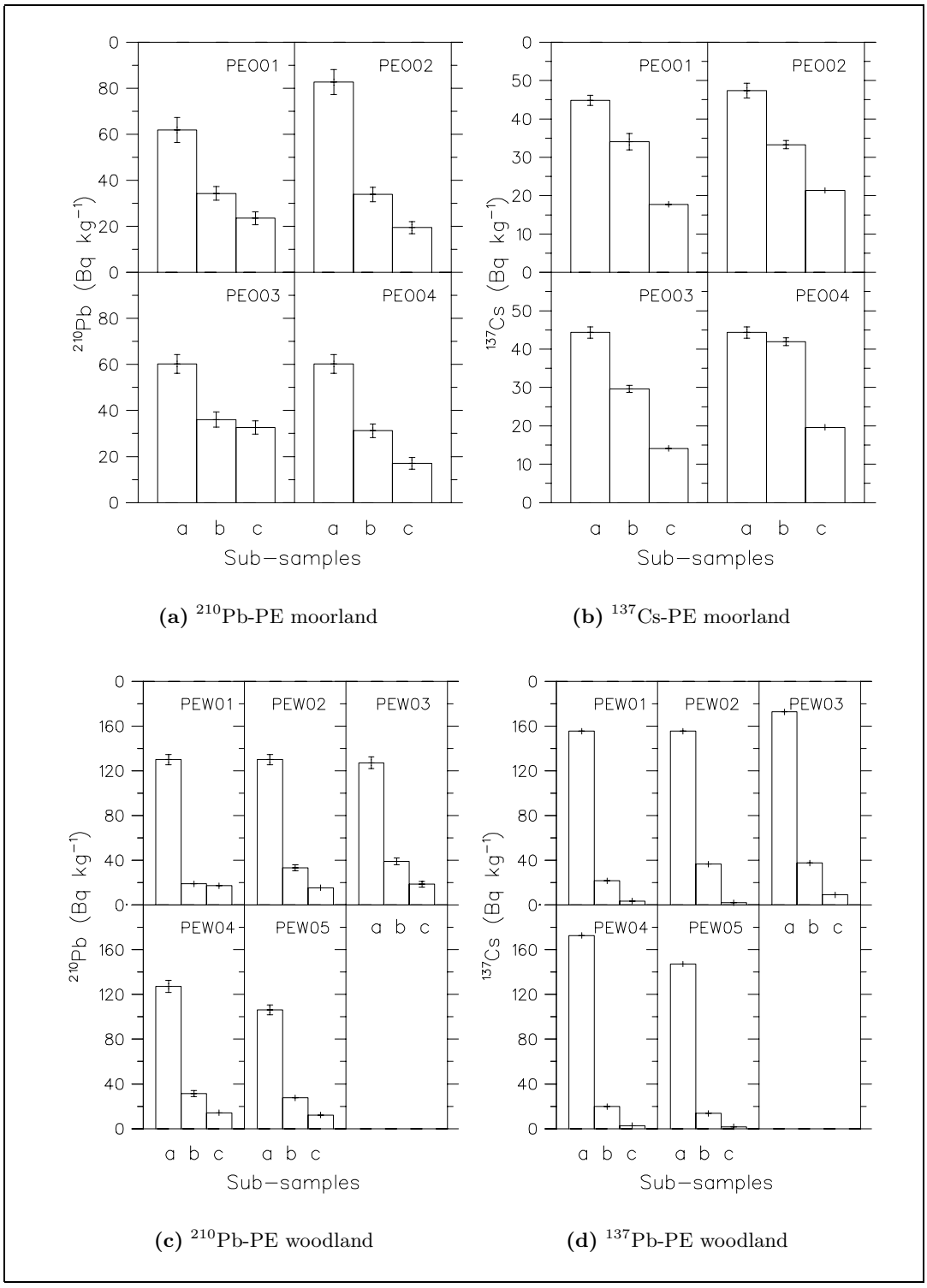

(a) ^{210}Pb-PE moorland

(b) ^{137}Cs-PE moorland

(c) ^{210}Pb-PE woodland

(d) ^{137}Pb-PE woodland

Figure 4.9: *Distribution of ^{210}Pb and ^{137}Cs specific activities with soil depth at the Pentland site: (a) and (b) show the ^{210}Pb and ^{137}Cs activities in the open grassland soil, respectively: (c) and (d) show ^{210}Pb and ^{137}Cs activities in soil under the woodland canopy, respecticely.*

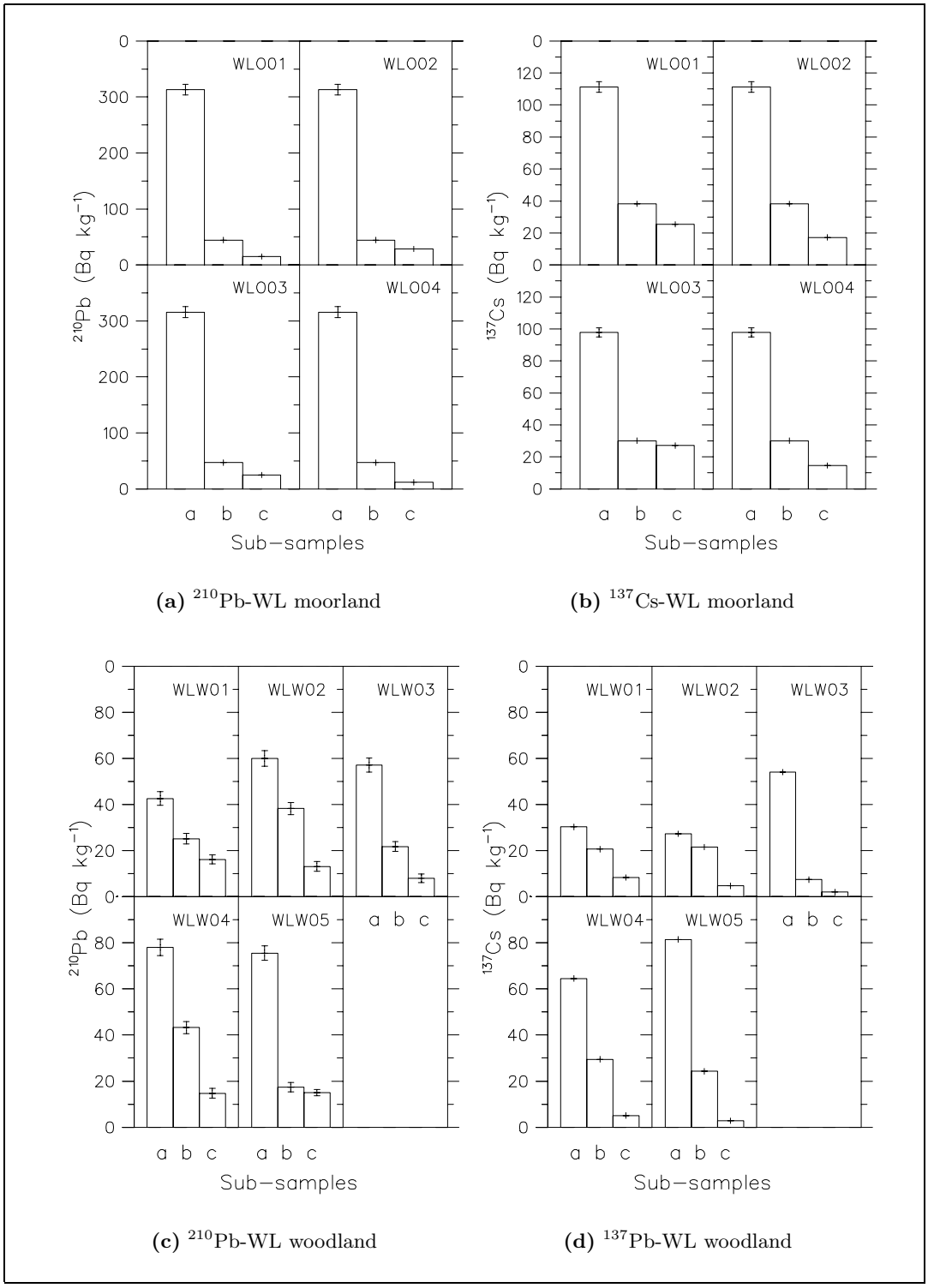

(a) ^{210}Pb-WL moorland

(b) ^{137}Cs-WL moorland

(c) ^{210}Pb-WL woodland

(d) ^{137}Pb-WL woodland

Figure 4.10: *Distribution of ^{210}Pb and ^{137}Cs specific activities with soil depth at the West Linton site: (a) and (b) show the ^{210}Pb and ^{137}Cs activities in the open grassland soil, respectively: (c) and (d) show ^{210}Pb and ^{137}Cs activities in soil under the woodland canopy, respecticely.*

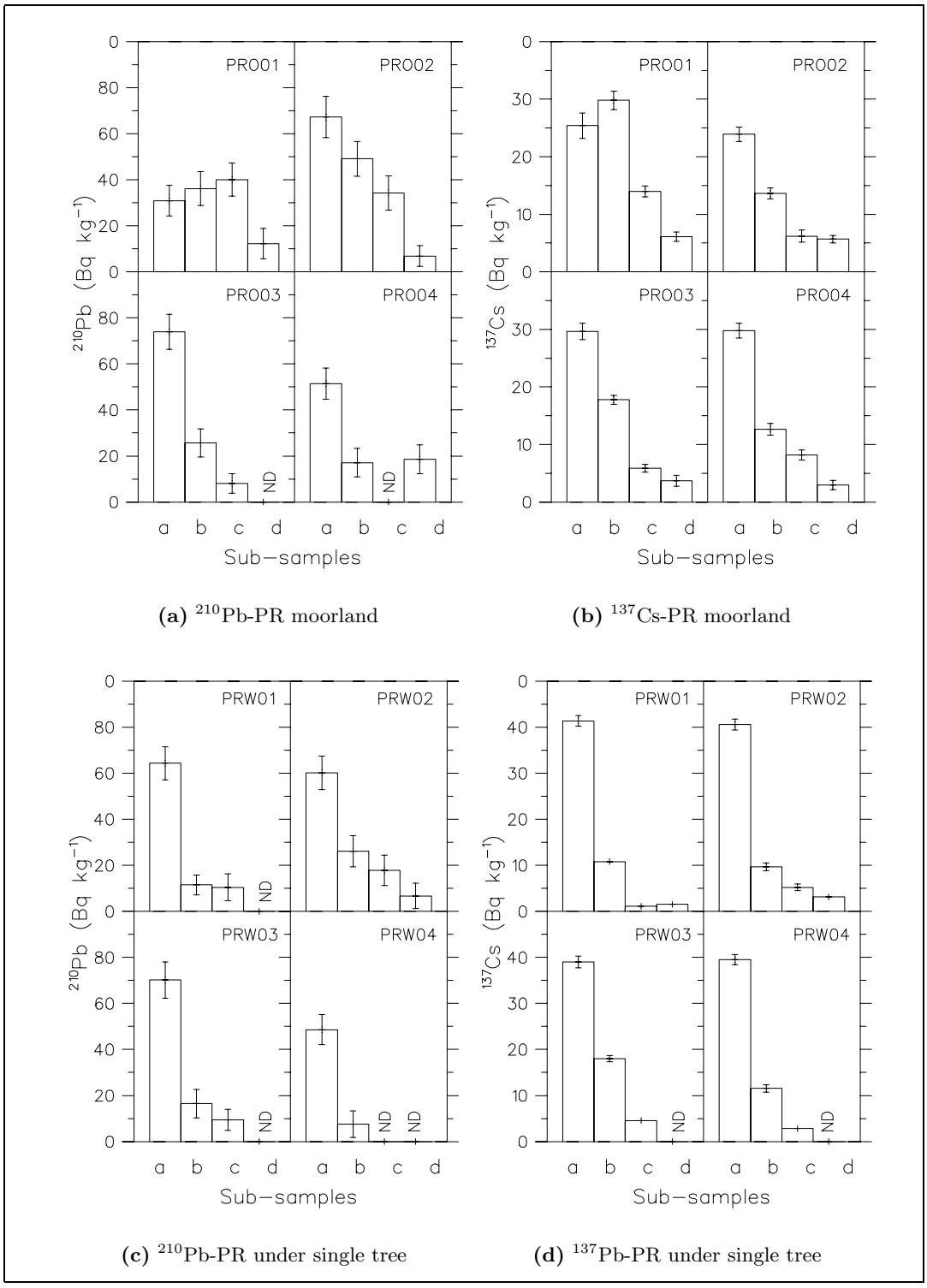

(a) ^{210}Pb-PR moorland

(b) ^{137}Cs-PR moorland

(c) ^{210}Pb-PR under single tree

(d) ^{137}Pb-PR under single tree

Figure 4.11: *Distribution of ^{210}Pb and ^{137}Cs specific activities with soil depth at Prestonfield site: (a) and (b) show the ^{210}Pb and ^{137}Cs activities in the open grassland soil, respectively: (c) and (d) show ^{210}Pb and ^{137}Cs activities in soil under the sycamore tree, respecticely.* (ND = Not Detected).

4.3.2 Inventories of ^{210}Pb and ^{137}Cs in Soils

Tables 4.2 to 4.6 give both ^{210}Pb and ^{137}Cs inventories in open grassland and under forest canopy soils at each site. The average inventories for open grassland and woodland (or under single oak and sycamore trees for CEH and Prestonfield sites, respectively) soils are also given. Intra-site variability within sites are indicated by the coefficient of variability (CoV in %).

CEH Edinburgh Site

Table 4.2: *The ^{210}Pb and ^{137}Cs inventories in soil sampled at the Centre for Ecology and Hydrology site. CoV (in %) measures the intra-site variability.*

Core Identity	Open Grassland (Bq m^{-2})		Single Tree (Bq m^{-2})	
	^{210}Pb	^{137}Cs	^{210}Pb	^{137}Cs
CEO/W01	3685 ± 97	1205 ± 24	3093 ± 104	2056 ± 41
CEO/W02	2661 ± 72	1248 ± 23	2290 ± 64	1416 ± 29
CEO/W03	2765 ± 80	1462 ± 28	3134 ± 89	1211 ± 51
CEW04	-	-	3156 ± 86	1626 ± 43
CEW05	-	-	2866 ± 80	1544 ± 36
CEW06	-	-	3053 ± 63	1294 ± 27
Mean	3037 ± 564	1305 ± 138	2932 ± 331	1524 ± 302
CoV (%)	19	11	11	20

Cramond Site

Table 4.3: *The ^{210}Pb and ^{137}Cs soil inventories at the Cramond site. CoV (in %) measures the intra-site variability.*

Core Number	Open Grassland (Bq m^{-2})		Woodland Canopy (Bq m^{-2})	
	^{210}Pb	^{137}Cs	^{210}Pb	^{137}Cs
CRO/W01	4073 ± 153	1504 ± 44	1724 ± 68	1509 ± 29
CRO/W02	3479 ± 127	1571 ± 51	2781 ± 111	1993 ± 42
CRO/W03	4011 ± 139	1314 ± 42	2272 ± 86	1991 ± 43
CRO/W04	3010 ± 101	1323 ± 38	2404 ± 89	2093 ± 40
CRW05	-	-	1914 ± 72	2003 ± 38
Mean	3643 ± 499	1428 ± 129	2223 ± 410	1918 ± 232
CoV (%)	14	9	18	8

Pentlands Site

Table 4.4: *The ^{210}Pb and ^{137}Cs inventories at the Pentland site. CoV (in %) measures the intra-site variability.*

Core Number	Open Grassland (Bq m^{-2})		Woodland Canopy (Bq m^{-2})	
	^{210}Pb	^{137}Cs	^{210}Pb	^{137}Cs
PEO/W01	2575 ± 92	2073 ± 54	3227 ± 81	3010 ± 37
PEO/W02	2827 ± 93	2452 ± 49	3389 ± 79	3273 ± 37
PEO/W03	2222 ± 66	1483 ± 30	3500 ± 95	3331 ± 44
PEO/W04	2231 ± 71	2379 ± 41	3274 ± 91	2592 ± 37
PEW05	-	-	2797 ± 73	2390 ± 32
Mean	2464 ± 293	2097 ± 441	3237 ± 268	2919 ± 415
CoV (%)	12	20	8	14

West Linton Site

Table 4.5: *The ^{210}Pb and ^{137}Cs inventories at West Linton Site. CoV (in %) measures the intra-site variability.*

Core Number	Open Grassland (Bq m^{-2})		Woodland Canopy (Bq m^{-2})	
	^{210}Pb	^{137}Cs	^{210}Pb	^{137}Cs
WLO/W01	2662 ± 75	2005 ± 38	3635 ± 113	2358 ± 42
WLO/W02	2739 ± 71	1347 ± 27	4061 ± 126	1907 ± 38
WLO/W03	2517 ± 72	1558 ± 33	3779 ± 133	2283 ± 48
WLO/W04	2366 ± 64	1503 ± 45	4637 ± 132	3076 ± 46
WLW05	-	-	3874 ± 106	3251 ± 40
Mean	2571 ± 165	1603 ± 282	3997 ± 390	2575 ± 567
CoV (%)	6	18	10	22

Prestonfield Site

Table 4.6: *The ^{210}Pb and ^{137}Cs inventories at the Prestonfield site. CoV (in %) measures the intra-site variability.*

Core Number	Open Grassland (Bq m^{-2})		Single Tree (Bq m^{-2})	
	^{210}Pb	^{137}Cs	^{210}Pb	^{137}Cs
PRO/W01	2317 ± 109	1322 ± 50	1904 ± 98	1127 ± 31
PRO/W02	3036 ± 132	1380 ± 80	3669 ± 162	1436 ± 55
PRO/W03	2061 ± 104	1263 ± 55	2001 ± 111	1398 ± 37
PRO/W04	1982 ± 116	1254 ± 124	1249 ± 84	1313 ± 41
mean	2349 ± 480	1305 ± 58	2206 ± 1031	1318 ± 138
CoV (%)	20	4	47	10

4.3.2.1 The ^{210}Pb Grassland:Woodland Ratio

Inventories of ^{210}Pb in open grassland relative to woodland vegetation soils for each site were determined. A one-tail student's *t*-test showed that there were no significant differences (P<0.05) in the mean ^{210}Pb inventories on open grassland and woodland soils at CEH and Prestonfield sites ($t = 0.36$; $df = 7$ and $t = 0.25$; $df = 6$, respectively) as shown by box plots in figure 4.12 (A & E). The woodland canopy effect was observed at the Pentland and West Linton golf course sites ($t = 4.14$; $df = 7$ and $t = 6.78$; $df = 7$, respectively), giving woodland/grassland inventory ratios of 1.31 ± 0.19 and 1.55 ± 0.18, respectively (figure 4.12 (C & D)). Conflicting results were, however, obtained for Cramond soils, figure 4.12 (B), indicating a significantly low ($t = 4.70$; $df = 7$) ^{210}Pb inventory under the forest canopy relative to the adjacent open grassland areas.

Although the enhancement factors obtained from the two sites, Pentland and West Linton, are more variable; 31% and 55%, respectively, their mean value (43%) compares to an average enhancement of 37% found by Moghaddam [105] for the deposition of ^{210}Pb inside forest canopies relative to adjacent open grassland soils at Dunslair Heights (southeast Scotland). These results are also within the 22% to 60% range of enhancement factors for ^{210}Pb inventories throughout the west midlands of England soils under the woodland relative to open grass areas reported by Fowler *et al.* (in press, 2003). During deposition (wet and/or dry), some of the ^{210}Pb-rich aerosols are

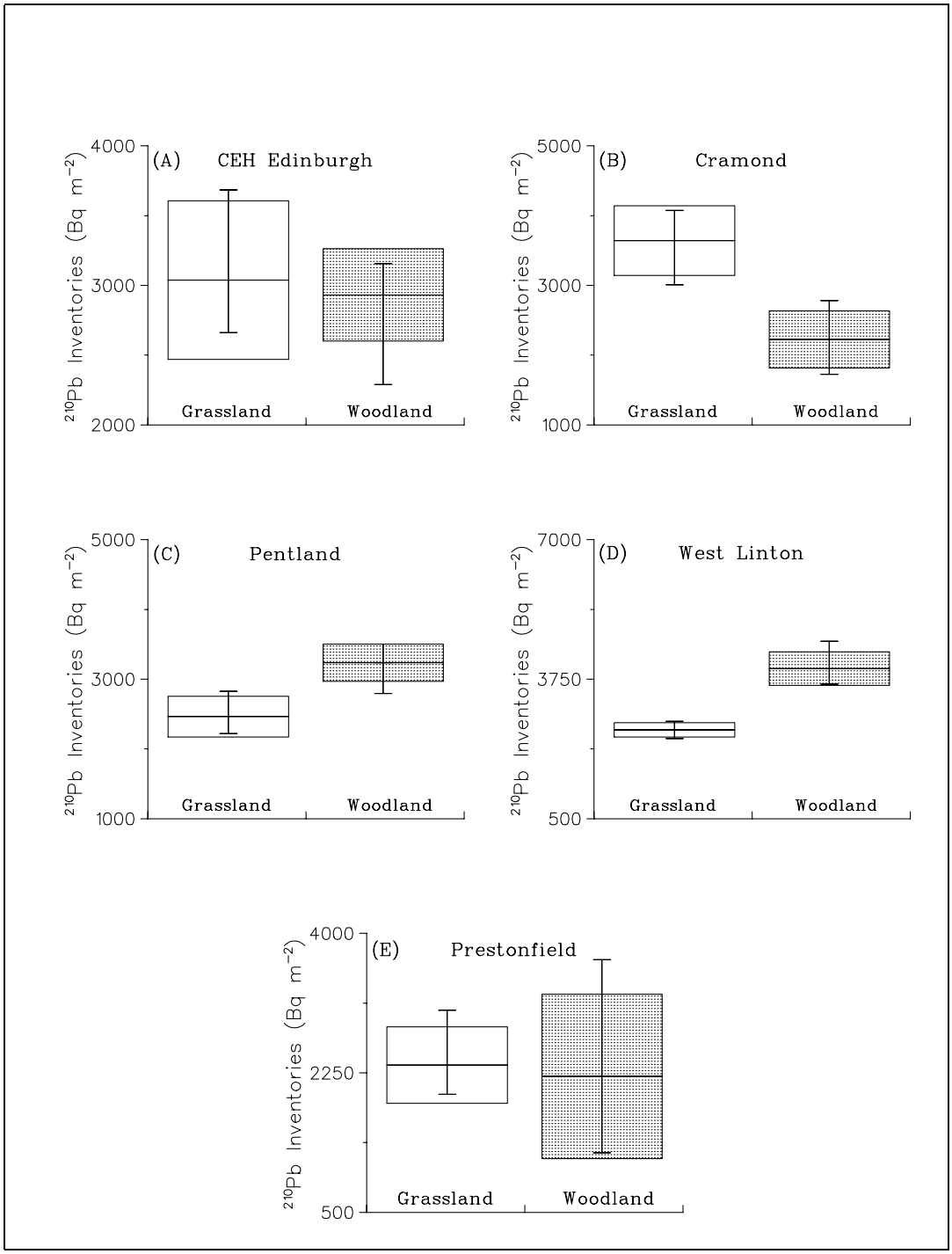

Figure 4.12: *Box plots for ^{210}Pb mean inventories in soils sampled at Edinburgh sites: (A) CEH, (B) Cramond, (C) Pentland, (D) West Linton and (D) Prestonfield. The box heights extend to ± standard deviation from the mean (centred horizontal lines). The lines with error bars extend from the minimum to the maximum values obtained from single cores at each site.*

captured and retained by foliage before reaching the ground through leaf senescence and wash off by rain. In areas where trees are of a dense canopy, leaves deposit ^{210}Pb-carrier aerosols below the canopy and decompose to become part of the topmost soils. ^{210}Pb is efficiently retained in soils by organic matter as reported by Lewis [94] and by Graustein and Turekian [89]. The efficiency with which ^{210}Pb-carrier aerosols are captured by leaves depends, among other things, on the density and morphology of the woodland canopy.

Both Pentland and West Linton golf forest canopies were composed of relatively tall (∼15 m) and dense deciduous woodland, giving rise to the expected higher ^{210}Pb inventories in woodland soils relative to adjacent open grassland areas. The large difference in enhancement factors in ^{210}Pb inventories due to the presence of woodland between the Pentland and West Linton sites (*i.e.*, 31% and 55%, respectively) were attributed to the positions of the sites relative to the prevailing winds. West Linton is situated on a relatively flat area, whereas, the Pentland site was on a hill-end, at a leeward side of the prevailing winds. Therefore, the high woodland enhancement factor at West Linton, compared to that at Pentland hills site may be due to the increased turbulence inside the canopy resulting from the alteration of the vertical wind profile and hence an increase in interception and impaction of particles. This process is expected to be less efficient in delivering aerosols at the Pentland woodland forest, since some particulate matter would be deposited on the wind-facing side of the hills, before reaching the sampled area.

Insignificant differences in the ^{210}Pb soil inventories under single tree canopies, relative to respective open grassland areas sampled from CEH and Prestonfield were not unexpected because the ^{210}Pb captured by the trees only increase the soil inventories if the leaves fall vertically to the soil beneath the trees. In practice, falling leaves for single trees are dispersed over a much larger area. The high open grassland ^{210}Pb inventory at Cramond relative to the woodland canopy may be due to some form of soil disturbance as was revealed by specific activity distribution with depth in figure 4.8 (section 4.3.1).

4.3.2.2 The ^{137}Cs Grassland:Woodland Ratio

The ^{137}Cs inventories measured at the five sampling sites also follow the same trend (except for Cramond site) as that found in unsupported ^{210}Pb deposited on open grassland, relative to woodland canopy soils (figure 4.13 (A to E)). No significant difference ($P<0.05$) was observed in mean ^{137}Cs inventories between open grassland and woodland soils at CEH and Prestonfield ($t = 1.17$; $df = 7$ and $t = 0.18$, $df = 6$, respectively) sites. Significantly higher ^{137}Cs soil inventories in woodland canopy soils relative to open land were measured at Pentland ($t = 2.87$; $df = 7$) and West Linton ($t = 3.10$; $df = 7$). The woodland/grassland inventory ratios were calculated to be 1.39 $\pm$ 0.35 (for Pentland soils) and 1.61 $\pm$ 0.45 (for West Linton soils), giving an average of woodland enhancement factor of 50%. Although the woodland canopy enhancement factor relative to open grassland is high compared with an average of 30% reported by Bunzl and Kracke [119] and 35% obtained by Moghaddam for Dunslair Heights soils [105], it is consistent with the 43% obtained with the ^{210}Pb inventories at the sites and also compares well with 49% and 54% for Geescroft and Broadbalk deciduous forest, respectively, reported by Choubedar [28].

The woodland enhancement factor of 1.34 $\pm$ 0.20 ($t = 3.74$; $df = 7$), given by ^{137}Cs inventories at Cramond remains unexplainable, considering the fact that the reverse was true for ^{210}Pb deposited at the site (see section 4.3.2.1).

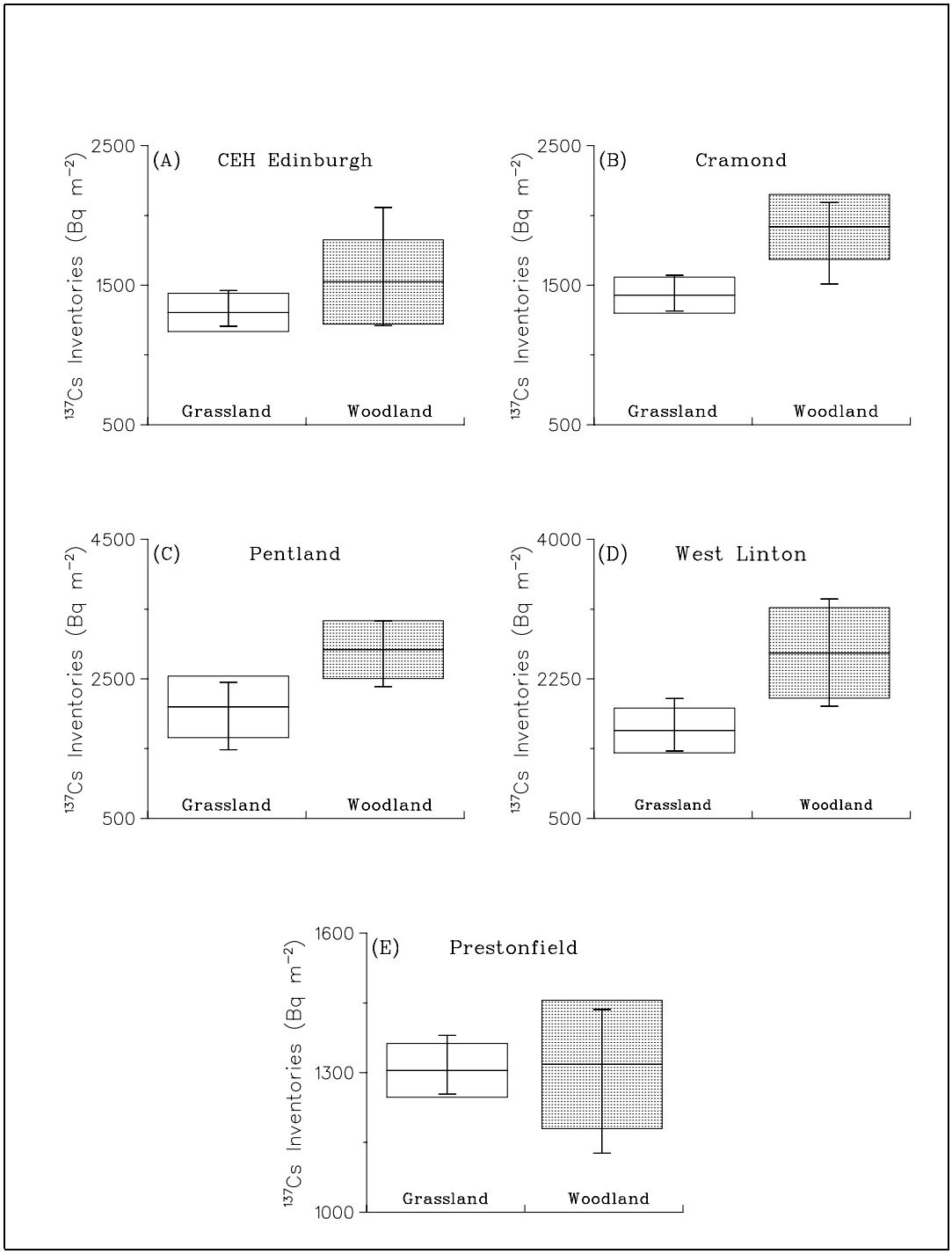

Figure 4.13: *Box plots for ^{137}Cs mean inventories in soils sampled at Edinburgh sites (A) CEH, (B) Cramond, (C) Pentland, (D) West Linton and (D) Prestonfield. The box heights extends to ± standard deviation from the mean (centred horizontal lines). The lines with error bars extend from the minimum to the maximum values obtained from single cores at each site.*

4.3.3 Atmospheric Fluxes of ^{210}Pb

Under reasonable assumptions that the soils have not been disturbed for ∼100 years and that the rate of ^{210}Pb decay and the atmospheric deposition rate are at steady state [89], the mean ^{210}Pb flux on the open grassland was estimated to be 81 ± 10 Bq m^{-2} y^{-1}, and 113 ± 16 Bq m^{-2} y^{-1} for woodland canopy soils. The fluxes reported here do not include measurements obtained from Cramond soils due to the possibility of the site having been disturbed within the past 30 years as reported earlier. Furthermore, woodland sample inventories at CEH and Prestonfield were treated as the open grassland sample means and therefore were considered in estimating open grassland ^{210}Pb fluxes. Table 4.7 gives a summary of the estimated ^{210}Pb fluxes at each site.

Table 4.7: *The ^{210}Pb mean fluxes at open field and under the woodland canopies for Edinburgh sites.*

Sampled Site	Rainfall (mm/yr)	^{210}Pb (Bq m^{-2} y^{-1})		Wood/Open Ratio
		Grassland	Woodland	
PE	850	77 ± 9	101 ± 8	1.31 ± 0.19
WL	1000	80 ± 5	124 ± 12	1.55 ± 0.18
[a]CE	900	94 ± 18	91 ± 10	0.97 ± 0.20
[a]PR	700	73 ± 15	69 ± 32	0.95 ± 0.48
[b]CR	700	113 ± 16	69 ± 13	0.61 ± 0.14
Mean	830	[†]81 ± 10	[‡]113 ± 16	[‡]1.43 ± 0.17

[a]Single Tree sites
[b]Poor values due to site characteristics
[†]Mean for sites: CE, PE, WL and PR only (*see text*).
[‡]Mean for sites: PE and WL only (*see text*).

The mean ^{210}Pb fluxes obtained in this study are within the range reported for Scotland. For example, Mac Kenzie *et al.* [120], reported a ^{210}Pb flux range of 67-106 Bq m^{-2} y^{-1} for Fenwick where the mean rainfall is 1400 mm/yr, while Pulford *et al.* [117] reports flux range of 83 to >116 Bq m^{-2} y^{-1} at Inverness (rainfall = 950 mm/yr). Moghaddam [105] also found mean ^{210}Pb fluxes of 72 Bq m^{-2} y^{-1} in open moorland and 99 Bq m^{-2} y^{-1} in soils under Norway spruce (*Picea Abies*) canopy, respectively, where the annual mean rainfall at site was 1200 mm/yr.

Considering an annual average rainfall of 830 mm/yr for Edinburgh, presented in table 4.7 (based on the 30-year annual average rainfall map [121]), the mean ^{210}Pb flux was estimated to be 98 ± 12 and 136 ± 23 Bq m^{-2} y^{-1} *per metre of rainfall* (which corresponds to derived mean ^{210}Pb concentrations in rainfall, expressed in mBq l^{-1}) on open grassland and woodland canopy soils, respectively. The open grassland flux compares well with the UK mean ^{210}Pb flux of 77 ± 14 m^{-2} y^{-1} *per metre of rainfall* reported by Smith *et al.* [118]. However, the derived mean ^{210}Pb concentration is about 56% higher than that of 63 mBq l^{-1} measured directly in bulk precipitation by Choubedar at Edinburgh for the period 1997-1999 [28]. Mean ^{210}Pb rainfall concentrations obtained in this way, although used by others, are misleading because the main reason for apparently large concentrations in rain deduced using this argument is that the value contains ^{210}Pb dry deposited.

4.3.4 Concentrations of ^{210}Pb and ^{7}Be in Precipitation and Foliage

Concentrations of ^{210}Pb and ^{7}Be in bulk precipitation, throughfall and foliage (Sitka spruce age-graded needles and three deciduous tree leaves) were measured. Litterfall from the Sitka forest plantation was also collected and measured for the ^{210}Pb activity. No attempt was, however, made to measure the activity of ^{7}Be in litterfall due to its short half-life. Data for both ^{210}Pb and ^{7}Be concentrations and activities of individual events during the collection period in bulk precipitation and throughfall samples are given in appendix C.

4.3.4.1 Bulk Precipitation and Throughfall Concentrations of ^{210}Pb

The total rainfall amount over a 358-day collection period was 1184 mm. The concentrations for ^{210}Pb and ^{7}Be for the 14 bulk precipitation samples collected ranged from 0.9 ± 0.1 to 79.2 ± 8.4 mBq l^{-1} and 30.3 ± 0.5 to 741.7 ± 20.9 mBq l^{-1} respectively. The volume-weighted annual average concentrations were 54 ± 3 mBq l^{-1} for ^{210}Pb and 909 ± 47 mBq l^{-1} for ^{7}Be. The corresponding inventories varied from 0.3 ± 0.1 to 15.7 ± 1.7 Bq m^{-2} for ^{210}Pb and from 3.8 ± 0.1 to 222.6 ± 6.3 Bq m^{-2} for ^{7}Be. The annual depositional fluxes for ^{210}Pb and ^{7}Be were 64 ± 4 and 1235 ± 62

Bq m^{-2} y^{-1} respectively. Both the annual average concentrations and depositional fluxes were determined by correcting the corresponding integrated activities over the 358-day collection period to one year. The ^{210}Pb retained in foliage was estimated by plotting a graph of bulk precipitation *versus* throughfall (in mBq l^{-1}), presented in figure 4.14.

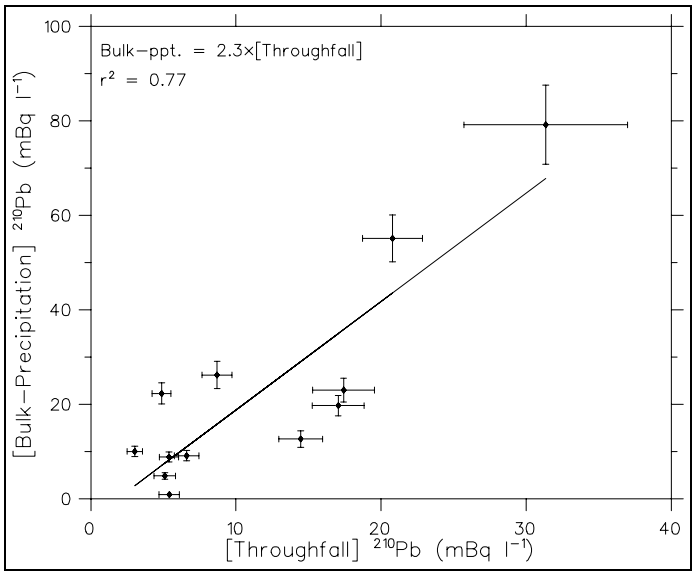

Figure 4.14: *A graph showing bulk precipitation versus throughfall ^{210}Pb concentrations at Deepsyke forest plantation.*

Rainfall losses approximately half the ^{210}Pb by passing through foliage. This figure is, however, subject to uncertainties. Rain serves to deposit particles on foliage, as well as dislodge particulate matter from foliage. Furthermore, some fraction of the rain contents that come into contact with foliage will also be distributed to twig and stem tissue in accordance with the distribution of tissue surface area. These factors will play a major role in the measured activities of radioactive aerosols received as throughfall. On considering these factors, the ^{210}Pb bulk precipitation/throughfall ratio of 2.3 could be interpreted as a mere indication of particulate matter being brought to foliar surfaces by rain, rather that the efficiency with which the Sitka spruce needles retains ^{210}Pb-carrier aerosols in bulk precipitation. Previous investigations by Russell *et al.* [122] have revealed a high contamination surface density of radioactive aerosols (^{7}Be, ^{144}Ce, ^{141}Ce and ^{95}Zr) in twig and limb surfaces of pine, oak and maple trees.

The annual average ^{7}Be concentrations in rainfall exceed that in Sitka spruce throughfall by a factor of ∼9. Unlike ^{210}Pb, there was no significant correlation in bulk precipitation and throughfall concentrations. Lack of correlation in the measured concentrations of ^{7}Be in rain and throughfall samples may be attributed to the irregular collection periods during the sampling exercise. The isotope of ^{7}Be is short-lived ($t_{1/2} = 53$ days), whereas ^{210}Pb has a half-life of 22.3 years. Therefore, large errors in measured ^{7}Be concentrations in samples exposed for longer periods are expected, despite the fact that correction procedures were applied to compensate for loss in decay of ^{7}Be. Decay correction procedures become more reliable only if the accumulation rate of the isotope is also known, or can be estimated for the period the collectors were exposed to the atmosphere. Table 4.8 presents a summary of volume-weighted annual average concentrations and annual fluxes of both ^{210}Pb and ^{7}Be over the collection period.

Table 4.8: *The ^{210}Pb and ^{7}Be annual average concentrations and fluxes in the bulk-precipitation and throughfall samples.*

Isotope	Concentrations (mBq l^{-1})		Annual Fluxes (Bq m^{-2} y^{-1})	
Name	†Bulk	‡Thru	Bulk	Thru
^{210}Pb	54 ± 3	13 ± 1	64 ± 4	5.4 ± 0.3
^{7}Be	909 ± 47	96 ± 4	1235 ± 62	34.1 ± 4.8

†Bulk precipitation.
‡Throughfall.

4.3.4.2 Concentrations of ^{210}Pb and ^{7}Be in Foliage

The activity distributions of ^{210}Pb and ^{7}Be in age graded Sitka spruce needles were measured and the results are presented in figure 4.15 (see data in table C.3, appendix C). Both ^{210}Pb and ^{7}Be were observed to accumulate until a 'quas-equilibrium' was reached, signifying that a balanced process between accretion and loss of particulate matter is maintained with time. Despite the fact that both ^{210}Pb and ^{7}Be concentrations are reasonably constant from year to year, ^{210}Pb activities (figure 4.15 (A)) in leaf needles reached their maximum more quickly compared to ^{7}Be for the same class of needle ages. The difference in the time at which a steady state is reached suggests

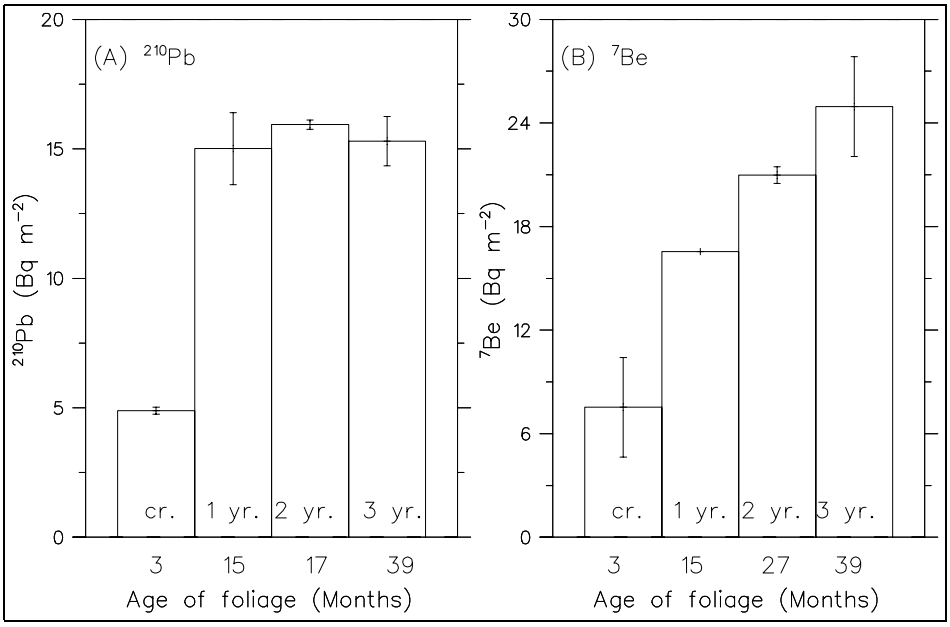

Figure 4.15: *Distribution of: (A) ^{210}Pb and (B) ^{7}Be in Sitka spruce leaf needles, based on averages for the 2001 and 2002 measurements: cr. = current year shoots (∼2.5 months old); 1 yr. = previous year needles (∼15 months old), etc.*

that, even though the deposition behaviour of the two isotopes are similar, the two may be associated with dissimilar aerosol size distribution. Moore *et al.* [10] has found ^{210}Pb distributions as a function of particle size to be almost always $\leq$0.3 μm, while Crecelius [72] reported ^{7}Be to be mostly submicron. Because the leaves loose their stickiness and hairy structure with age, hence decreasing their particle retaining efficiency, relatively large particles are more likely to dislodge first during periods of high wind turbulence and intense rain than very fine particles. These features compare well with those obtained from sequential measurements of ^{210}Pb and ^{7}Be conducted with oak, lime and sycamore foliage as depicted in figure 4.16 (see data in table C.4, appendix C). However, both ^{7}Be and ^{210}Pb activities declined with almost the same time constants in measurements conducted with sycamore foliage. This could be due to the fact that the sycamore leaves started to become scenescent during August, and had started to fall off the tree by September/October, thus, loosing most of the particulate matter they had retained early compared to other tree species.

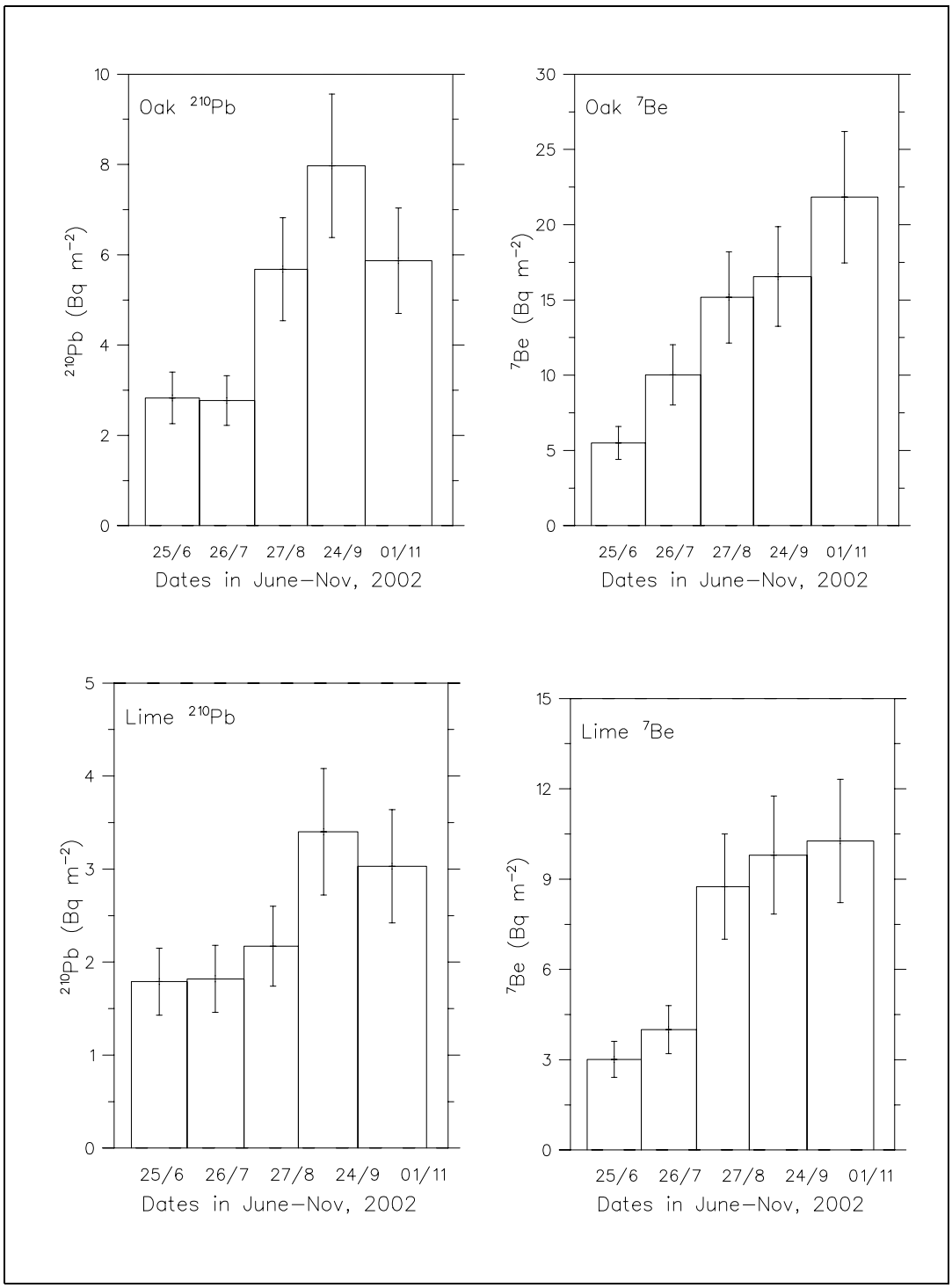

Figure 4.16: (Continued on next page) *^{210}Pb and ^{7}Be in oak, lime and sycamore leaf samples. The measurements were made after about three months since leafing, and continued on approximately 30-day intervals until leaves became senescent.*

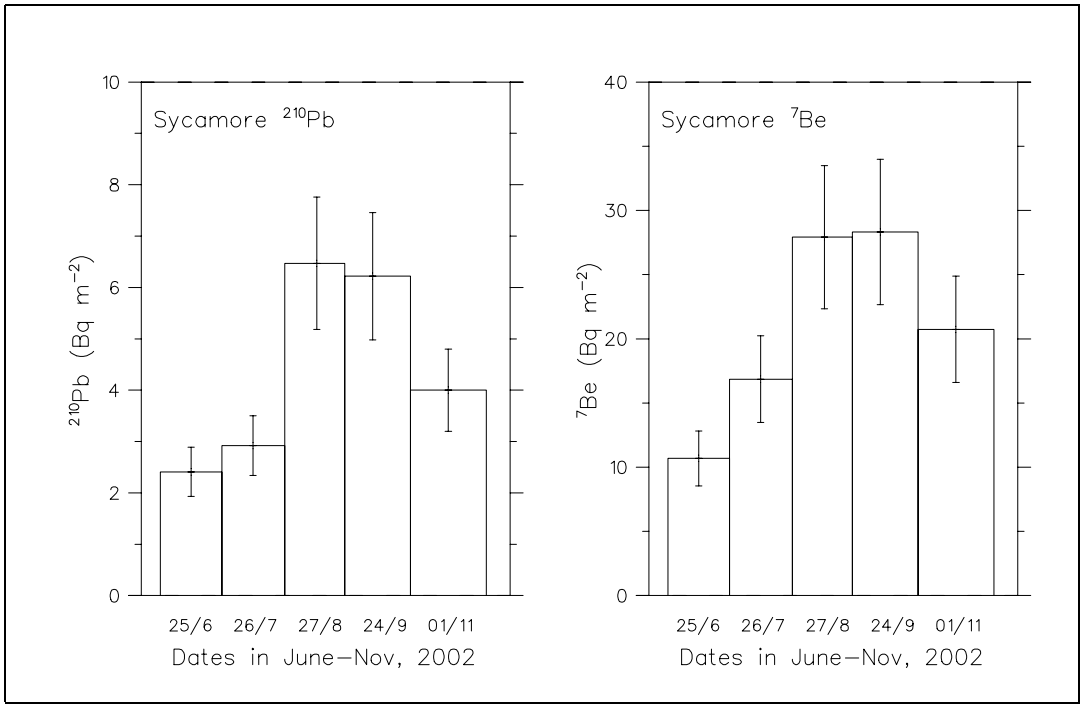

Figure 4.16: *^{210}Pb and ^{7}Be in oak, lime and sycamore leaf samples. The measurements were made after about three months since leafing, and continued on approximately 30-day intervals until leaves became senescent* (continued from previous page).

4.3.5 Deposition Mechanism of ^{210}Pb in Woodland Soils

By comparing ^{210}Pb fluxes in both woodland and open grassland soils at West Linton with ^{210}Pb fluxes measured in bulk precipitation, throughfall, litterfall and Sitka spruce needles, a clear picture of the main factor contributing to enhancement in the depositional flux in woodland relative to open grassland soils can be drawn (figures 4.17). The West Linton golf course was chosen because of its proximity to Deepsyke plantation.

Particles are captured and retained by foliar surfaces, until such time when a quasi-steady state is maintained between accumulation and wash off by precipitation before leaf senescence. Some of the particles may deposit to the ground by gravitational settling and as throughfall, as indicated by the 5 Bq m^{-2} y^{-1} of ^{210}Pb in Sitka spruce throughfall. The bulk of ^{210}Pb flux under woodland canopy (*i.e.*, 118 Bq m^{-2} y^{-1}), is due to contribution from litterfall. Some additional flux to woodland soil, although not measured in this work, may be due to other processes such as stem flow.

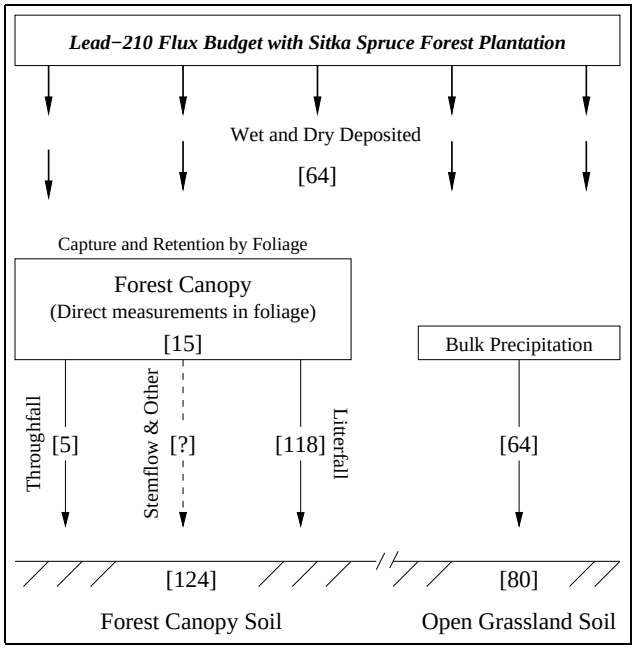

Figure 4.17: *A schematic representation of ^{210}Pb fluxes measured in soils at West Linton and at a Sitka spruce forest plantation at Deepsyke. The numbers in square brackets are expressed in $Bq\ m^{-2}\ y^{-1}$.*

Considering both ^{210}Pb and ^{137}Cs inventory measurements made in CEH Edinburgh and Prestonfied golf course soils, and the fact that there was lack of significant enhancement of radioisotopes under woodland relative to open grassland soils, it can be concluded that the main contributing factor to the elevated deposition fluxes in forest soils is due to litterfall. Large quantities of aerosol-rich litter are removed from trees under unshielded woodland canopies by wind. Although there are contributions from throughfall and gravitational settling of bounced off particles, these do not significantly enhance fluxes of aerosols shown in figures 4.12 and 4.13.

The ^{7}Be activity was not measured in soil due to its short half-life. Furthermore, the ^{137}Cs activities were insignificant in foliage samples. This was not unexpected because ^{137}Cs was only present almost entirely in the environment due to nuclear weapons testing and Chernobyl nuclear power plant accident and consequently most of the ^{137}Cs activity in the atmosphere has fallen to very small values.

4.3.6 Dry Deposition and Deposition Velocities

Taking ^{210}Pb wet deposition of 64 ± 4 Bq m^{-2} y^{-1} reported earlier in section 4.3.4 as the long-term average, the dry deposition of submicron atmospheric particulates can be estimated by subtracting this average wet deposition from the total fluxes obtained for open grassland and woodland soils. Determining the quantity of dry deposition flux is important in that it provides the means of estimating the dry deposition velocity (v_{dd}), if the ambient air ^{210}Pb concentration is known. The average ^{210}Pb dry deposition in open grassland surfaces was found to be 17 ± 9 Bq m^{-2} y^{-1} and that for woodland surfaces was 49 ± 12 Bq m^{-2} y^{-1}, representing contributions of approximately 21% and 43%, respectively, of the total deposition. Other indirect methods used to evaluate deposition flux contributions due to dry deposition processes involve taking the difference between the wet only and bulk precipitation activity measurements or measurement of bulk (wet plus dry) precipitation and extrapolating to zero precipitation to estimate the dry deposition flux. Contributions due to dry deposition of up to 41% of the bulk deposition flux for ^{210}Pb was reported by Choubedar [28] using the latter method, whereas, ≤12% was calculated by Todd *et al.* [75] for both ^{210}Pb and ^{7}Be using the former. Although ^{210}Pb and ^{7}Be measurements were made in bulk precipitation collected in this work, it was inappropriate to apply the zero precipitation extrapolation method because of the small population size of collected samples.

Considering the ^{210}Pb and ^{7}Be mean air concentration measurements of 0.21 ± 0.17 and 2.50 ± 1.24 mBq m^{-3}, respectively, reported in chapter 3 and applying equation 1.1, dry deposition velocities were estimated to be 2.6 ± 1.3 mm s^{-1} for open field surfaces and 7.4 ± 1.8 mm s^{-1} for woodland surfaces. Both these values are large compared to the reported wind tunnel dry deposited measurements by Gallagher [123]. However, the derived dry deposition fluxes reported here compare well with those reported in other studies under natural conditions. Choubedar [28] reported ^{210}Pb dry deposition velocities 4.6 and 8.9 mm s^{-1} for grassland and woodland areas, respectively, while Fowler *et al.* (in press, 2003) reports an average for 3.3 mm s^{-1} in grassland and 9.0 mm s^{-1} in woodland areas.

The wet ^{210}Pb and ^{7}Be deposition velocities (v_{wd}) and washout ratio (α), using the bulk precipitation data, were also calculated. The washout ratios were estimated by means of equation 1.2, (assuming the density of air at standard temperature and pressure to be 1.2 kg m^{-3}) and the results are presented in table 4.9.

Table 4.9: *Wet deposition velocities for ^{210}Pb and ^{7}Be estimated from rain and surface air concentrations measured in this work.*

Isotope	Flux Bq m^{-2} y^{-1}	c_r mBq l^{-1}	c_a mBq m^{-3}	α	$^{\dagger}v_{wd}$ mm s^{-1}
^{210}Pb	64 ± 4	54 ± 3	0.21 ± 0.02	309 ± 34	9.7 ± 1.1
^{7}Be	1235 ± 62	909 ± 47	2.50 ± 0.12	436 ± 30	15.9 ± 1.1

†Wet deposition velocity.

The wet deposition velocity of ^{7}Be is about 60% greater than that of ^{210}Pb. This difference, however, may be attributed to the fact that surface level air concentrations were used, rather than an average of a vertical concentration profile. Because the concentration of ^{7}Be in air is higher in the upper troposphere than surface level air, and that scavenging of submicron particles by precipitation is mainly from in cloud, rather than below cloud processes [29], the calculated ^{7}Be wet deposition velocity may be slightly overestimated, while that of ^{210}Pb is underestimated. Thus, it can be concluded that the two deposition velocities are in reasonable agreement, suggesting that removal of the two aerosol carriers are governed by similar processes.

No attempt was made to estimate effective deposition velocities of both ^{210}Pb and ^{7}Be on foliage measured in this work. Successful application of deposition velocity concept in leaf samples would require knowledge of contributions of isotopes due to root uptake, growth dilution, addition and removal of particulates to and from vegetation, surfaces the biomass density of each vegetation species as well as the surface level air concentrations of ^{210}Pb and ^{7}Be for each period of exposure.

4.4 Conclusions

This chapter reports the effect of vegetation on the deposition of submicron atmospheric particulates using ^{210}Pb and ^{137}Cs soil inventory measurements at Edinburgh and the surrounding areas. The following are the main results obtained:

- Soil inventories of ^{210}Pb beneath woodland revealed an average enhancement of 43% of atmospheric particulate matter relative to open grassland areas, whereas ^{137}Cs soil inventory measurements provided an average increase by 50%.

- Conflicting results obtained from the Cramond site may be due to soil disturbance, possibly when the layout of the golf course was being changed.

- High ^{210}Pb and ^{137}Cs inventories under forest soils relative to open areas are largely due to carrier isotope-rich senescent leaves depositing under dense forest canopies. This was supported by lack of significant enhancements in both ^{210}Pb inventories in soils under single and isolated trees. Furthermore, measurements of ^{210}Pb and ^{7}Be in foliage, using both direct and throughfall technique, revealed that these carrier aerosols are captured and retained by foliage during wet and dry deposition processes before depositing to the ground as litterfall. Some of the aerosol may deposit through washout processes due to rain and by gravitational settling.

- The dry deposition velocites (v_{dd}) of ^{210}Pb-carrier aerosol for open field surfaces and woodland surfaces were estimated to be 2.6 $\pm$ 1.3 and 7.4 $\pm$ 1.8 mm s^{-1}, respectively.

Chapter 5

Effects of Topography on ^{210}Pb and ^{137}Cs Deposition

5.1 Introduction

The fallout of naturally occurring (^{210}Pb) and the anthropogenic (^{137}Cs) radionuclides provides important tools for studying pollutant transport processes and deposition fluxes to terrestrial ecosystems. Although there is a large body of data on ^{210}Pb and ^{137}Cs world-wide, this is mainly limited to relatively lowland areas. Aerosol deposition flux measurements over mountain terrain is complicated in several ways by the meteorological conditions that are typical of high elevations. High elevation sites induce additional deposition processes that are not major contributors to deposition in lowland sites. These processes affect the efficiency with which aerosols are scavenged from the atmosphere. Recently, studies involving measurements of major ionic concentrations as a function of elevation have been conducted to improve the estimates of acid quantities deposited in elevated sites. Results presented by Fowler [37] from 20 precipitation events measured at eight levels between 244 and 847 m asl., on the western slopes of Great Dun Fell (Cumbria, UK), indicate an increased ionic concentration of 2.2 to 3.1 between the valley (∼250 m asl.) and the summit (∼847 m above sea level). The increased concentrations of ions observed was interpreted as resulting from the seeder-feeder process, a mechanism first put forward by Bergeron [36], who proposed that rain falling from the high altitude (seeder) clouds washout small droplets within the low-level cap (feeder) clouds formed by ascent over the hills and consequently grow by accreting cloud drops (figure 1.2). The seeder-feeder mechanism

was also supported by theoretical studies of Storebø [124], Bader and Roach [125] and by Hill *et al.* [126], who presented eight detailed case studies of orographic rain falling over the hills of south Wales using data obtained from scanning radar combined with a network of autographic raingauges. Hill *et al.* found that the orographic rainfall enhancement depended on the low-level wind speed, and that over 80% of the total orographic enhancement occurred in the lowest 1500 m above the hill. Model studies of the seeder-feeder effect by Jones and Choularton [38] support this interpretation and also show that the rainfall enhancement and deposition are a function of topography and spatial scale. These results are valuable to improve the wet deposition map of the UK, particularly over the Pennines, the Lake District and Snowdonia where the seeder-feeder effect constitutes a large fraction of annual deposition [39].

Following the observations described above, a technique pointed out by Graustein and Turekian [90], which involves the use of fallout ^{210}Pb and ^{137}Cs accumulated in undisturbed soils to measure the rate of aerosol deposition, was employed to make inferences regarding the above mechanisms. The use of soil samples as long-term collectors of atmospheric deposition has advantages over direct collection of precipitation in that: (1) there is a greatly reduced time and expense required for sampling and (2) the deposition rates are relatively free of artefacts introduced by artificial collection apparatus. Therefore, the ^{210}Pb and ^{137}Cs measurement in soils provides practical studies of effect of local variables such as topography, cloud and vegetation, on the inventories of aerosols on the land surfaces. This chapter reports ^{210}Pb and ^{137}Cs inventories measured in soils collected from lowland and moderately high-elevated sites in mid-Wales (55.0°N, 04.0°W). The measurements were carried out for the following reasons:

- To determine whether high elevation sites have an influence on the long-term annual average wet deposition of ^{210}Pb and ^{137}Cs isotopes.

- To determine whether the presence of clouds frequently shrouding hilltops have a significant influence on the deposition of ^{210}Pb and ^{137}Cs, assuming constant concentrations of the isotopes in rainfall and negligible contributions from dry deposition processes.

5.2 Sampling Location and Site Description

Four sites in mid-Wales were selected for this study: (1) Ynys Hir (YH), grid reference no. SN 682 963; (2) Bryn Mawr (BM), grid reference no. SN 727 902; (3) Plynlimon Mountain (PL), grid reference no. SN 819 883; and (4) Tanllwyth Valley (TN), grid reference no. SN 855 868. Sites 3 and 4 are situated within the Hafren Forest Plantation. The four sites were situated 7.5, 15, 24 and 28 km, respectively from the west coast, lying approximately along a transect leading ESE of the Grid North. The sampling expedition were in two phases: one on June, 6^{th} 2002 for YH and BM and the last one on June, 7^{th} 2002 for PL and TN sites. Figure 5.1 shows the map of Wales, indicating approximate locations of the sites.

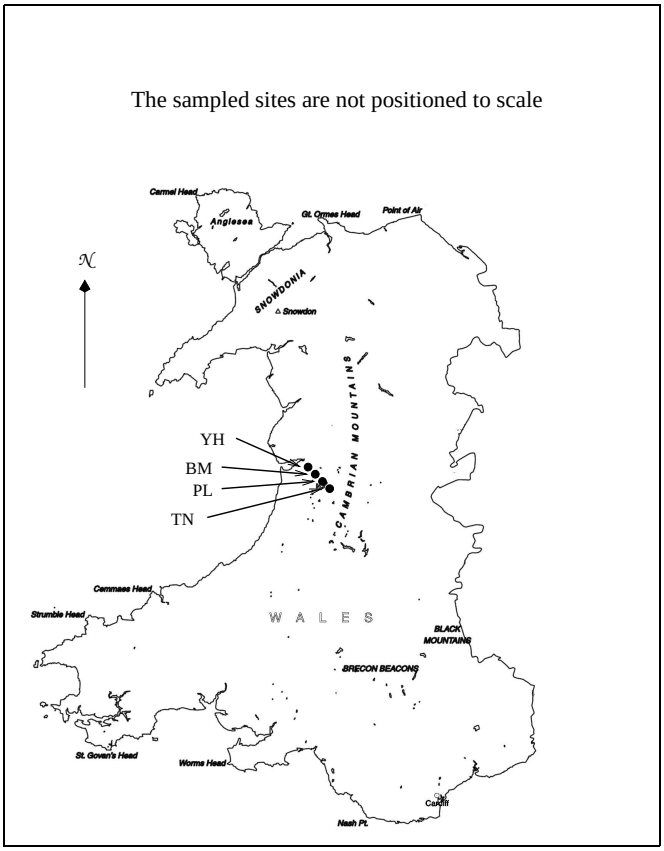

Figure 5.1: *A map of Wales showing approximate positions of sampled sites: Ynys Hir (YH), Bryn Mawr (BM), Plynlimon (PL) and Tanllwyth Valley (TN).*

The land and rainfall profiles of the transect, presented in figure 5.2, were drawn based on the information obtained from Ordnance survey maps [127] and the 30-yr annual

average rainfall map of the British Isles [121], respectively. The hill profile was drawn based on contours, assuming a straight line between contor positions, whereas, the rainfall profile was interpolated from a ∼5 km resolution rainfall isopleth map.

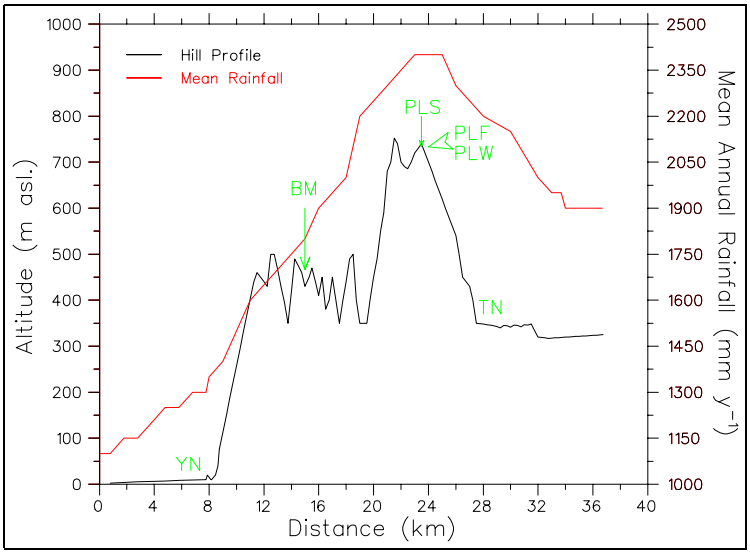

Figure 5.2: *Variation in altitude (black line) and rainfall rainfall (red line) with distance from the coast. The profiles stretch from the west coast of Britain, making a 35 km transect, running approximately ESE of the Grid North, through Yyns Hir (YN), Bryn Mawr (BM), Plynlimon (PL) and Tanllwyth (TN) sites.*

5.2.1 Ynys Hir Site

Ynys Hir was selected on the basis that it will provide inventories representative of low altitude sites. Furthermore, due to its proximity to the coast, the rainfall at the site was not expected to be enhanced significantly by the seeder feeder process. The site was located within the Ynys Hir Nature Reserve Park (altitude = 15 m asl.) situated about 7.5 km from the coast, next the mouth of River Dovey. The site receives a mean annual rainfall of 1300 mm. Five samples were obtained from soils under a moderately dense (10-15 m high) oak woodland canopy. The soil was rich in mineral content, and contained rocks (mostly slate). Adjacent to the oak woodland was a moorland area lying on a very gentle slope. Three samples were obtained from the moorland area and two more samples were obtained further away from the slope, inside a fence that demarcated the two areas. The soil within the fenced area was organic-rich and

was covered with relatively tall (∼10 cm) grass. A set of five more samples were obtained under an approximately 15 m-tall birch woodland canopy that was about 100 m southwest of the oak woodland area. The soil under the birch woodland was very wet and was composed mostly of organic matter and decaying litter. All samples from this site were obtained to a depth of 20 cm with the help of a spade, covering an area of 10 × 10 cm. Each sample was subdivided according to 0-5 cm, 5-10 cm and 10-20 cm depth intervals. Figure 5.3 presents a sketch of the sampled areas at Ynys Hir site.

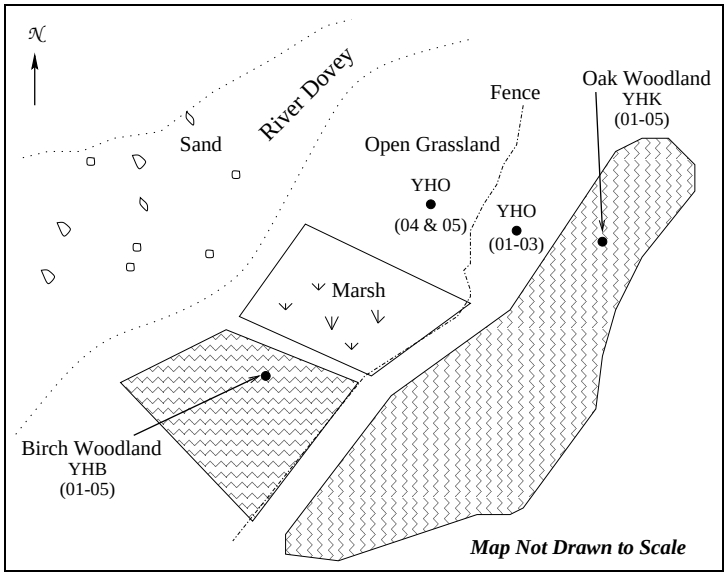

Figure 5.3: *A map of Ynys Hir showing sampled areas at site. YHO is the open grassland (moorland) area. YHK and YHB are the oak and the birch woodland areas, respectively.*

5.2.2 Bryn Mawr Site

The choice of the Bryn Mawr site was based on its enhanced rainfall due to the extent of land mass from the coast and rise in altitude relative to the Ynys Hir site. Thus, this site was expected to provide information on the effect of increased annual average rainfall on the deposition of ^{210}Pb and ^{137}Cs relative to that at the coast. The site is located about 15 km from the west coast, inland. This site lies on a hill end, at an altitude of ∼430 m asl., and receives a mean annual rainfall of 1800 mm. There was a fence running through the moorland area, probably separating the grazing from

non-grazing areas. The woodland was that of Sitka spruce, ∼20 m high. Moorland samples were obtained from the narrow strip of an ungrazed (∼10 cm tall grass) area between the fence and the edge of the woodland. A total of 6 samples were obtained from the moorland area: the first three were sampled about 10 metres from the road that ran through the woodland, and the last three were sampled about 20 more metres away from the road, at a boundary of the forest edge and the moorland area. The soils were rich with organic material within the first 10 cm of the profile. However, at depths beyond 10 cm, the soils were composed mostly of some mineral matter. Seven samples were obtained under the woodland canopy: one at about 3 m from the canopy edge; three at 5 m into the woodland; two at about 10 m from the edge of the woodland canopy; and the last sample was obtained approximately 15 cm inside the woodland. Samples were obtained using a 10.4 cm diameter corer. Figure 5.4 shows a sketch map of sampled areas at Bryn Mawr site.

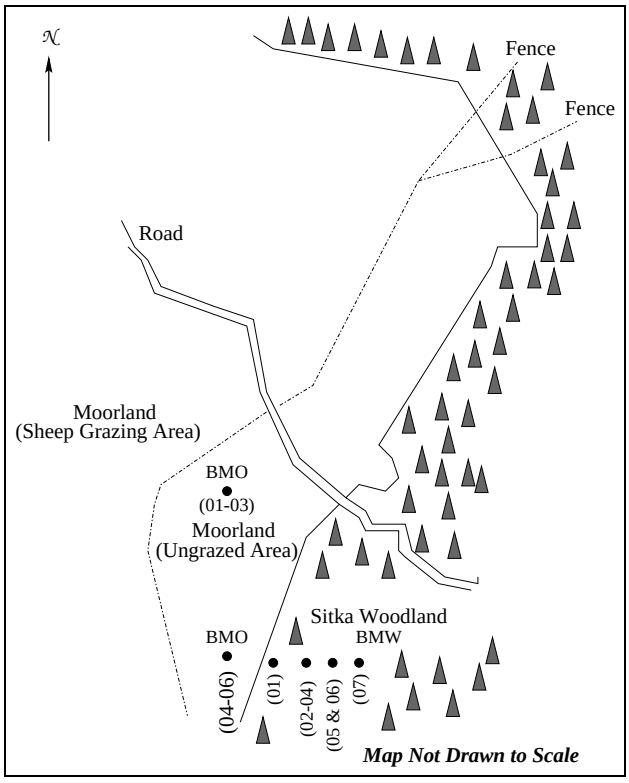

Figure 5.4: *A map of Bryn Mawr showing sampled areas at site. BMO and BMW are the open grassland (moorland) and the woodland areas, respectively.*

5.2.3 Plynlimon Site

Plynlimon was selected for sampling with the aim of investigating the effect of meteorological conditions at the mountain summit on the deposition of aerosols by comparing the measured inventories of ^{210}Pb and ^{137}Cs at this site with those for the low elevation sites. The site was located approximately 24 km from the west coast, at the summit of Plynlimon mountain, (altitude ∼741 m asl). The mean annual rainfall at this site is 2400 mm. Two open grassland areas were selected for sampling: one at the summit (741 m asl.) and the other site approximately 200 m to the eastern side of the summit, at an altitude of approximately 700 m asl. The grass at the summit was relatively short compared to the 10-15 cm tall grass at the site on the eastern side of the summit, suggesting that the area was almost certainly grazed. The two sites were divided by a fence that ran over the mountain. There were some tree stumps at the ungrazed moorland area, indicating that the site was once forested. Adjacent to this site was a Sitka spruce woodland. Four samples were obtained from the grazed moorland area at the summit, and five were sampled from the moorland area that was within the fenced area. The soils on both areas were composed mainly of organic matter at topmost sections, and mineral matter at depths >10 cm. Five more samples were obtained under the Sitka spruce woodland. The woodland samples, except one presented as PLW02, were composed of decaying litter at the topmost 5 cm of the core; organic matter at 5-10 cm; and mineral matter at depths >10 cm. The first two subsections of the core sample presented by PLW02 were organic rich, whereas the 10-15 cm subsection was composed of reddish-brown mineral soil. At a depth greater than 10 cm, there was another layer of organic matter, suggesting that the soil may have been disturbed. This sample was sectioned into four 5-cm thick subsamples. Figure 5.5 shows the sampled areas at Plynlimon (and the Tanllwyth site, see next section).

5.2.4 Tanllwyth Valley Site

Tanllwyth was selected because of its position on a leeward side of the Plynlimon mountain, so as provide information on the 'shadow effect' in the deposition of at-

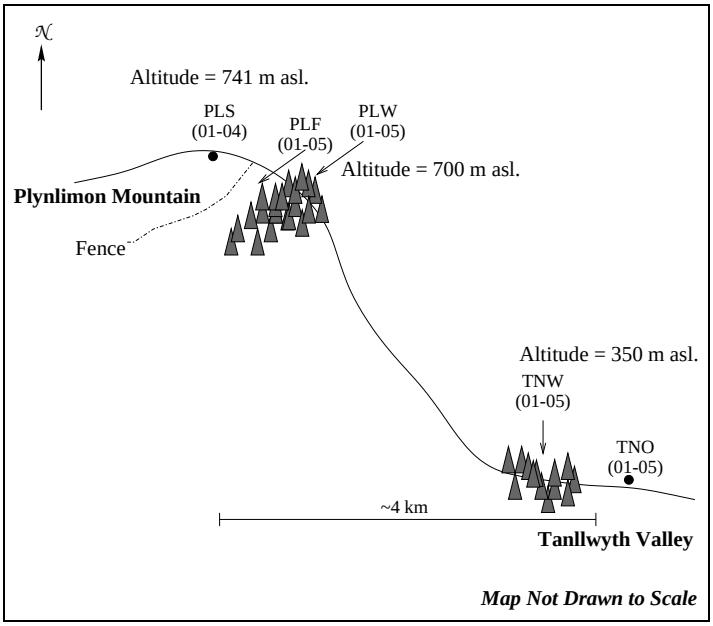

Figure 5.5: *A map of Plynlimon Mountain and Tanllwyth Valley showing sampled areas at the two sites. PLS is the (grazed) moorland area at the summit; PLF and PLW are moorland (ungrazed open grassland) and the Sitka woodland, both within the fenced area, respectively. At Tanllwyth site, TNO and TNW are the moorland and the Sitka woodland areas, respectively.*

mospheric aerosols. The site (figure 5.5) is situated 28 kilometres west of the coast, approximately 4 km on the eastern side of Plynlimon mountain, at an altitude of about 350 m asl., receiving the mean annual rainfall of 2000 mm. A total of ten samples were collected from Tanllwyth: five were sampled from soils under a Sitka woodland canopy and the other five from the nearby moorland area. Core samples no. TNW(01 & 05), obtained under the woodland canopy, were sampled from soils between the rows of the tree stands, whereas, TNW(02-04) were obtained on the soil ridges, along the stands. The topmost part (0-5 cm) of the woodland samples were composed mostly of litterfall. Beyond 5 cm, the soils were composed of organic material. The moorland area was covered with ∼20 cm tall grass, and the soils were very wet and poorly drained.

5.3 Results and Discussion

Specific activities (in Bq kg^{-1}) and inventories (in Bq m^{-2}) of ^{210}Pb and ^{137}Cs in soils sampled from mid-Wales are presented in this section. Intra-site variabilities were also measured by means of the coefficient of variability (as defined in the previous chapter). Details of the sampling procedures, analytical methods and data acquisition and analyses were presented in chapters 2 and 4. Figures 5.6 to 5.9 give the ^{210}Pb and ^{137}Cs specific activities as functions of soil depth. Data for these figures are presented in appendix B, table B.2.

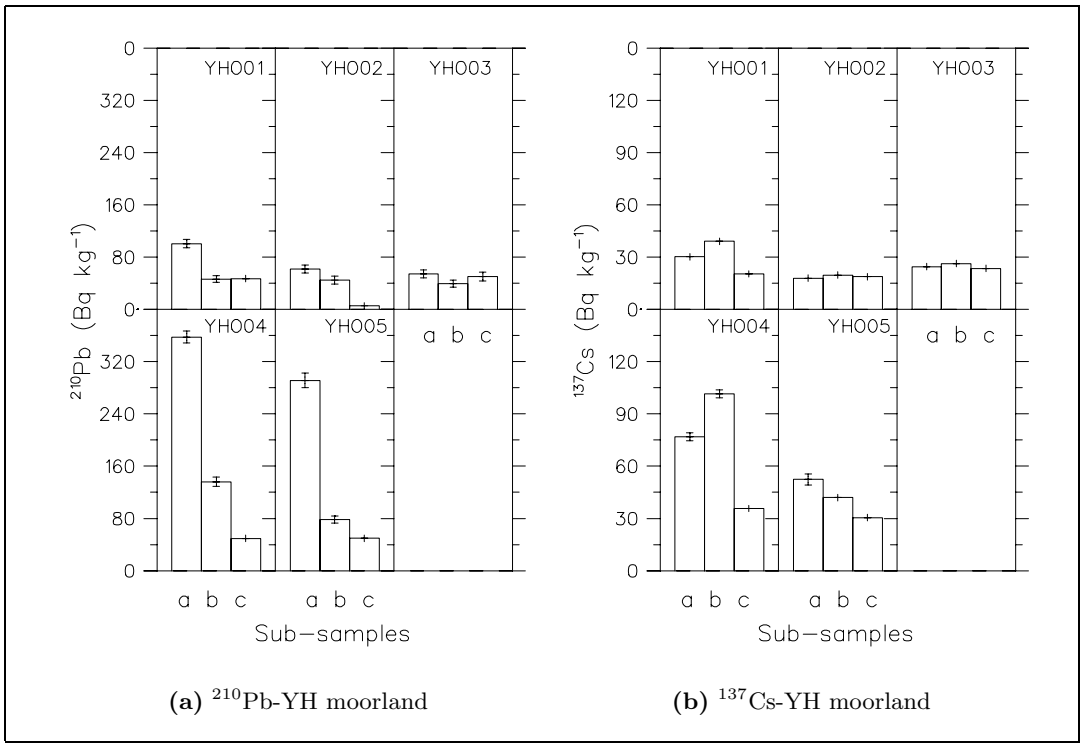

(a) ^{210}Pb-YH moorland **(b)** ^{137}Cs-YH moorland

Figure 5.6: (Continued on next page). *Variation in ^{210}Pb and ^{137}Cs specific activities with soil depth at Ynys Hir site: (a) and (b) are the ^{210}Pb and ^{137}Cs activities in moorland soils: (c) and (d) are the ^{210}Pb and ^{137}Cs activities in oak woodland canopy soils: and (e) and (f) are the ^{210}Pb and ^{137}Cs activities in birch woodland canopy soils.*

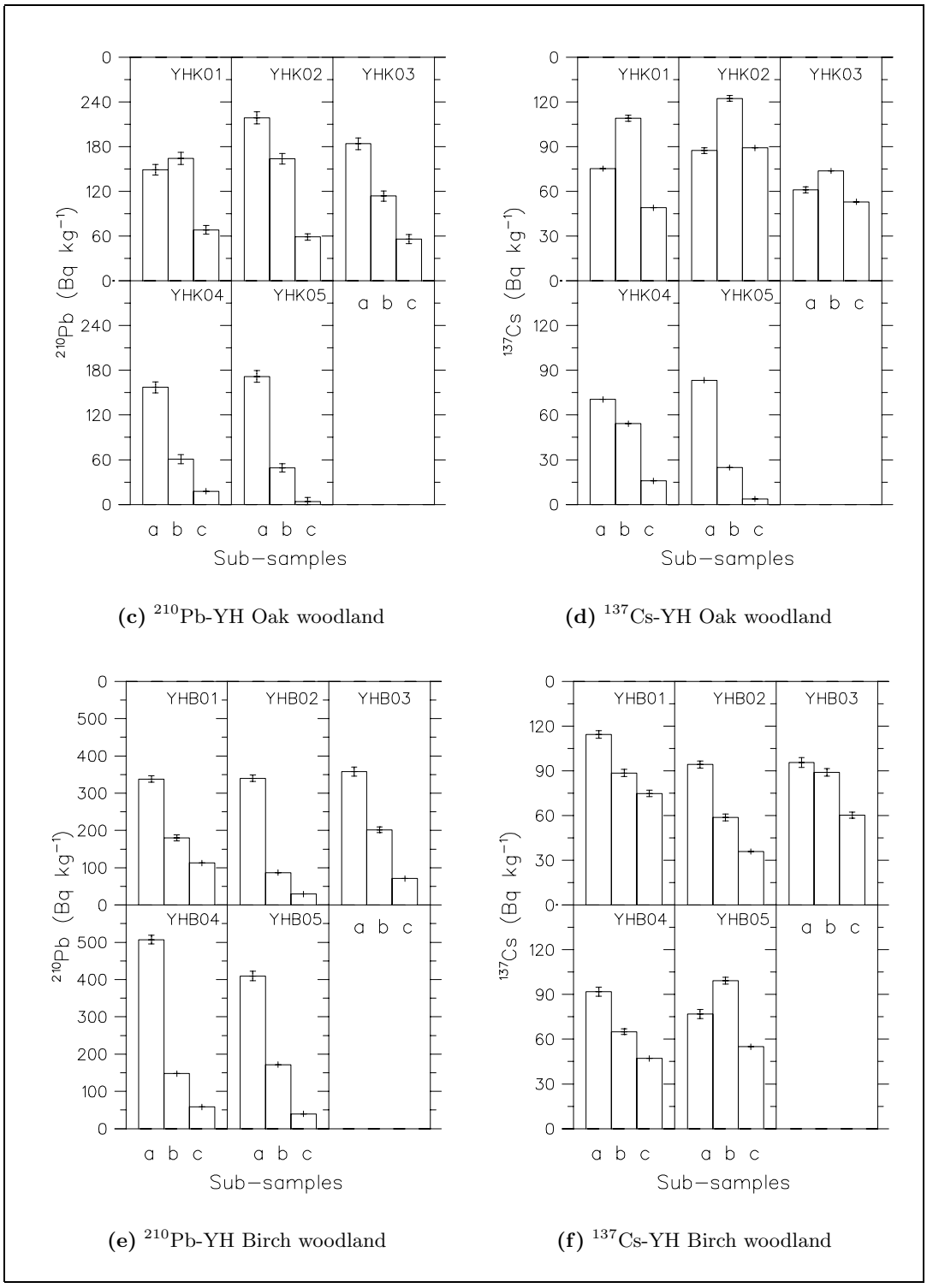

(c) ^{210}Pb-YH Oak woodland

(d) ^{137}Cs-YH Oak woodland

(e) ^{210}Pb-YH Birch woodland

(f) ^{137}Cs-YH Birch woodland

Figure 5.6: *Variation in ^{210}Pb and ^{137}Cs specific activities with soil depth at Ynys Hir site: (a) and (b) are the ^{210}Pb and ^{137}Cs activities in moorland soils: (c) and (d) are the ^{210}Pb and ^{137}Cs activities in oak woodland canopy soils: and (e) and (f) are the ^{210}Pb and ^{137}Cs activities in birch woodland canopy soils* (continued from previous page).

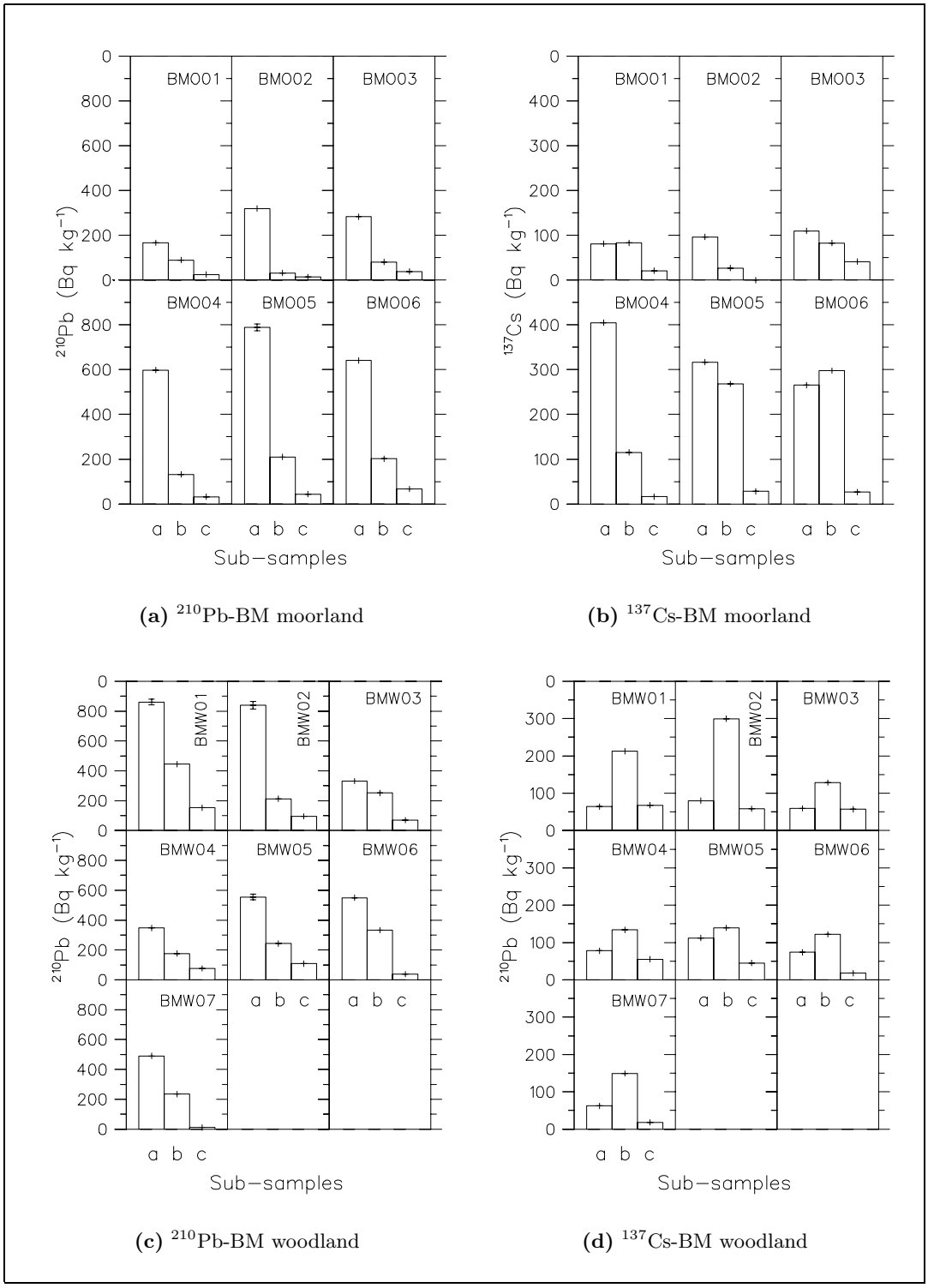

(a) ^{210}Pb-BM moorland

(b) ^{137}Cs-BM moorland

(c) ^{210}Pb-BM woodland

(d) ^{137}Cs-BM woodland

Figure 5.7: *Variation in ^{210}Pb and ^{137}Cs specific activities with soil depth at Bryn Mawr site: (a) and (b) are the ^{210}Pb and ^{137}Cs activities in moorland soils: (c) and (d) are the ^{210}Pb and ^{137}Cs activities in woodland canopy soils.*

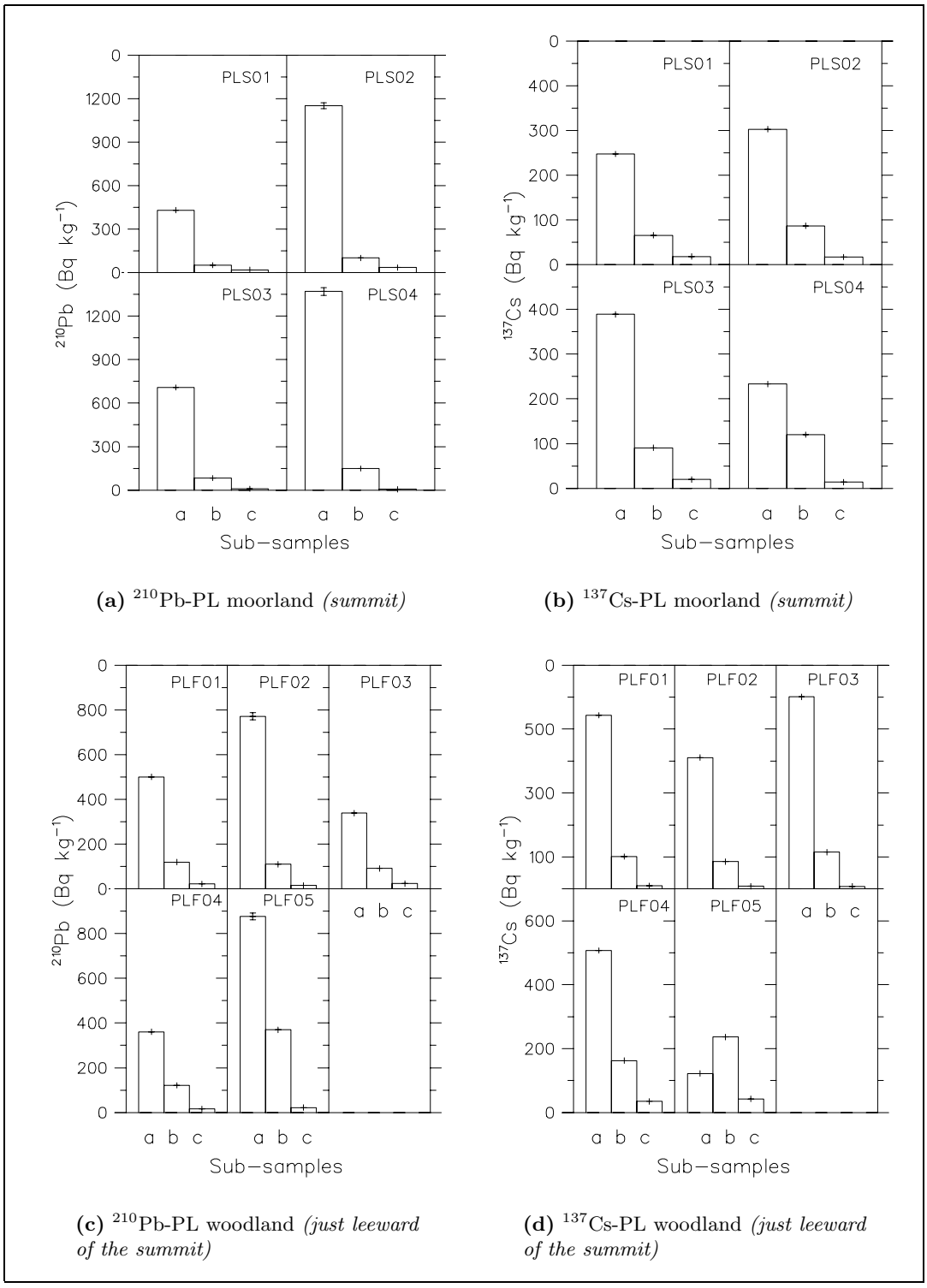

(a) ^{210}Pb-PL moorland *(summit)*

(b) ^{137}Cs-PL moorland *(summit)*

(c) ^{210}Pb-PL woodland *(just leeward of the summit)*

(d) ^{137}Cs-PL woodland *(just leeward of the summit)*

Figure 5.8: (Continued on next page). *Variation in ^{210}Pb and ^{137}Cs specific activities with soil depth at Plynlimon site: (a) and (b) are the ^{210}Pb and ^{137}Cs activities in moorland soils at the summit: (c) and (d) are the ^{210}Pb and ^{137}Cs activities in moorland soils just leeward of the summit: (e) and (f) are the ^{210}Pb and ^{137}Cs activities in woodland canopy soils: (g) and (h) are the ^{210}Pb and ^{137}Cs activities in the disturbed (PLW02) woodland sample.*

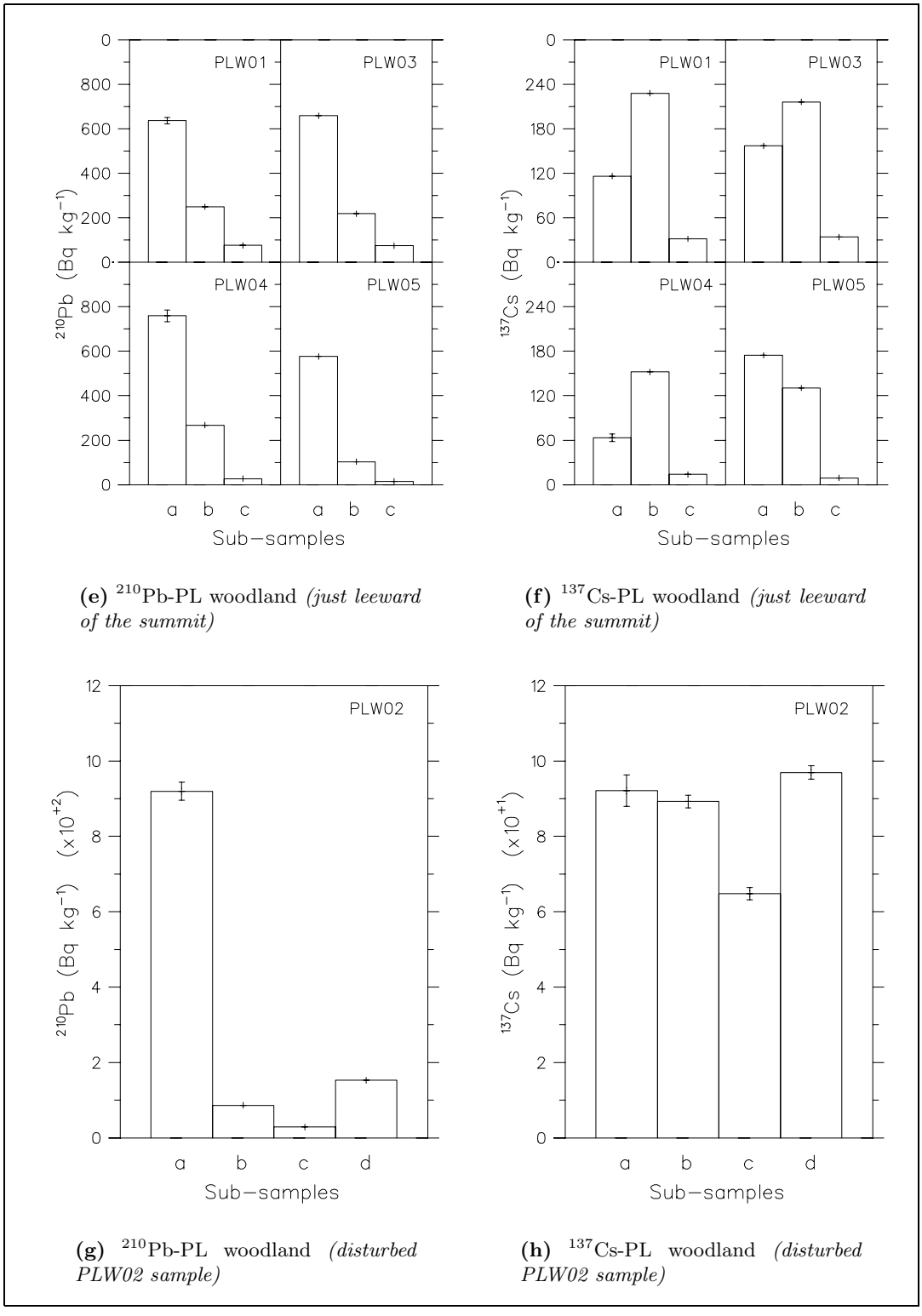

(e) ^{210}Pb-PL woodland *(just leeward of the summit)*

(f) ^{137}Cs-PL woodland *(just leeward of the summit)*

(g) ^{210}Pb-PL woodland *(disturbed PLW02 sample)*

(h) ^{137}Cs-PL woodland *(disturbed PLW02 sample)*

Figure 5.8: *Variation in ^{210}Pb and ^{137}Cs specific activities with soil depth at Plynlimon site: (a) and (b) are the ^{210}Pb and ^{137}Cs activities in moorland soils at the summit: (c) and (d) are the ^{210}Pb and ^{137}Cs activities in moorland soils just leeward of the summit: (e) and (f) are the ^{210}Pb and ^{137}Cs activities in woodland canopy soils: (g) and (h) are the ^{210}Pb and ^{137}Cs activities in the disturbed (PLW02) woodland sample* (continued from previous page).

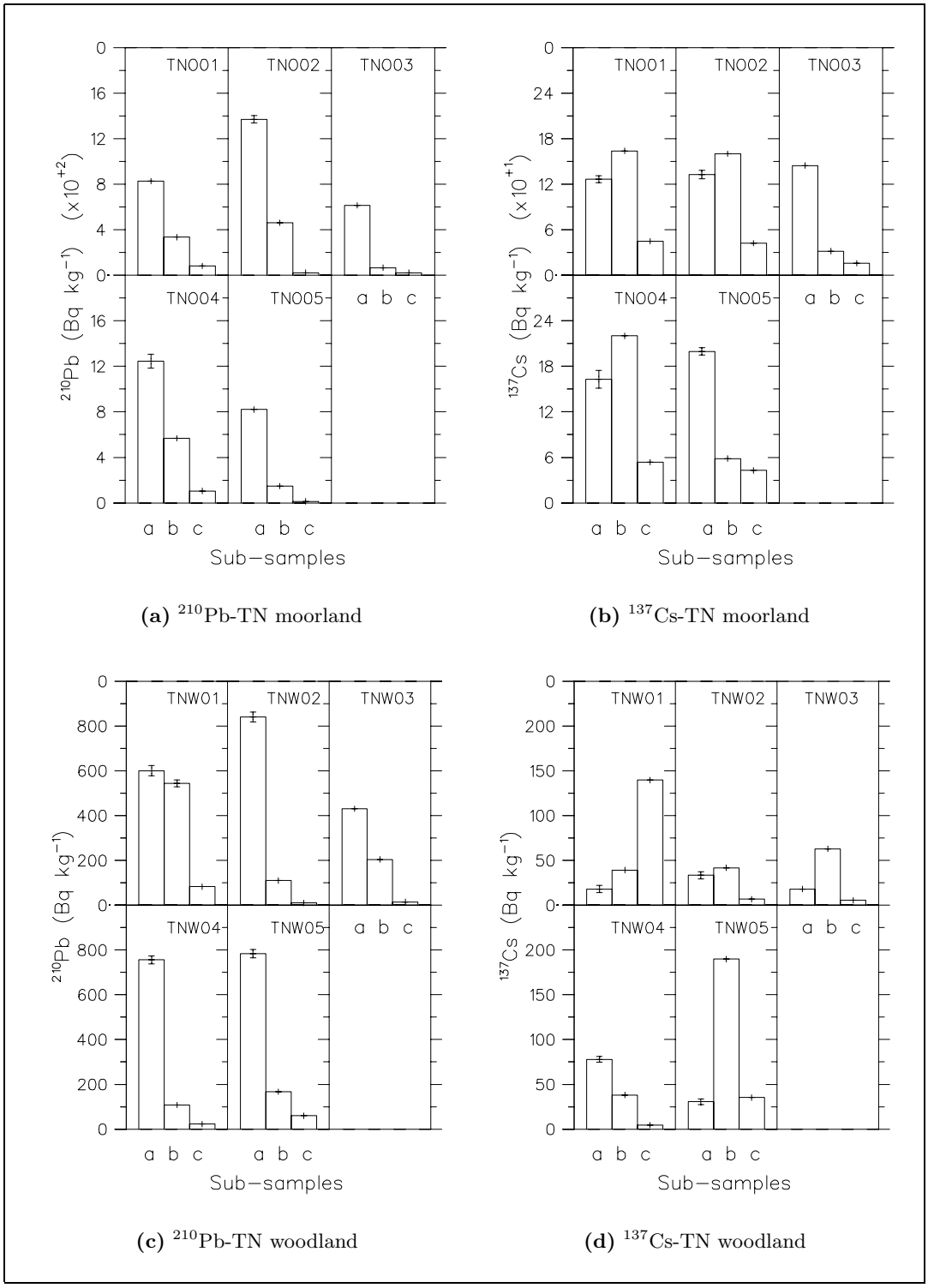

(a) ^{210}Pb-TN moorland

(b) ^{137}Cs-TN moorland

(c) ^{210}Pb-TN woodland

(d) ^{137}Cs-TN woodland

Figure 5.9: *Variation in ^{210}Pb and ^{137}Cs specific activities with soil depth at Tanllwyth Valley site: (a) and (b) are the ^{210}Pb and ^{137}Cs activities in moorland soils: (c) and (d) are the ^{210}Pb and ^{137}Cs activities in woodland canopy soils.*

5.3.1 Variation in ^{210}Pb and ^{137}Cs Activities with Soil Depth

When comparing the activity profiles presented by samples YHO(01, 02 & 03) to the ones presented by YHO(04 & 05) in figure 5.6 (a), it appears that there are two distinct features that indicate differences between the two sets of samples: (1) the fallout ^{210}Pb specific activities at the topmost sections of the soils (at 0-5 cm depth interval) ranged between 50 and 100 Bq kg^{-1} for YHO(01, 02 & 03) samples compared to the 300 to 350 Bq kg^{-1} range presented by samples YHO(04 & 05): and (2) there are no significant variations in the ^{210}Pb concentrations between the first and the subsequent subsections of soils in the YHO(01, 02 & 03) samples, compared to samples presented by YHO(04 & 05). Both sets of samples were obtained on a moorland area, however, samples presented by YHO(01, 02 & 03) were taken on a very gentle slope, whereas, the other two samples (YHO(04 & 05)) were obtained from a relatively flat area, within a fence and presumably free from grazing. Different features presented by the two sets of samples suggest that, soils presented by YHO(01, 02 & 03) may have been subjected to some form of human activity influencing the vertical distribution ^{210}Pb in soils presented in these samples. The area where YHO(01, 02 & 03) were sampled was prone to human disturbance due to its proximity to the access footpath into the Nature Reserve. The variation in ^{210}Pb activities with soil depths for soils sampled under oak (YHK, except for YHK01) and birch (YHB) woodland canopies, presented in figures 5.6 (c) and (e), respectively, showed an expected exponential decrease with increase in depth. It was, however, difficult to ascribe the anomaly presented by YHK01 to any form of site characteristics.

Considering the ^{210}Pb activity profiles in Bryn Mawr moorland soils, figure 5.7 (a), the concentrations of ^{210}Pb in BMO(01-03) samples were relatively low when compared with those in BMO(04-06) samples. However, their activity distributions with soil depths depicted a similar trend (*i.e.*, an expected exponential decrease with increase in depth). The difference presented by the two sets may be attributed to site characteristics. Samples presented by BMO(04-06) were obtained at a boundary between the forest edge, facing the prevailing westerly winds, and the moorland area, whereas BMO(01-03) were sampled a few metres away from the forest edge, but next

to the access road into the forest. Thus, relatively high ^{210}Pb concentrations reflected by BMO(04-06) may be influenced by bounced off particles from the forest edge due to increased turbulence resulting from the sudden change in surface roughness. A clear forest-edge effect was detected with the woodland BMW(01 to 07) samples, in figure 5.7 (c). It was found that the ^{210}Pb concentrations in BMW01 are relatively higher when compared to the other six samples presented by BMW(02 to 07). It appears that there is a gradual decrease, from BMW01 to BMW03, in the ^{210}Pb concentrations suggesting that forest edge effect diminishes with distance into the woodland. BMW01 was sampled approximately 3 m from the edge of the woodland. Samples BMW(02-04), BMW(05 & 06) and BMW07 were obtained approximately 5, 10 and 15 m into the woodland, respectively.

The concentrations of ^{210}Pb in soils obtained from the summit of Plynlimon (PLS-samples), presented in figure 5.8 (a), decrease exponentially with soil depth, however, ^{210}Pb concentrations in the topmost subsections of PLS(01 & 03) were significantly lower than those in PLS(02 & 04) samples. Similarly, topmost subsections of PLF(01, 03 & 04), obtained on a moorland, just leeward of the summit were also low when compared to PLF(02 & 05), given in figure 5.8 (c). The variabilities in activities of ^{210}Pb at the top sections of the core profiles may be attributed to lateral redistribution of ^{210}Pb influenced by the local undulations. Furthermore, almost all the ^{210}Pb in both PLS and PLF samples were confined at the topmost 10 cm of sections of the cores, suggesting very little permeability of the fallout component of ^{210}Pb at depths greater than 10 cm at this site. It appears that the organic matter confined at the top 10 cm of Plynlimon soils efficiently retains most of the fallout ^{210}Pb, in support of the findings reported by most authors (for example, Lewis [94] and Nozaki *et al.* [52]). There are, however, no pronounced variabilities in the ^{210}Pb concentrations for soils obtained under the woodland area at this site, as indicated by figure 5.8 (e), probably because most the ^{210}Pb in soils under forest canopies reach the ground surface as litterfall and are trapped in place because of shielding provided by the canopy. As already discussed in section 5.2.3, the ^{210}Pb distribution given by PLW02 in figure 5.8 (g) was attributed to soils disturbance.

Specific activity distributions of ^{210}Pb with soil profiles at Tanllwyth present the expected exponential decrease with increase in soil depths for samples obtained from both moorland and woodland areas (figure 5.9). Like in Plynlimon soils, most of the ^{210}Pb was confined to the top 10 cm of the core samples.

The activity profiles of ^{137}Cs also follow a similar trend as that presented by the ^{210}Pb activity distributions with depth in most soils, for example: Ynys Hir, figure 5.6 (f); Bryn Mawr, figure 5.7 (b); and Plynlimon, figure 5.8 (b) and (d). However, most soils exhibited subsurface maximum concentrations of ^{137}Cs, mostly in woodland canopy samples. Two possible explanations could be given: (1) Older deeper organic matter contains the litter from the Chernobyl event and the upper horizon therefore contains much smaller ^{137}Cs concentrations, or that: (2) The high mobility of ^{137}Cs in woodland canopy soils may be influenced by the high organic matter content in woodland soils. Greater depth of penetration of ^{137}Cs in organic rich soils, relative to mineral soils measured in catchments in Cumbria was reported by Smith *et al.* [118]. They attributed this to the very low dry bulk densities of highly organic soils. Most studies involving ^{137}Cs activity *versus* depth profile have indicated well defined subsurface peaks. This pattern of distribution has been attributed to contributions of weapons test ^{137}Cs fallout to the content in soils by most authors, for example, Smith *et al.* [118], Livens *et al.* [128] and Bonnett and Cambray [129]. Data obtained from this study are, however, too sparse to justify any speculation that may link features depicted by ^{137}Cs activity distribution is soils to any possible correlation.

5.3.2 Inventories of ^{210}Pb and ^{137}Cs in Soils

Tables 5.1 to 5.4 give the integrated ^{210}Pb and ^{137}Cs soil inventories in each sample from the sites. The mean inventories in both moorland and woodland canopy samples and the intra-site variabilities (indicated by % CoV) in the inventories measured between sample replicates, are also presented.

Ynys Hir Site

Inventories of ^{210}Pb and ^{137}Cs in moorland soil samples (YHO), and in oak and birch woodland canopy soils (YHK and YHB, respectively) are presented in table 5.1.

Table 5.1: *The ^{210}Pb and ^{137}Cs inventories in soils sampled from Ynys Hir. CoV (in %) measures intra-site variabilities.*

Core Number	Inventories (Bq m^{-2})	
	^{210}Pb	^{137}Cs
YHO01	3992 ± 195	1957 ± 44
YHO02	4012 ± 365	2041 ± 71
YHO03	3847 ± 295	1953 ± 61
YHO04	4103 ± 107	1803 ± 31
YHO05	3176 ± 112	1174 ± 33
Mean	3826 ± 375	1786 ± 352
CoV (%)	10	20
YHK01	5775 ± 225	3620 ± 45
YHK02	6872 ± 189	5391 ± 49
YHK03	5042 ± 220	3196 ± 51
YHK04	5885 ± 258	3503 ± 55
YHK05	5550 ± 300	2776 ± 58
Mean	5825 ± 669	3697 ± 1002
CoV (%)	11	27
YHB01	3166 ± 66	1379 ± 21
YHB02	2648 ± 60	1158 ± 21
YHB03	3820 ± 92	1562 ± 29
YHB04	3773 ± 72	1230 ± 21
YHB05	3561 ± 87	1493 ± 27
Mean	3394 ± 439	1364 ± 153
CoV (%)	13	11

On comparing ^{210}Pb and ^{137}CS concentrations in soils between samples presented by YHO(01-03) with YHO(04 & 05) samples, discussed in section 5.3.1, it was found that the latter samples presented relatively lower concentrations than the former, however, when these results are presented as Bq m^{-2}, the coefficients of variation indicate insignificant variabilities (CoV = 10% and 20% in ^{210}Pb and ^{137}Cs, respectively) in the deposition of the two isotopes. This was due to the effect of different dry bulk densities of the two sets of samples. The YHO(04 & 05) samples contained high content of organic material. Thus, their dry bulk densities were relatively lower when

compared to the mineral-rich YHO(01-03) samples.

Inventories of both ^{210}Pb and ^{137}Cs in soils under oak woodland were significantly higher ($P < 0.0002$; $t = 6.55$, $df = 8$ and $P < 0.0009$; $t = 5.13$, $df = 8$, respectively) than inventories measured in soil sampled under the birch woodland canopy. Soils under the birch woodland were very wet, suggesting that the area might have been frequently covered with water during periods of heavy rains. Therefore, lower inventories of ^{210}Pb and ^{137}Cs measured at this area, relative to those measured in oak woodland soils may be ascribed to lack of permeability of the fallout material due to washout of the top soils. Thus, ^{210}Pb and ^{137}Cs inventories measured under birch woodland soils may not represent typical woodland soil inventories expected at this site. It was therefore found reasonable to remove these values from the final interpretation of these results presented in section 5.3.3.

Bry Mawr Site

Inventories of ^{210}Pb and ^{137}Cs in BMO(01-03) soils were generally lower than those for BMO(04-06) samples, table 5.2.

Table 5.2: *The ^{210}Pb and ^{137}Cs inventories at the Bryn Mawr site. CoV (in %) measures the intra-site variability.*

Core Number	Open Grassland (Bq m^{-2})		Woodland Canopy (Bq m^{-2})	
	^{210}Pb	^{137}Cs	^{210}Pb	^{137}Cs
BMO/W01	3022 ± 169	2208 ± 39	12419 ± 180	3499 ± 40
BMO/W02	3822 ± 293	1454 ± 40	8749 ± 195	5549 ± 53
BMO/W03	4768 ± 173	3145 ± 43	6940 ± 198	3075 ± 46
BMO/W04	7673 ± 209	5430 ± 55	7566 ± 157	3378 ± 44
BMO/W05	8155 ± 197	6305 ± 60	7022 ± 155	2508 ± 32
BMO/W06	7712 ± 196	5906 ± 59	6718 ± 230	2111 ± 50
BMW07	-	-	5396 ± 219	2767 ± 61
Mean	5859 ± 2253	4075 ± 2068	7830 ± 2258	3270 ± 1116
CoV (%)	38	50	29	34

The mean ^{210}Pb inventories in soils presented by BMO(01-03) and BMO(04-06) were 3871 ± 874 and 7847 ± 268, respectively, providing a difference of a factor of ∼2. Similarly, the mean ^{137}Cs inventories in soils presented by BMO(01-03) that BMO(04-

06) were 2269 ± 847 and 5880 ± 438, respectively, giving a difference of a factor of ∼2.6. Two possible explanations for these observations are given: (1) higher ^{210}Pb and ^{137}Cs inventories in moorland soils sampled at a woodland boundary suggest that these soils may be receiving additional input of fallout material influenced by the adjacent forest edge. Because the forest stand was oriented approximately at right angles to the westerly prevailing winds, the edge of the forest presented a sudden change in surface roughness, and consequently an alteration in the vertical wind profile, resulting in increased interception and impaction of particle and cloud droplets, and possible bounce-off of particles depending on the turbulence intensities and: (2) it is also possible that the BMO(01-03) samples may also be losing some of their topmost material from erosion, due their proximity to the road. The latter explanation is supported by lack of pronounced forest-edge effect in ^{137}Cs inventories measured in woodland soils, as discussed below.

A significant influence of the forest edge was observed with the ^{210}Pb inventory measured in a sample obtained at 3 m from the wind-facing edge, presented by BMW01. A sample obtained ∼5 m from the forest edge (BMW02), into the woodland canopy, indicated a sharp reduction in the ^{210}Pb inventory. Furthermore, inventories of ^{210}Pb in subsequent samples were getting progressively lower with increase in distance into the forest stand. The forest edge effect was, however, not detected with the ^{137}Cs measurements. This could be due to the insignificant level of ^{137}Cs concentrations in the environment. The ^{137}Cs inventories measured in soils are a legacy of the nuclear weapons testing and the 1986 Chernobyl nuclear reactor accident. Thus, unlike ^{210}Pb, there is no constant supply of ^{137}Cs to the ecosystem. Given that the levels of ^{137}Cs were significantly lower in BMO(01-03) than in BMO(04-06) soils, then it may be possible that this lower level of both ^{210}Pb and ^{137}Cs in BMO(01-03) were due to the removal of topmost material of soils due to erosion. It was found reasonable to remove the ^{210}Pb inventory measured in BMW01 from subsequent analyses because it was not representative of moorland soil inventories due to its enhancement from the forest edge-effect. Thus, the mean ^{210}Pb soil inventory in woodland was estimated to be 7065 ± 1096 (CoV = 16%).

Plynlimon Mountain Site

The mean ^{210}Pb and ^{137}Cs inventories in moorland soils sampled at Plynlimon sites are presented in table 5.3.

Table 5.3: *The ^{210}Pb and ^{137}Cs inventories at the Plynlimon site. CoV (in %) measures the intra-site variability.*

Core Number	Inventories (Bq m^{-2})	
	^{210}Pb	^{137}Cs
PLS01	7695 ± 243	5753 ± 58
PLS02	10293 ± 258	3752 ± 58
PLS03	8671 ± 293	6546 ± 81
PLS04	10323 ± 223	3856 ± 45
Mean	9246 ± 1290	4977 ± 1393
CoV (%)	14	28
PLF01	8210 ± 228	8023 ± 77
PLF02	8887 ± 214	5053 ± 62
PLF03	7506 ± 191	7152 ± 56
PLF04	6110 ± 185	8821 ± 70
PLF05	9025 ± 195	4217 ± 60
Mean	7948 ± 1192	6653 ± 1957
CoV (%)	15	29
PLW01	7954 ± 150	3781 ± 39
PLW02	10011 ± 195	5120 ± 48
PLW03	7169 ± 189	3952 ± 51
PLW04	8303 ± 228	2482 ± 49
PLW05	6527 ± 279	3470 ± 57
Mean	7993 ± 1323	3761 ± 949
CoV (%)	16	25

The mean ^{210}Pb in summit (PLS) samples was significantly higher ($P < 0.08$; $t = 1.57$, $df = 7$) that inventories measured at an area just at the leeward side of the summit (PLF-samples). The PLF samples were obtained approximately 200 m on the eastern side of summit, at an altitude of ∼700 m asl. Relatively high ^{210}Pb inventories measured in PLS samples may be attributed to contributions from occult deposition due to the presence of cap clouds in contact with the summit. Furthermore, assuming a constant surface roughness over the mountain, extending from the windward side of the summit to an area where PLF samples were extruded, then the zone of frequently high mean wind speeds is expected just at the summit. Consequently, a maximum

turbulent deposition of cloud droplets also is expected to be centred at and just upwind of the mountain summit. Thus, the PLF moorland area is sheltered from high winds and also the site is in a zone of cloud evaporation due to descending moist air. Field measurements conducted by Fowler *et al.* [130] at Great Dun Fell, a site 620 m above sea level, indicated that input due to occult deposition was responsible for about 8% of the rainfall total to moorland vegetation. Based on the ^{210}Pb inventories in soils discussed above, and assuming a 10% input due to occult deposition at this site, occult deposition at the leeward site is accountable for about 795 Bq m^{-2} of ^{210}Pb deposition, 7153 Bq m^{-2} is due to deposition by rainfall. Assuming a negligible contribution of dry deposition to the total deposition at a mountain site and also that, due to the short distance between sites, the ^{210}Pb deposition in rainfall is the same at both the summit and downwind sites, then occult deposition at the summit (PLS-site) is estimated to contribute ∼2100 Bq m^{-2} of ^{210}Pb inventory in soil. This figure represents 23% of the total deposition of ^{210}Pb and 29% of the amount deposited in rainfall. However, this figure may be an underestimate, as pointed out in the discussion below.

Interestingly, the mean ^{210}Pb inventory in woodland canopy soils was not significantly different ($P < 0.27$; $t = 0.66$, $df = 7$) from the mean ^{210}Pb inventory measured in moorland (PLF-samples). Given the increased aerodynamic surface roughness due to the presence of woodland canopy, and the high elevation of this site, a significantly larger ^{210}Pb inventory under forest canopy soils relative to the adjacent moorland soils was expected. Lack of enhanced ^{210}Pb inventories over that of the adjacent moorland area at this site may be attributed to land use. The forest of Plynlimon (Hafren forest) was planted over a period of 40 years, beginning in the 1930s. From 1985, some parts of the forest were clear-felled as part of the experiment in progress to investigate some of the environmental impacts of forestry practice upon upland waters [131] [132]. Based on this information, the lack of a difference in the ^{210}Pb inventories between the two sites suggest that the PLF samples may have been obtained from a felled area. Because the clearing commenced in 1985 (∼20 yrs ago), the moorland soils may still possess properties typical of woodland canopy soils. This would result in the ^{210}Pb inventory measured at this site being higher than expected. Bonnett and

Appleby [133] reported unsupported ^{210}Pb core inventory of 6070 Bq m^{-2} at a site in Llyn Llygad Rheidol, at an altitude of ∼600 m (rainfall; 2000 mm/yr.) on the north western slopes of Plynlimon. This sites was only 2.5 km west of the sampled sites at Plynlimon, reported in this study. Based on the ^{210}Pb inventory presented by Bonnett and Appleby and assuming a linear dependence of the ^{210}Pb deposition on the amount of rainfall, the moorland ^{210}Pb inventory at the PLF site sampled in this study was estimated as 7000 Bq m^{-2}. This figure is not unreasonable, considering that the altitude and rainfall at site are 700 m asl. and 2400 mm/yr, respectively. Based on this result, occult deposition at summit (PLS-site) is estimated to account for ∼2946 Bq m^{-2} of the ^{210}Pb inventory in soil. This figure represents 32% of the total deposition of ^{210}Pb and 48% of the amount deposited in rainfall. This figure is significantly greater than the estimated 20% reported by Dollard *et al.* [134], based on measurements conducted at Great Dun Fell, for occult deposition of chemical species in areas prone to low cloud. However, the results for different specific sites could be different.

Inventories of ^{137}Cs in soils from Plynlimon site do not follow the same trend as that presented by ^{210}Pb: (1) the mean ^{137}Cs inventory in the summit soils were significantly lower ($P < 0.10$; $t = 1.44$, $df = 7$) than ^{137}Cs inventories in PLF soils: and (2) the mean ^{137}Cs inventory in moorland soils was significantly higher ($P < 0.008$; $t = 3.13$, $df = 7$) than that in adjacent woodland soils. High levels of ^{137}Cs inventories in PLF samples, just below the summit, relative to the summit inventories may be attributed to the Chernobyl component of ^{137}Cs (discussed in section 5.3.3.3). Lower ^{137}Cs inventory in woodland soils may be explained by the degree of disturbance in these soils when the trees were planted.

Tanllwyth Valley Site

Soil inventories of ^{210}Pb and ^{137}Cs sampled at Tanllwyth, on the eastern slopes of Plynlimon ∼4 km from the summit are presented in table 5.4.

Table 5.4: *The ^{210}Pb and ^{137}Cs inventories at the Tanllwyth Valley site. CoV (in %) measures the intra-site variability.*

Core Number	Open Grassland (Bq m^{-2})		Woodland Canopy (Bq m^{-2})	
	^{210}Pb	^{137}Cs	^{210}Pb	^{137}Cs
TNO/W01	6503 ± 131	2260 ± 34	8772 ± 262	5626 ± 74
TNO/W02	6692 ± 155	2638 ± 39	8488 ± 414	1366 ± 89
TNO/W03	6086 ± 109	1925 ± 32	8202 ± 347	1708 ± 62
TNO/W04	8910 ± 245	2469 ± 51	8156 ± 324	1430 ± 63
TNO/W05	6496 ± 134	2317 ± 42	8798 ± 283	4706 ± 71
Mean	6937 ± 1125	2322 ± 266	8483 ± 304	2967 ± 2037
CoV (%)	16	11	4	69

The coefficient of variation in the distribution of ^{210}Pb on both moorland and woodland samples of 16% and 4%, respectively suggest a fairly uniform deposition of the radioisotope. Similarly, a fairly uniform distribution in ^{137}Cs deposited in the moorland was also obtained. However, this was not the case with soils obtained under the woodland canopy, indicated by a CoV of ∼69%. Relatively higher inventories in core samples TNW(01 & 05) may be due to the mobility of ^{137}Cs within the soils influenced by the heterogeneity of the ground surface. The TNW(01 & 05) soils were sampled between the rows of the Sitka tree stands, whereas the rest of the samples were obtained on the ridges that were along rows. Thus, an additional input of ^{137}Cs in TNW(01 & 05) may be influenced by the gradual release from the ridges.

5.3.3 Deposition of ^{210}Pb and ^{137}Cs at Sites

As discussed in sections 5.2.3 and 5.3.2, samples presented by YNB(01-05), BMW01 (^{210}Pb inventory, only) and PLW02 are not considered in these discussions. Because the removal of atmospheric ^{210}Pb and ^{137}Cs occurs primarily through wet deposition processes and the inventories of these isotopes in soils are expected to be closely associated with the rainfall pattern, it is useful to first discuss the mean annual rainfall at these sites. The annual average rainfall, obtained from the mean annual rainfall map of Britain [121], varied greatly between sites. The profiles of the variation in rainfall with altitude over the transect considered in this study are presented in figure 5.2.

The mean rainfall at the coast (Ynys Hir site) is 1300 mm yr^{-1}, and increases going inland with altitude. Taking the rainfall amount of 1300 mm/yr at Ynys Hir to represent the non-enhanced west coast rainfall (although rainfall at the coast is about 100 or 200 mm/yr higher than that at the coast, see figure 5.2), the enhancement factors in rain falling over Bryn Mawr, Plynlimon and Tanllwyth, due to orography, were calculated to be 1.38 (430m asl.), 1.85 (741 and 700 m asl.) and 1.54 (350 m asl.), respectively. Pedgley [135], put forward two principal reasons for heavy rainfall over mountain areas: (1) mountains act as barrier to moist airstreams. The moist airstreams are therefore forced to rise, producing clouds by the processes of expansion and cooling of the rising air, and: (2) when the days are sunny, mountains act as high-level heat sources. Thus, convective cloud formation may result, even when the effect in (1) is negligible. Enhanced rainfall over moderately sized hills of western Britain has been attributed to the effect of orography on frontal systems coming from the Atlantic Ocean, mainly from westerly and/or south-westerly directions [136]. Considering the mean annual rainfall at these sites, it seems that the rainfall is already significantly enhanced at Bryn Mawr (∼430 m asl.) due to uplifting of airmasses by the extent of land (15 km) from the coast. Fowler *et al.* [37], using rainfall measurements collected at a hill site in Cumbria, found that a rise in altitude of 600 m from the base of the hill summit was accompanied by an increase approximately a factor of two in the amount of rainfall measured at the hill summit.

5.3.3.1 Profile of ^{210}Pb Deposition

The distribution of ^{210}Pb deposited at these sites is characterised by the mean inventory values increasing with increase in altitude for both woodland and open grassland soils. The profile of ^{210}Pb deposition as a function of altitude is presented in figure 5.10. In moorland soils, the ratios of the inventories for Bryn Mawr, Plynlimon (PLS and PLF) and Tanllwyth relative to the coastal ^{210}Pb inventories measured for Ynys Hir increased by factors of 1.5 ± 0.6, 2.4 ± 0.3, 2.1 ± 0.3 and 1.8 ± 0.3, respectively. The decrease in the enhancement factors from the 2.4 ± 0.3, presented by the ^{210}Pb inventories in summit (PLS) soils to 1.8 ± 0.3 at Tanllwyth indicates

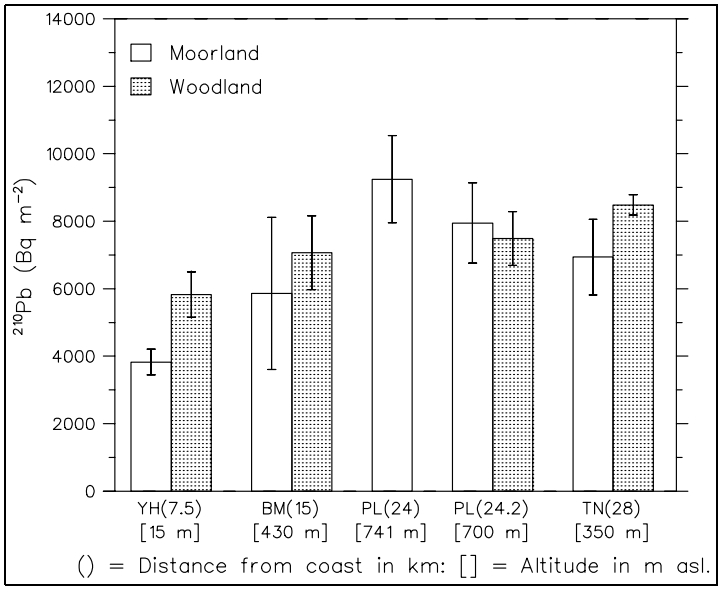

Figure 5.10: *Variation in ^{210}Pb inventories (open and woodland soils) with altitude:* numbers in round brackets '()' indicate site distance in kilometres, from the west coast; numbers in square bracket '[ ]' indicate site altitude, in metres above sea level.

that the seeder-feeder process becomes less effective as the altitude decreased, moving eastwards of the mountain summit. Thus, the zone of maximum ^{210}Pb deposition is indicated to be at the summit (given by the PLS samples) for the sampled sites along this transect.

Considering the rainfall enhancement factors of 1.38, 1.85 and 1.54 over that recorded for Ynys Hir (1300 mm/yr) at the coast for Bryn Mawr, Plynlimon and Tanllwyth sites, respectively, it is possible to determine whether or not ^{210}Pb concentration in rain water and cloud water is enhanced at the summit of Plynlimon as would be expected. The enhancement factor for ^{210}Pb concentration due to the input of liquid water content at the summit of Plynlimon relative to that in the rainfall deposited at the coast is being enhanced by a factor of 1.3 $\pm$ 0.4. Assuming a 48% contribution of ^{210}Pb deposited in rainfall, inferred based on the results of Bonnet and Appleby [133], the ^{210}Pb concentration in cloud water at the summit becomes 1.9 $\pm$ 0.6 greater than that in the frontal rain. For the purpose of comparisons, table 5.5 presents enhancement factors (summit/valley and cloud/rain) for concentrations of major ions [37] and ^{210}Pb [21], conducted at Great Dun Fell.

Table 5.5: *The ratios of major ions and ^{210}Pb concentrations in feeder/seeder rain and feeder cloud/seeder rain.*

References	Fowler *et al.* (1988)					Mourne (1993)	This study
Species	H^+	NH_4^+	Cl^-	NO_3^-	SO_4^{2-}	^{210}Pb	^{210}Pb
summit/valley	2.9	3.1	2.9	2.3	2.2	1.6	1.3 ± 0.4
cloud/rain	3.9	2.4	2.6	2.8	2.0	2.2	1.9 ± 0.6

The lower ratios obtained for the ^{210}Pb concentrations obtained in this study may be due to a number of factors: (1) the spatial resolution of the rainfall isopleths used for estimating the mean rainfall for these sites was relatively poor. Overestimating the mean rainfall at the summit sites may lead to an underestimate in feeder/seeder ratios, and consequently, lower ratios of ^{210}Pb concentrations in cloud water to the ^{210}Pb concentrations in the seeder rain; (2) it is possible that the zone of maximum deposition may not be located at the sampled area, but centred elsewhere over the 4-kilometre stretch (taking the E-W transect) of the summit. Due to practical reasons, only one area was selected at the summit to represent ^{210}Pb inventories at the Plynlimon highest sites: and (3) the ^{210}Pb inventories in PLF soils may be lower than the estimated 7948 Bq m^{-2}, due to reasons stated earlier. The enhancement of ^{210}Pb concentration due to the input of liquid water deposited at Tanllwyth, over that at Ynys Hir was 1.2 ± 0.3, indicating that the input of cloud water deposition is less effective at this site, given its position and altitude, relative to Plynlimon mountain.

5.3.3.2 Effects of Woodland on ^{210}Pb Deposition

On considering inventories measured in soils under the wooded areas, significantly higher ^{210}Pb inventories in forest soils relative to the nearby moorland areas were measured in all but the Plynlimon (PLW and PLF) sites, indicated by the following percentage increase: 52% at YNYS Hir; 34% at Bryn Mawr (with the BMW01 inventory included in this calculation) and 22% at Tanllwyth. The mean enhancement factor for these sites (36%) is in line with the 43% reported in chapter 4 for lowland sites sampled in Edinburgh soils, indicating the influence of afforestation in the deposition of submicrometre particles to terrestrial surfaces. Due to the absence of wooded

areas over the summit of Plynlimon, it was not possible to estimate contributions due to occult deposition at the summit over that of the summit moorland soils. Because occult deposition increases with altitude, and that the increase becomes greater with wind speeds (and hence greater deposition by turbulence) as well as the duration of the clouds shrouding high elevations [137], significantly high ^{210}Pb inventories in woodland canopy soils would be expected due to increased surface roughness, influenced by afforestation. Fowler *et al.* [130] estimated that afforestation would increase the wet deposition input of major ions by approximately 50%. Over moorland vegetation, they estimated that cloud water deposition increases the wet deposition by approximately 12%.

The variations in ^{210}Pb inventories in both moorland and woodland soils with the mean annual precipitation are presented in figure 5.11 (A) and (B), respectively.

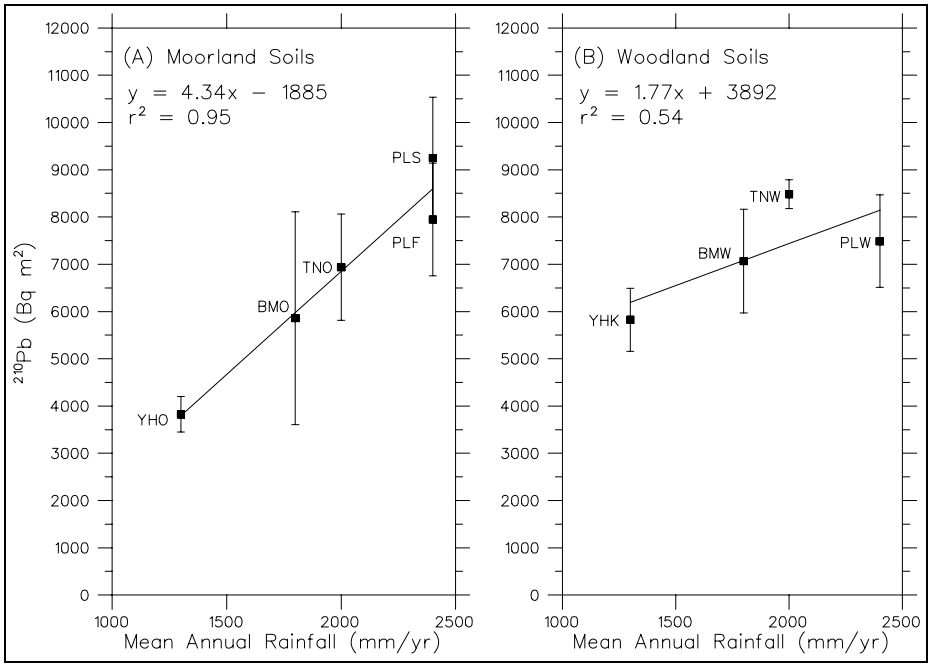

Figure 5.11: *Variation in ^{210}Pb inventories in; (A) moorland and (B) woodland soils with the mean annual rainfall.*

In moorland soils, the ^{210}Pb inventories are correlated strongly ($r^2 = 0.95$) with the amount of rainfall suggesting that the fallout of ^{210}Pb aerosols is mainly through wet deposition processes. Inventories of ^{210}Pb in woodland soils show a weak correlation with rainfall. Furthermore, the rate of increase of ^{210}Pb with increase in precipitation

is smaller than expected. A weak correlation in the deposited ^{210}Pb in woodland soils with rainfall is due to the fact that, the presence of a forest canopy alters the wet deposition pathways typical to open grassland areas (see chapter 4). The relatively small increase in ^{210}Pb inventories (even smaller than that obtained for moorland soils) may be attributed to the degree of disturbance in woodland soils (discussed in the next section).

5.3.3.3 Profile of ^{137}Cs Deposition

The distribution of ^{137}Cs inventories in soils as a function of altitude is presented in figure 5.12.

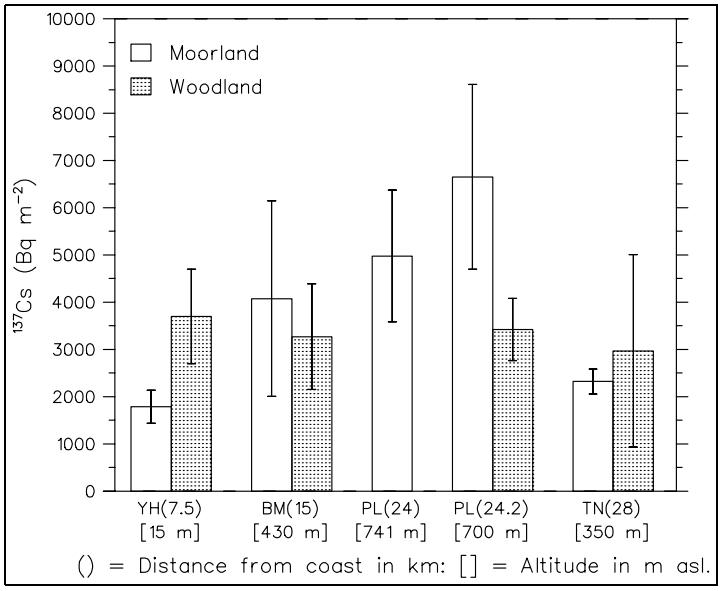

Figure 5.12: *Variation in ^{137}Cs inventories (open and woodland soils) with altitude:* numbers in round brackets '()' indicate site distance in kilometres, from the west coast; numbers in square bracket '[ ]' indicate site altitude, in metres above sea level.

The ^{137}Cs inventories in moorland soils indicated an increase with altitude, however, there is an insignificant variation (P = 0.85) with altitude in the deposition ^{137}Cs in woodland soils. The spatial patterns of ^{137}Cs deposited in soils can be due to a number of factors: (1) the non-uniform geographical distribution of rainfall, leading to wide variations in the deposition of total ^{137}Cs; (2) the local variations in rain falling over the regions of interest in this study, coincident with the initial fallout

plume from the Chernobyl accident; (3) the surface run-off of ^{137}Cs, particularly at high altitude, influenced by the increased gradient of the slopes; and (4) leaching loss of ^{137}Cs mobilized by rain.

The fallout ^{137}Cs present in the environment was due to the nuclear weapons testing and Chernobyl reactor accident. The component of ^{137}Cs resulting from nuclear weapon testing, ^{137}Cs(B), was injected into the upper troposphere and the stratosphere [138], and became well mixed throughout the northern hemisphere before depositing mainly through wet deposition processes over a number of years. Peirson and Salmon [139] found that, for seven sites in the UK situated far from the nuclear weapons test sites, there was a linear dependence of surface concentrations of ^{137}Cs with the mean annual rainfall. Thus, the distribution of ^{137}Cs(B) inventories in soils is expected to be linearly correlated with rainfall. On the other hand, the ^{137}Cs due to the Chernobyl reactor accident, ^{137}Cs(C), was not injected in the upper troposphere. Most of the activity delivered to the UK soils was mainly through convective precipitation events over the first week of May 1986, especially over the uplands of Wales, northern England and SW Scotland [88]. Thus, its spatial variability is likely to be greater, and unlike ^{137}Cs(B), the ^{137}Cs(C) deposits are not likely to be linearly dependent on rainfall amount.

No attempt was made to separate the ^{137}Cs(B) from the ^{137}Cs(C) deposited in this study, however, the measured total ^{137}Cs inventories in soils from these sites suggest the following: assuming that the ^{137}Cs(B) deposition are linearly related to the mean annual rainfall, higher than expected total inventories ^{137}Cs in soils between sites may be attributed to the large deposition and accumulation in soil of ^{137}Cs(C) influenced by rain coincident with the Chernobyl plume, whereas, the smaller than expected values would indicate removal of topsoil material and/or possibly, vertical migration beyond the sampled depth. Figure 5.13 presents the variation in the total measured ^{137}Cs inventories in soils with the mean precipitation.

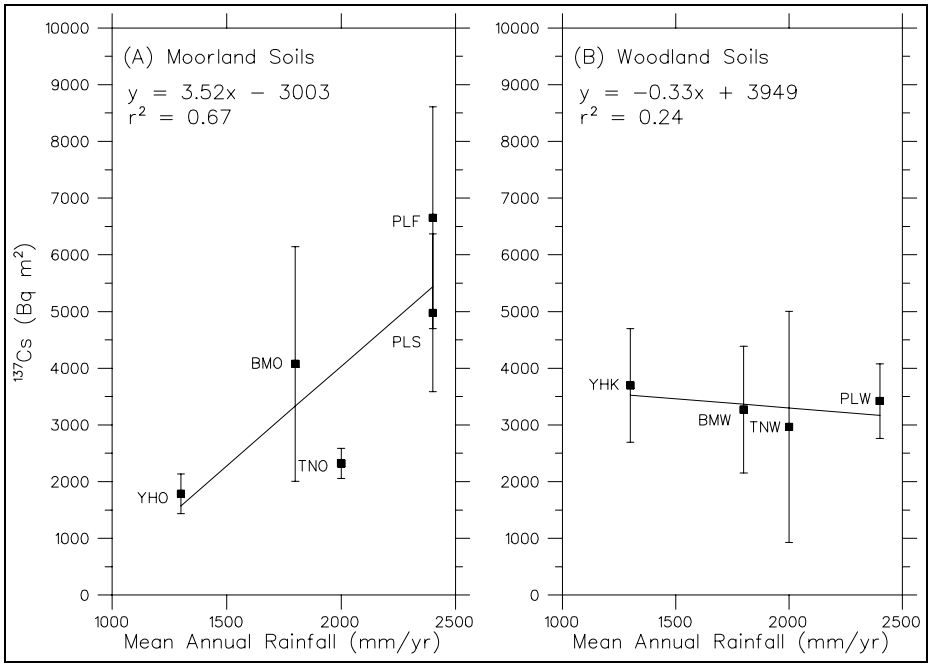

Figure 5.13: *Variation in ^{137}Cs inventories in; (A) moorland and (B) woodland soils with the mean annual rainfall.*

Looking at figure 5.13 (A), the measured inventories of ^{137}Cs in moorland soils increased with the increase in the amount of rainfall at the rates similar to those of ^{210}Pb. The mean ^{137}Cs inventory in PLF moorland soils was higher than that of the PLS samples. Although the mean inventories of the two sets of samples were insignificantly different (P = 0.19), the mean ^{137}Cs inventory in PLF moorland soils was not expected to be higher than that of the PLS samples. However, the increased inventory measured in the PLF samples may be attributed to loss of topmost soil material from the summit transported downwards, during periods of heavy rains. PLF samples were obtained ∼40 m below the summit. The grass over the sampled PLF area was relatively dense, and the site characteristics indicated that it might have been afforested. It seems reasonable that these features may possibly act as a 'sponge' to trap material coming down the slope. Lower than expected ^{137}Cs inventories at Tanllwyth may be due to two possible factors: (1) low fallout ^{137}Cs(C) at site: and/or (2) removal of the topmost soils containing the pre-Chernobyl ^{137}Cs deposits during the 1973 and 1977 floods [140], and/or infiltration of ^{137}Cs below the sampled depths. However, the activity profiles presented in figure 5.9 (b), show that more than 80% of the ^{137}Cs

was deposited in the upper 10 cm of the soils. Thus, low levels of ^{137}Cs inventories in moorland soils are due to particulate erosion. Low levels of ^{137}Cs(C) were reported by Bonnett *et al.* [141] in the area bordered by the Afon Hore and Tanllwyth rivers. They also attributed this to the removal of radiocesium by erosion.

A plot of ^{137}Cs inventories in woodland soils *versus* the mean annual precipitation, in figure 5.13 (B), indicate a little change in ^{137}Cs inventories with rainfall. It is expected that levels of ^{137}Cs should increase significantly with rainfall, and that the increase will be even higher in woodland soils when compared with that in moorland for each site, given the higher surface roughness provided by vegetation canopies. The uniform inter-site distribution of ^{137}Cs inventories, particularly at Bryn Mawr, Plynlimon and Tanllwyth is most likely due to the large uptake of ^{137}Cs by the trees than moorland sites. Large uptake of ^{137}Cs by vegetation in soils rich in organic have been reported by other workes, for example, Barber [142] and Livens *et al.* [128].

5.3.4 Fluxes and Concentrations of ^{210}Pb in Rainfall

The total ^{210}Pb flux to the ground surface at each site, and the ^{210}Pb concentrations in rain are presented in table 5.6.

Table 5.6: *The ^{210}Pb fluxes and concentrations for both moorland and woodland soils at each site.*

Sites	Altitude (m asl.)	^{210}Pb fluxes (Bq m^{-2} y^{-1})		^{210}Pb conc. (mBq l^{-1})
		Moorland	Woodland	
Ynys Hir	15	119 ± 12	181 ± 21	92 ± 9
Tanllwyth	350	216 ± 35	264 ± 9	108 ± 17
Bryn Mawr	430	182 ± 70	220 ± 34	101 ± 39
Plynlimon (PLF)	700	247 ± 37	233 ± 30	103 ± 15
Plynlimon (PLS)	741	286 ± 40	-	120 ± 17

The ^{210}Pb flux was obtained by multiplying the ^{210}Pb decay constant (λ) by the measured ^{210}Pb mean inventories (see equation 4.2). The derived ^{210}Pb concentrations were estimated based on the 30-year mean annual average rainfall at each site. The derived average concentrations of ^{210}Pb for the sampled moorland sites show a factor of ∼1.3 between the coast and the summit of Plynlimon mountain, in support of the

suggestion of the seeder-feeder scavenging process whereby the rain from high altitude frontal clouds scavenge the feeder clouds containing relatively high concentrations of ^{210}Pb than that in rainfall. It should be noted though that the values presented here are overestimates, since the processes of dry and occult deposition are included. Furthermore, the errors associated with these values may be large since the rainfall data used were interpolated from a low resolution rainfall isopleth map.

5.4 Conclusions

The effect of topography in the deposition of ^{210}Pb and ^{137}Cs using soil inventory measurements has been investigated at selected sites of low and moderately high altitudes in mid-Wales. The following are the main results obtained:

- Inventories of ^{210}Pb measured in moorland soils increased by a factor of 2.4 ± 0.4 with increase in altitude between the coast (15 m asl.) and the summit of Plynlimon (741 asl), whereas, rainfall exceeded that at the coast by a factor of ∼1.8. Furthermore, the increase in ^{210}Pb inventories in moorland soils was linearly proportional to the amount of rain, indicating that the deposition of ^{210}Pb aerosols is mainly through wet deposition processes.

- The ratio of ^{210}Pb concentrations in liquid water deposited at the summit to that in rainfall deposited at the coast was 1.3 ± 0.4. This indicates that the mountain site is an efficient collector of ^{210}Pb aerosols influenced by the seeder-feeder processes. Furthermore, the presence of cap-clouds that frequently shroud Plynlimon increases the ^{210}Pb concentration by 1.9 ± 0.6 over that in frontal rain.

- The mean enhancement factor in the deposition of ^{210}Pb in woodland canopy soils, relative to moorland soils for Ynys Hir, Bry Mawr and Tanllwyth sites was 36%. This is in line with the 43% reported in chapter 4 for lowland sites sampled in Edinburgh soils, indicating the influence of afforestation in the deposition of submicrometre particles to terrestrial surfaces.

Chapter 6

Summary and Further Work

6.1 Summary

Surface level air concentration measurements of ^{210}Pb and ^{7}Be were made to investigate factors affecting the concentrations of the isotopes in air. The influence of vegetation and topography in the deposition of atmospheric aerosols was investigated by means of quantitative measurements of ^{210}Pb and ^{137}Cs inventories in soils. Rain, throughfall and vegetation measurements of ^{210}Pb and ^{7}Be concentrations were also made to investigate the main pathways of submicrometre particles influecing the increased ^{210}Pb and ^{137}Cs measurements in woodland canopy soils. A summary of the main results obtained and suggestions for further work, is presented in this chapter.

6.1.1 Concentrations of ^{210}Pb and ^{7}Be in Air

Table 6.1 presents the mean ^{210}Pb concentrations in air obtained from this study, and compared with other results published in literature [143].

Table 6.1: *The ^{210}Pb concentrations in surface level air from this study, compared to other places in Europe.*

Location (latitude/longitude)	Name of Place	Altitude (m asl.)	Precipitation (mm/yr.)	^{210}Pb Conc. (mBq m^{-3})
55.7°N, 12.1°E (DE)	Riso	10	587	0.21
48.2°N, 11.6°E (GE)	Munich	490	1048	0.59
51.5°N, 01.5°W (UK)	Chilton	350	741	0.23
53.4°N, 06.2°W (UK)	Dublin	-	900	0.24
51.9°N, 10.2°W (UK)	Caherciveen	-	1470	0.17
†55.9°N, 03.2°W (UK)	Edinburgh	80	790	0.21

†This Study.
(DE) = Denmark; (GE) = Germany; (UK) = United Kingdom.

The concentrations of both ^{210}Pb and ^{7}Be in air were found to exhibit relatively low values during periods of low atmospheric pressure and relatively high values during high pressure periods. It was also found that periods of increased and decreased rainfall were associated with periods of low and high atmospheric pressure, respectively. Hence, it was concluded that the variation of these isotopes with pressure may be mainly due to the strong washout effects of the lower atmosphere by precipitation. Washout by rainfall is also able to explain the observed correlation in the monthly mean concentrations of ^{210}Pb and ^{7}Be. In addition, the ^{210}Pb results indicate that high concentrations correlated with air flow arriving from the continent and/or air that has resided longer over the continent.

The mean ^{210}Pb concentration obtained from this study (0.21 ± 0.17 mBq m^{-3}) compares well with other measurements in the UK, such as at Chilton (51.5°N, 01.5°W) and Dublin (53.4°N, 06.2°W). The lower concentrations at Caherciveen (51.9°N, 10.2°W) may be due to the relatively high rainfall at the site, considering that the location is at the west coast of Ireland. Over the continental area, for example, at Munich (48.2°N, 11.6°E), the mean ^{210}Pb concentration is higher.

The mean ^{7}Be concentration of 2.50 ± 1.24 mBq m^{-3}, reported in this study compares well with the other low-altitude ^{7}Be concentrations reported in literature for the northern midlatitudes areas: for example; 2.10 mBq m^{-3} reported for Chilton (UK) [70]; 1.43 mBq m^{-3} for Sutton (UK), 2.55 mBq m^{-3} for Mace Head (Ireland)

and 2.78 mBq m^{-3} for Berlin (Germany), cited from Brost *et al.* [66].

6.1.2 Inventories of ^{210}Pb and ^{137}Cs in Soils

Inventories of ^{210}Pb and ^{137}Cs in soils measured under moderately dense woodland canopies indicated average enhancements of 43% and 50% relative to nearby moorland areas, respectively. Because woodland and moorland sites were chosen to be in close proximity at each sampling location, the long-term average rainfall can be assumed to be the same for each of the woodland to moorland inventory comparisons. Thus, it was concluded that the enhancement in the deposition of ^{210}Pb and ^{137}Cs is most likely due to dry and/or occult deposited particles on the tree leaves. Direct measurements of ^{210}Pb and ^{7}Be concentrations in age graded Sitka needles and the sequential measurements of deciduous tree leaves: oak, lime and sycamore, showed that foliar surfaces do indeed capture and retain the ^{210}Pb carrier aerosols before they deposit as litterfall directly under the tree canopies, thus supporting such a mechanism. The results for ^{210}Pb and ^{137}Cs inventories in soils under moderately dense vegetation canopies and under single trees presented here, show that senescent tree leaves are the main pathway of providing enhanced ^{210}Pb and ^{137}Cs deposition in forested areas.

Measurements of ^{210}Pb inventories at a transect through the Plynlimon mountain (at mid-Wales) show that the increase in the ^{210}Pb concentrations in rain at the summit of the Plynlimon is a factor of 1.3 ± 0.4 higher than that at the west coast (Ynys Hir site). This increase is consistent with the orographic enhancement expected to arise through the seeder feeder process. The ^{210}Pb concentration in cloud water at the summit of Plynlimon was found to be 1.9 ± 0.6 greater than that in the frontal rain. These results indicate the importance of occult deposition in the deposition of submicrometre particles, particularly in high elevated sites, where cloud cover frequency is relatively high. For the purpose of comparison with other results reported in literature for most UK sites, the ^{210}Pb deposition flux (in Bq m^{-2} y^{-1}) are presented in figure 6.1.

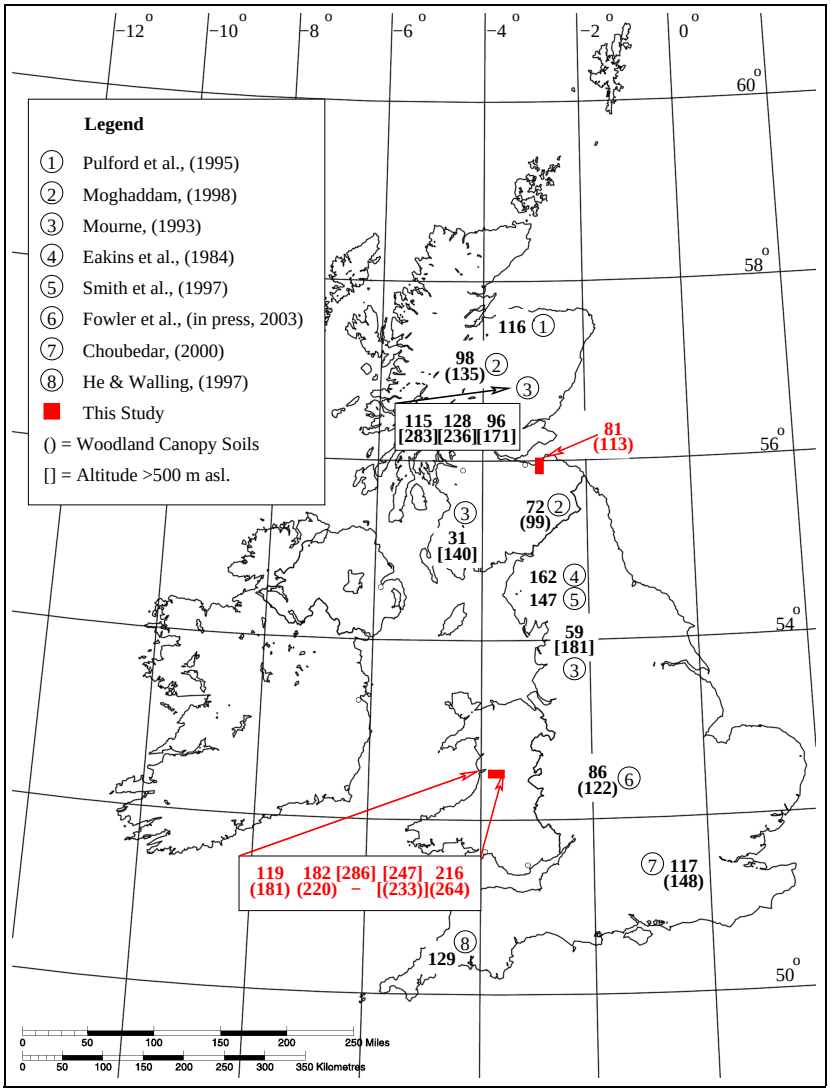

Figure 6.1: *The measured ^{210}Pb deposition fluxes in this study compared with fluxes reported from literature.*

When considering the sites where both moorland and woodland soils (figures shown in round brackets) were measured, it can be clearly seen that there is an enhancement in the deposition fluxes of ^{210}Pb, ranging between 26% and 38%, due to the presence of woodland canopies. Similarly, the ^{210}Pb fluxes measured at high altitude sites (figures shown in square brackets) also show significantly high values (enhanced by factors of 1.8 to 4.5), indicating the importance of the seeder-feeder effect in the deposition of ^{210}Pb-carrier aerosols over hill sites.

The main aim of this study was to investigate the influence of vegetation and topography on the deposition of the atmospheric particulates. The results have shown that, both wooded areas and high altitude sites increase the deposition fluxes of ^{210}Pb and ^{137}Cs carrier aerosols. Because ^{210}Pb, ^{137}Cs and ^{7}Be attach to the same carrier aerosols as most of the pollutant species such as sulphur and nitrogen, these can provide important input data for modelling of acid rain deposition. With respect to the influence of vegetation canopy in the deposition of the atmospheric aerosols, the results obtained from this study may be of practical importance in the current development regarding the beneficial effects of trees in urban air quality in that: although the application of urban woodland may improve the local air quality by increasing the uptake rates of gaseous, particulate and aerosol pollutant from the atmosphere [144], this application must be considered together with the long-term effects of the deposited pollutants which accumulate in the woodland soils.

6.2 Suggestion for Future Work

The technique involving the use of radionuclide in studying the deposition of atmospheric particulates has proven to be effective and relatively inexpensive. However, the spectroscopic analysis is time consuming. The following are suggestions for improvement of this work:

- Daily collection of air samples would be helpful in order to effectively relate the concentrations of the isotopes in air with the meteorological variables for relatively shorter time periods, rather that for several days (*i.e.* 3 to 4 days in this case). Furthermore, the monitoring programme needs to be extended to several years of data collection in order to be able to separate the weather-related from the climate-related meteorological variables that affect the concentrations of the isotopes in air.

- Vegetation sampling needs to be complemented with air and rain sampling for the exposure periods. This would help in providing estimated accumulation rates of the ^{210}Pb and ^{7}Be isotopes on foliage, since these are governed, among other things, by the ambient concentrations of the isotopes and the washout effects by rainfall. The sampling frequency of foliage also needs to be increased, *eg.*, to biweekly sampling.

- It would be useful to extend the soil sampling to three or more individual mountains, for example, sampling on several east-west transect from the west coast. Furthermore, over the hill/mountain profile, more sampling sites would improve the resolution.

- Large number of samples from several sites could be collected and bulked for counting. This would help to improve reliability of results and also in making progress to this study.

Appendix A

Air Samples

A.1 Surface Air Sample Concentrations

Table A.1: *The ^{210}Pb and ^{7}Be Concentrations in air: (55.9°N, 03.2°W).*

The ^{210}Pb and ^{7}Be Concentrations in Air Samples				
Collection Dates	Duration (Hrs)	Concentrations (mBq m^{-3})		†Rainfall (mm)
		^{210}Pb	^{7}Be	
28/06/02	Deployed			
07/07/02	216.29	0.053 ± 0.003	1.043 ± 0.018	20.6
14/07/02	165.06	0.052 ± 0.003	0.760 ± 0.014	6.5
21/07/02	170.70	0.101 ± 0.005	1.713 ± 0.023	22.2
30/07/02	219.26	0.118 ± 0.005	1.678 ± 0.020	28.6
07/08/02	185.82	0.165 ± 0.005	1.317 ± 0.021	57.0
14/08/02	167.59	0.093 ± 0.005	1.591 ± 0.023	45.2
18/08/02	99.71	0.091 ± 0.006	1.167 ± 0.029	2.4
21/08/02	71.78	0.058 ± 0.006	0.819 ± 0.035	10.9
24/08/02	75.18	0.128 ± 0.009	1.441 ± 0.037	2.9
27/08/02	71.50	0.135 ± 0.011	2.382 ± 0.087	1.1
30/08/02	70.91	0.090 ± 0.009	0.862 ± 0.044	8.1
02/09/02	71.99	0.117 ± 0.009	1.848 ± 0.043	12.4
05/09/02	32.49	0.084 ± 0.012	2.144 ± 0.103	0.0
08/09/02	68.09	0.176 ± 0.020	2.348 ± 0.058	20.4
11/09/02	73.02	0.318 ± 0.016	2.705 ± 0.054	19.0
14/09/02	76.42	0.711 ± 0.018	3.474 ± 0.050	0.0
17/09/02	66.95	0.385 ± 0.018	2.871 ± 0.062	0.0
20/09/02	69.48	0.214 ± 0.011	3.886 ± 0.054	0.0

continued on next page

continued from previous page

Collection Dates	Duration (Hrs)	Concentrations (mBq m^{-3}) ^{210}Pb	Concentrations (mBq m^{-3}) ^{7}Be	†Rainfall (mm)
23/09/02	73.33	0.278 ± 0.013	3.295 ± 0.051	0.0
26/09/02	72.09	0.325 ± 0.013	4.577 ± 0.057	0.5
29/09/02	72.59	0.338 ± 0.013	4.175 ± 0.054	0.0
02/10/02	72.74	0.582 ± 0.016	3.339 ± 0.050	0.1
05/10/02	72.36	0.313 ± 0.013	2.844 ± 0.048	3.1
08/10/02	71.24	0.260 ± 0.014	2.400 ± 0.055	1.4
11/10/02	73.91	0.371 ± 0.014	3.643 ± 0.052	0.8
14/10/02	66.41	0.241 ± 0.013	2.419 ± 0.052	55.9
17/10/02	77.47	0.220 ± 0.010	1.579 ± 0.040	11.5
20/10/02	72.62	0.065 ± 0.006	1.666 ± 0.043	0.8
23/10/02	65.93	0.055 ± 0.005	0.864 ± 0.039	63.0
26/10/02	59.96	0.149 ± 0.011	3.200 ± 0.056	13.5
29/10/02	85.65	0.110 ± 0.008	1.758 ± 0.040	21.9
01/11/02	76.83	0.168 ± 0.011	2.621 ± 0.047	1.9
04/11/02	72.64	0.052 ± 0.006	1.490 ± 0.044	10.7
07/11/02	65.09	0.107 ± 0.009	2.345 ± 0.050	8.1
10/11/02	81.47	0.108 ± 0.008	2.491 ± 0.042	7.3
13/11/02	63.37	0.087 ± 0.008	3.307 ± 0.052	2.7
17/11/02	95.76	0.034 ± 0.004	0.634 ± 0.024	23.9
20/11/02	70.22	0.150 ± 0.010	1.900 ± 0.040	0.0
24/11/02	101.33	0.132 ± 0.007	1.645 ± 0.030	3.5
27/11/02	71.10	0.128 ± 0.009	1.819 ± 0.039	0.4
30/11/02	62.22	0.061 ± 0.006	1.562 ± 0.035	11.7
03/12/02	73.75	0.068 ± 0.006	1.195 ± 0.034	3.0
06/12/02	74.32	0.119 ± 0.008	1.236 ± 0.033	0.4
09/12/02	90.88	0.284 ± 0.011	2.726 ± 0.039	0.8
12/12/02	72.10	0.250 ± 0.012	4.478 ± 0.054	1.1
15/12/02	70.83	0.573 ± 0.016	4.212 ± 0.053	12.0
18/12/02	70.72	0.288 ± 0.012	2.272 ± 0.043	5.1
22/12/02	94.90	0.233 ± 0.010	1.731 ± 0.032	2.1
25/12/02	72.48	0.046 ± 0.005	0.790 ± 0.032	14.4
29/12/02	96.01	0.164 ± 0.008	0.843 ± 0.024	9.1
01/01/03	79.82	0.237 ± 0.011	1.724 ± 0.035	17.8
04/01/03	68.06	0.193 ± 0.011	2.024 ± 0.041	0.4
07/01/03	74.10	0.250 ± 0.012	2.520 ± 0.042	12.8
10/01/03	73.42	0.210 ± 0.012	3.212 ± 0.048	0.0
13/01/03	70.19	0.130 ± 0.009	2.942 ± 0.046	6.9
16/01/03	69.73	0.069 ± 0.006	1.761 ± 0.038	6.9

continued on next page

continued from previous page

Collection Dates	Duration (Hrs)	Concentrations (mBq m^{-3})		†Rainfall (mm)
		^{210}Pb	^{7}Be	
19/01/03	72.73	0.088 ± 0.008	2.560 ± 0.046	13.9
22/01/03	25.88	0.139 ± 0.014	1.877 ± 0.082	5.6
25/01/03	75.60	0.035 ± 0.004	1.177 ± 0.034	6.2
28/01/03	63.37	0.058 ± 0.006	1.181 ± 0.037	3.4
31/01/03	73.21	0.049 ± 0.005	1.655 ± 0.037	0.0
03/02/03	72.00	0.022 ± 0.003	1.359 ± 0.036	6.9
06/02/03	71.13	0.040 ± 0.004	1.752 ± 0.038	0.7
09/02/03	73.16	0.058 ± 0.006	0.959 ± 0.033	3.8
12/02/03	70.66	0.008 ± 0.001	0.713 ± 0.031	1.6
16/02/03	100.39	0.305 ± 0.010	3.419 ± 0.040	0.1
19/02/03	68.53	0.282 ± 0.013	3.600 ± 0.051	0.0
23/02/03	96.69	0.426 ± 0.013	2.369 ± 0.039	0.0
26/02/03	71.38	0.437 ± 0.015	2.379 ± 0.045	0.0
01/03/03	79.07	0.564 ± 0.016	3.695 ± 0.050	0.1
04/03/03	63.69	0.111 ± 0.009	1.496 ± 0.040	9.8
07/03/03	74.77	0.070 ± 0.006	1.866 ± 0.037	1.6
10/03/03	69.97	0.147 ± 0.010	2.404 ± 0.044	3.1
13/03/03	70.94	0.143 ± 0.009	2.252 ± 0.041	5.7
16/03/03	76.30	0.175 ± 0.009	2.172 ± 0.041	0.0
19/03/03	67.14	0.415 ± 0.015	3.194 ± 0.049	0.0
23/03/03	100.48	0.293 ± 0.011	3.804 ± 0.042	0.0
26/03/03	65.93	0.634 ± 0.017	5.299 ± 0.060	0.0
30/03/03	98.82	0.633 ± 0.018	4.759 ± 0.047	0.0
02/04/03	68.49	0.154 ± 0.012	5.125 ± 0.066	4.5
06/04/03	99.09	0.199 ± 0.009	2.591 ± 0.035	0.0
09/04/03	67.08	0.302 ± 0.013	4.371 ± 0.055	0.0
12/04/03	80.89	0.469 ± 0.015	6.539 ± 0.063	0.0
16/04/03	86.94	0.714 ± 0.015	5.988 ± 0.054	0.0
19/04/03	81.82	0.742 ± 0.016	5.864 ± 0.056	0.0
22/04/03	63.87	0.724 ± 0.018	4.994 ± 0.060	0.8
25/04/03	71.10	0.606 ± 0.016	3.733 ± 0.050	0.1
28/04/03	73.57	0.239 ± 0.011	2.852 ± 0.044	9.1
01/05/03	72.00	0.129 ± 0.009	2.584 ± 0.052	35.2
04/05/03	69.89	0.107 ± 0.008	2.523 ± 0.044	10.8
07/05/03	72.13	0.128 ± 0.009	3.225 ± 0.048	9.0
11/05/03	97.99	0.089 ± 0.007	2.272 ± 0.035	5.9
14/05/03	69.59	0.084 ± 0.012	1.848 ± 0.068	4.6
17/05/03	75.96	0.045 ± 0.005	1.671 ± 0.036	8.4

continued on next page

continued from previous page				
Collection Dates	Duration (Hrs)	Concentrations (mBq m^{-3})		†Rainfall (mm)
		^{210}Pb	^{7}Be	
20/05/03	67.81	0.124 ± 0.009	1.592 ± 0.039	7.9
23/05/03	29.80	0.102 ± 0.011	0.961 ± 0.068	1.6
26/05/03	69.52	0.061 ± 0.006	1.339 ± 0.036	7.3
29/05/03	78.45	0.196 ± 0.012	3.849 ± 0.049	0.3
01/06/03	66.05	0.416 ± 0.015	3.980 ± 0.056	3.1
04/06/03	71.31	0.184 ± 0.011	2.741 ± 0.045	0.2
07/06/03	76.52	0.093 ± 0.008	2.769 ± 0.043	2.9
10/06/03	67.66	0.114 ± 0.009	3.981 ± 0.054	9.0
13/06/03	71.58	0.100 ± 0.008	2.018 ± 0.040	5.9
16/06/03	73.05	0.100 ± 0.008	2.210 ± 0.042	0.0
19/06/03	71.57	0.156 ± 0.010	2.401 ± 0.043	0.0
23/06/03	97.47	0.127 ± 0.008	2.695 ± 0.037	1.2
26/06/03	69.80	0.107 ± 0.008	1.817 ± 0.039	0.0
29/06/03	74.96	0.220 ± 0.011	2.672 ± 0.042	6.8

†Hourly rainfall data.

Appendix B

Soil Samples

Notes

Soils were excavated using corers, except for the Ynys Hir site in Mid-Wales where a spade was used. Most soils where sampled to a depth of 20 cm. The cores were sectioned according to 0-5 cm, 5-10 cm and 10-20 cm, represented by letters *a*, *b* and *c*, respectively (except for soils from the CEH Edinburgh, Prestonfield at the Edinburgh sites, and sample PLW02 sampled at Wales where samples were sectioned at 0-5, 5-10, 10-15 and 15-20 cm depth intervals, represented by the letters letters; *a*, *b*, *c* and *d*, respectively). Thus, the inventories reported here are in Bq m^{-2} *per 5 cm depth intervals* for the firts two subsections, and Bq m^{-2} *per 10 cm depth intervals* for the last subsections (except for soils from the CEH Edinburgh, Prestonfield, and the PLWO2 sample, where the inventories for all the subsections are reported as Bq m^{-2} *per 5 cm depth intervals*, unless indicated otherwise. For all cases, $^{210}Pb_{tot.}$, $^{210}Pb_{sup.}$ and $^{210}Pb_{exs.}$ are the total Lead-210, supported Lead-210 and excess (unsupported) Lead-210, respectively (see definitions in main text).

B.1 The Edinburgh Sites

Table B.1: *Soils from the Centre for Ecology and Hydrology (CEH), Edinburgh.*

The ^{210}Pb and ^{137}Cs Specific Activities and Inventories in Soil Samples						
Sample	^{210}Pb and ^{137}Cs (Bq kg^{-1})				^{210}Pb and ^{137}Cs (Bq m^{-2})	
Identity	$^{210}Pb_{tot.}$	$^{210}Pb_{sup.}$	$^{210}Pb_{exs.}$	^{137}Cs	^{210}Pb	^{137}Cs
CEO01a	32.2 ± 2.2	1.9 ± 0.1	30.3 ± 2.2	7.8 ± 0.3	717 ± 48	184 ± 8
CEO01b	26.9 ± 1.3	9.1 ± 0.3	17.8 ± 1.3	7.5 ± 0.2	1064 ± 51	449 ± 14
CEO01c	25.4 ± 1.2	9.9 ± 0.3	15.5 ± 1.2	5.9 ± 0.2	1013 ± 48	384 ± 14
CEO01d	20.9 ± 1.1	9.5 ± 0.3	11.5 ± 1.2	2.4 ± 0.2	891 ± 48	187 ± 12
CEO02a	40.3 ± 2.3	10.7 ± 0.6	29.6 ± 2.4	11.1 ± 0.4	676 ± 39	254 ± 10
CEO02b	23.2 ± 1.1	11.5 ± 0.4	11.7 ± 1.1	9.6 ± 0.3	591 ± 28	486 ± 14
CEO02c	22.3 ± 1.1	12.0 ± 0.3	10.3 ± 1.2	5.7 ± 0.2	673 ± 34	369 ± 13
CEO02d	20.9 ± 1.2	11.5 ± 0.3	9.3 ± 1.3	1.8 ± 0.1	721 ± 42	140 ± 9
CEO03a	21.3 ± 1.1	9.6 ± 0.3	11.7 ± 1.2	9.6 ± 0.3	567 ± 30	462 ± 13
CEO03b	22.3 ± 1.1	10.3 ± 0.3	12.0 ± 1.2	6.7 ± 0.2	692 ± 35	388 ± 13
CEO03c	18.2 ± 1.1	10.2 ± 0.3	8.0 ± 1.1	2.4 ± 0.2	643 ± 39	190 ± 16
CEO03d	59.8 ± 2.9	12.7 ± 0.7	47.1 ± 3.0	33.4 ± 0.7	1702 ± 84	1209 ± 24
Mean ^{210}Pb and ^{137}Cs Inventory (Bq m^{-2})					3037 ± 564	1305 ± 138
CEW01a	59.7 ± 2.9	12.7 ± 0.7	47.1 ± 3.0	33.4 ± 0.7	1703 ± 84	1209 ± 24
CEW01b	24.5 ± 1.2	12.7 ± 0.4	11.8 ± 1.3	9.7 ± 0.3	738 ± 37	605 ± 16
CEW01c	21.0 ± 1.1	12.4 ± 0.4	8.6 ± 1.2	3.7 ± 0.2	330 ± 18	141 ± 8
CEW01d	20.1 ± 1.1	12.6 ± 0.4	7.5 ± 1.1	3.1 ± 0.2	323 ± 17	101 ± 3
CEW02a	52.0 ± 2.1	12.1 ± 0.5	39.8 ± 2.2	23.3 ± 1.0	1153 ± 47	674 ± 28
CEW02b	23.4 ± 1.3	13.0 ± 0.3	10.5 ± 1.3	7.6 ± 0.4	488 ± 27	352 ± 19
CEW02c	23.1 ± 1.4	12.3 ± 0.3	10.8 ± 1.4	4.7 ± 0.2	553 ± 33	243 ± 12
CEW02d	21.9 ± 1.2	13.3 ± 0.3	8.6 ± 1.3	2.4 ± 0.1	530 ± 29	147 ± 8
CEW03a	44.2 ± 2.3	10.8 ± 0.6	33.3 ± 2.4	14.1 ± 0.7	719 ± 37	305 ± 16
CEW03b	27.1 ± 1.4	11.8 ± 0.3	15.4 ± 1.5	8.5 ± 0.5	777 ± 41	430 ± 23
CEW03c	21.9 ± 1.4	12.5 ± 0.4	9.3 ± 1.4	6.8 ± 0.4	451 ± 28	329 ± 21
CEW03d	22.8 ± 1.2	11.3 ± 0.3	11.5 ± 1.3	4.9 ± 0.3	635 ± 34	273 ± 14
CEW04a	59.7 ± 3.1	10.3 ± 0.6	49.4 ± 3.1	28.6 ± 1.5	1272 ± 66	736 ± 38
CEW04b	23.6 ± 1.2	12.6 ± 0.4	11.0 ± 1.3	9.2 ± 0.5	524 ± 28	438 ± 23
CEW04c	24.3 ± 1.3	12.9 ± 0.4	11.4 ± 1.3	5.0 ± 0.3	534 ± 28	232 ± 12
CEW04d	22.5 ± 1.4	12.5 ± 0.3	10.1 ± 1.4	3.1 ± 0.2	716 ± 44	220 ± 14
CEW05a	69.0 ± 3.1	4.4 ± 0.2	64.6 ± 3.1	31.7 ± 1.4	1382 ± 63	678 ± 31
CEW05b	24.5 ± 1.2	12.4 ± 0.4	12.1 ± 1.3	9.7 ± 0.5	482 ± 24	388 ± 20
CEW05c	23.7 ± 1.3	13.0 ± 0.3	10.7 ± 1.4	5.7 ± 0.3	554 ± 31	296 ± 17
CEW05d	21.6 ± 1.4	12.8 ± 0.3	8.8 ± 1.4	3.3 ± 0.2	486 ± 31	181 ± 12

continued on next page

continued from previous page

Sample Identity	^{210}Pb and ^{137}Cs (Bq kg^{-1})				^{210}Pb and ^{137}Cs (Bq m^{-2})	
	^{210}Pb$_{tot.}$	^{210}Pb$_{sup.}$	^{210}Pb$_{exs.}$	^{137}Cs	^{210}Pb	^{137}Cs
CEW06a	64.0 ± 3.0	11.2 ± 0.6	52.8 ± 3.0	19.5 ± 0.9	1344 ± 62	498 ± 23
CEW06b	25.3 ± 1.4	12.4 ± 0.4	12.9 ± 1.4	8.5 ± 0.5	377 ± 21	249 ± 14
CEW06c	24.7 ± 1.3	12.5 ± 0.3	12.2 ± 1.4	6.6 ± 0.4	608 ± 33	327 ± 18
CEW06d	24.9 ± 1.2	12.2 ± 0.4	12.7 ± 1.3	3.9 ± 0.2	724 ± 35	222 ± 11
Mean ^{210}Pb and ^{137}Cs Inventory (Bq m^{-2})					2932 ± 331	1524 ± 302

Table B.2: *Soils from the Cramond Golf Course, Edinburgh.*

The ^{210}Pb and ^{137}Cs Specific Activities and Inventories in Soil Samples						
Sample Identity	^{210}Pb and ^{137}Cs (Bq kg^{-1})				^{210}Pb and ^{137}Cs (Bq m^{-2})	
	^{210}Pb$_{tot.}$	^{210}Pb$_{sup.}$	^{210}Pb$_{exs.}$	^{137}Cs	^{210}Pb	^{137}Cs
CRO01a	50.4 ± 2.8	16.8 ± 0.9	33.6 ± 2.9	10.2 ± 0.6	1061 ± 59	321 ± 18
CRO01b	35.8 ± 2.2	16.9 ± 0.6	18.9 ± 2.3	9.3 ± 0.4	891 ± 55	440 ± 20
CRO01c	37.7 ± 2.3	17.0 ± 0.6	20.6 ± 2.4	7.2 ± 0.3	2120 ± 130	743 ± 35
CRO02a	46.9 ± 2.5	16.1 ± 0.7	30.8 ± 2.6	9.8 ± 0.5	947 ± 50	302 ± 16
CRO02b	33.9 ± 2.1	17.0 ± 0.6	16.9 ± 2.2	9.4 ± 0.4	933 ± 59	518 ± 21
CRO02c	32.8 ± 2.1	17.6 ± 0.6	15.2 ± 2.1	7.2 ± 0.4	1599 ± 101	751 ± 44
CRO03a	61.2 ± 3.0	17.1 ± 0.9	44.0 ± 3.2	18.6 ± 0.8	1327 ± 66	561 ± 23
CRO03b	31.9 ± 2.1	17.0 ± 0.6	15.0 ± 2.2	8.4 ± 0.4	907 ± 60	507 ± 22
CRO03c	36.7 ± 2.2	18.0 ± 0.6	18.7 ± 2.3	2.6 ± 0.3	1777 ± 107	246 ± 28
CRO04a	65.1 ± 3.1	16.4 ± 0.9	48.7 ± 3.2	19.4 ± 0.7	1349 ± 65	537 ± 21
CRO04b	35.7 ± 2.2	19.0 ± 0.7	16.7 ± 2.3	9.2 ± 0.4	846 ± 52	465 ± 20
CRO04c	30.4 ± 2.1	21.7 ± 0.8	8.6 ± 2.3	3.4 ± 0.3	815 ± 57	320 ± 25
Mean ^{210}Pb and ^{137}Cs Inventory (Bq m^{-2})					3643 ± 499	1428 ± 129
CRW01a	47.0 ± 2.6	17.5 ± 0.7	29.5 ± 2.7	24.6 ± 0.6	865 ± 48	720 ± 18
CRW01b	30.8 ± 2.4	19.5 ± 0.7	11.3 ± 2.5	14.5 ± 0.5	405 ± 31	518 ± 18
CRW01c	31.3 ± 2.0	19.6 ± 0.6	11.7 ± 2.1	5.6 ± 0.3	573 ± 37	271 ± 14
CRW02a	45.7 ± 2.5	16.9 ± 0.7	28.8 ± 2.6	24.9 ± 0.7	620 ± 34	536 ± 14
CRW02b	42.5 ± 2.3	19.4 ± 0.7	23.1 ± 2.4	18.7 ± 0.5	715 ± 40	578 ± 16
CRW02c	36.4 ± 2.5	18.0 ± 0.7	18.5 ± 2.6	11.2 ± 0.5	1446 ± 98	878 ± 36
CRW03a	39.9 ± 2.4	18.0 ± 0.7	21.9 ± 2.5	22.5 ± 0.6	628 ± 38	645 ± 17
CRW03b	36.8 ± 2.3	18.2 ± 0.7	18.6 ± 2.4	20.0 ± 0.6	701 ± 44	756 ± 21

continued on next page

continued from previous page

Sample Identity	^{210}Pb and ^{137}Cs (Bq kg^{-1})				^{210}Pb and ^{137}Cs (Bq m^{-2})	
	$^{210}Pb_{tot.}$	$^{210}Pb_{sup.}$	$^{210}Pb_{exs.}$	^{137}Cs	^{210}Pb	^{137}Cs
CRW03c	32.0 ± 2.3	21.0 ± 0.7	11.0 ± 2.4	6.9 ± 0.4	943 ± 67	591 ± 34
CRW04a	49.2 ± 2.4	18.0 ± 0.7	31.2 ± 2.5	24.0 ± 0.6	763 ± 38	587 ± 14
CRW04b	38.1 ± 2.4	20.2 ± 0.7	17.9 ± 2.5	18.1 ± 0.5	779 ± 50	788 ± 23
CRW04c	30.3 ± 2.2	19.1 ± 0.7	11.2 ± 2.3	9.3 ± 0.4	862 ± 63	718 ± 29
CRW05a	41.3 ± 2.4	17.8 ± 0.7	23.5 ± 2.5	26.8 ± 0.6	607 ± 36	691 ± 17
CRW05b	43.8 ± 2.5	17.5 ± 0.7	26.3 ± 2.6	20.7 ± 0.6	1009 ± 58	796 ± 23
CRW05c	25.0 ± 1.9	20.8 ± 0.6	4.2 ± 2.0	7.2 ± 0.4	298 ± 22	516 ± 26
Mean ^{210}Pb and ^{137}Cs Inventory (Bq m^{-2})					2223 ± 410	1918 ± 232

Table B.3: *Soils from the Pentlands Golf Course, Edinburgh.*

The ^{210}Pb and ^{137}Cs Specific Activities and Inventories in Soil Samples						
Sample Identity	^{210}Pb and ^{137}Cs (Bq kg^{-1})				^{210}Pb and ^{137}Cs (Bq m^{-2})	
	$^{210}Pb_{tot.}$	$^{210}Pb_{sup.}$	$^{210}Pb_{exs.}$	^{137}Cs	^{210}Pb	^{137}Cs
PEO01a	76.8 ± 5.4	14.9 ± 0.8	61.8 ± 5.4	44.8 ± 1.3	793 ± 56	575 ± 17
PEO01b	56.7 ± 2.8	22.4 ± 0.7	34.3 ± 2.9	34.0 ± 2.1	641 ± 32	636 ± 40
PEO01c	45.9 ± 2.7	22.4 ± 0.7	23.5 ± 2.7	17.7 ± 0.7	1141 ± 66	861 ± 32
PEO02a	106.5 ± 5.2	23.9 ± 1.4	82.6 ± 5.4	47.4 ± 2.0	1060 ± 52	608 ± 25
PEO02b	53.2 ± 3.0	19.3 ± 0.8	33.8 ± 3.1	33.3 ± 1.0	838 ± 47	824 ± 26
PEO02c	38.7 ± 2.5	19.3 ± 0.7	19.5 ± 2.6	21.3 ± 0.7	929 ± 61	1020 ± 33
PEO03a	80.2 ± 4.0	20.0 ± 1.1	60.2 ± 4.1	44.3 ± 1.5	699 ± 35	514 ± 17
PEO03b	60.7 ± 3.2	24.6 ± 0.8	36.1 ± 3.3	29.7 ± 0.9	796 ± 42	654 ± 21
PEO03c	54.2 ± 2.7	21.6 ± 0.7	32.6 ± 2.8	14.1 ± 0.6	727 ± 37	315 ± 13
PEO04a	80.2 ± 4.0	20.0 ± 1.1	60.2 ± 4.1	44.3 ± 1.5	801 ± 40	589 ± 20
PEO04b	54.1 ± 2.9	22.9 ± 0.8	31.2 ± 3.0	41.9 ± 1.0	759 ± 40	1020 ± 25
PEO04c	37.9 ± 2.4	20.9 ± 0.7	17.1 ± 2.5	19.6 ± 0.7	671 ± 43	770 ± 27
Mean ^{210}Pb and ^{137}Cs Inventory (Bq m^{-2})					2464 ± 293	2097 ± 441
PEW01a	146.6 ± 4.4	16.5 ± 1.0	130.1 ± 4.6	155.5 ± 2.0	1912 ± 58	2285 ± 29
PEW01b	38.0 ± 2.3	19.1 ± 0.7	18.9 ± 2.5	21.6 ± 0.6	487 ± 30	557 ± 17
PEW01c	39.2 ± 2.3	21.9 ± 0.7	17.3 ± 2.4	3.5 ± 0.3	828 ± 48	168 ± 16
PEW02a	146.6 ± 4.4	16.5 ± 1.0	130.1 ± 4.6	155.5 ± 2.0	1912 ± 58	2285 ± 29
PEW02b	52.9 ± 2.6	19.6 ± 0.8	33.3 ± 2.7	36.6 ± 0.8	823 ± 40	903 ± 19

continued on next page

continued from previous page

Sample Identity	^{210}Pb and ^{137}Cs (Bq kg^{-1})				^{210}Pb and ^{137}Cs (Bq m^{-2})	
	^{210}Pb$_{tot.}$	^{210}Pb$_{sup.}$	^{210}Pb$_{exs.}$	^{137}Cs	^{210}Pb	^{137}Cs
PEW02c	37.3 ± 2.1	21.9 ± 0.7	15.4 ± 2.2	2.0 ± 0.3	654 ± 36	85 ± 12
PEW03a	144.6 ± 5.2	17.3 ± 1.2	127.3 ± 5.3	172.8 ± 2.4	1308 ± 47	1775 ± 24
PEW03b	58.6 ± 2.9	19.5 ± 0.8	39.1 ± 3.0	37.5 ± 0.9	1018 ± 51	977 ± 22
PEW03c	43.3 ± 2.4	24.7 ± 0.8	18.6 ± 2.5	9.2 ± 0.5	1175 ± 65	578 ± 29
PEW04a	144.6 ± 5.2	17.3 ± 1.2	127.3 ± 5.3	172.8 ± 2.4	1308 ± 47	1775 ± 24
PEW04b	49.3 ± 2.5	18.0 ± 0.7	31.3 ± 2.6	19.8 ± 0.6	997 ± 51	629 ± 20
PEW04c	33.3 ± 2.1	19.2 ± 0.7	14.1 ± 2.2	2.7 ± 0.3	970 ± 60	187 ± 20
PEW05a	124.5 ± 4.3	18.2 ± 1.0	106.3 ± 4.4	147.2 ± 1.9	1354 ± 47	1875 ± 25
PEW05b	45.5 ± 2.3	17.9 ± 0.7	27.6 ± 2.4	13.7 ± 0.5	879 ± 44	436 ± 15
PEW05c	30.9 ± 1.9	18.8 ± 0.7	12.1 ± 2.0	1.7 ± 0.3	565 ± 35	79 ± 12
Mean ^{210}Pb and ^{137}Cs Inventory (Bq m^{-2})					3237 ± 268	2919 ± 415

Table B.4: *Soils from the West Linton Golf Course, Edinburgh.*

The ^{210}Pb and ^{137}Cs Specific Activities and Inventories in Soil Samples						
Sample Identity	^{210}Pb and ^{137}Cs (Bq kg^{-1})				^{210}Pb and ^{137}Cs (Bq m^{-2})	
	^{210}Pb$_{tot.}$	^{210}Pb$_{sup.}$	^{210}Pb$_{exs.}$	^{137}Cs	^{210}Pb	^{137}Cs
WLO01a	316.2 ± 9.3	3.0 ± 0.7	313.2 ± 9.3	111.3 ± 3.3	1631 ± 48	580 ± 17
WLO01b	50.7 ± 3.0	6.4 ± 0.7	44.3 ± 3.1	38.2 ± 1.4	386 ± 23	333 ± 12
WLO01c	25.7 ± 2.1	10.6 ± 0.6	15.0 ± 2.2	25.4 ± 0.7	646 ± 53	1093 ± 32
WLO02a	316.2 ± 9.3	3.0 ± 0.7	313.2 ± 9.3	111.3 ± 3.3	1631 ± 48	580 ± 17
WLO02b	50.7 ± 3.0	6.4 ± 0.7	44.3 ± 3.1	38.2 ± 1.4	386 ± 23	333 ± 12
WLO02c	38.8 ± 2.6	10.2 ± 0.5	28.6 ± 2.6	17.2 ± 0.7	722 ± 47	434 ± 17
WLO03a	321.3 ± 9.7	5.6 ± 0.9	315.6 ± 9.7	97.8 ± 2.8	1344 ± 41	417 ± 12
WLO03b	49.0 ± 3.0	2.0 ± 0.4	47.0 ± 3.0	30.1 ± 1.2	309 ± 19	198 ± 8
WLO03c	37.0 ± 2.4	12.2 ± 0.7	24.8 ± 2.5	27.1 ± 0.8	864 ± 56	944 ± 29
WLO04a	321.3 ± 9.7	5.6 ± 0.9	315.6 ± 9.7	97.8 ± 2.8	1344 ± 41	417 ± 12
WLO04b	49.0 ± 3.0	2.0 ± 0.4	47.0 ± 3.0	30.1 ± 1.2	309 ± 19	198 ± 8
WLO04c	21.9 ± 1.4	10.2 ± 0.6	11.7 ± 1.5	14.6 ± 0.7	713 ± 45	888 ± 42
Mean ^{210}Pb and ^{137}Cs Inventory (Bq m^{-2})					2571 ± 165	1603 ± 282
WLW01a	53.7 ± 2.9	11.1 ± 0.7	42.6 ± 2.9	30.3 ± 0.8	1235 ± 66	878 ± 22
WLW01b	36.2 ± 2.2	11.0 ± 0.6	25.1 ± 2.3	20.6 ± 0.6	788 ± 49	646 ± 18
WLW01c	29.4 ± 1.9	13.3 ± 0.5	16.1 ± 1.9	8.3 ± 0.4	1613 ± 102	833 ± 38

continued on next page

continued from previous page

Sample Identity	^{210}Pb and ^{137}Cs (Bq kg^{-1})				^{210}Pb and ^{137}Cs (Bq m^{-2})	
	^{210}Pb$_{tot.}$	^{210}Pb$_{sup.}$	^{210}Pb$_{exs.}$	^{137}Cs	^{210}Pb	^{137}Cs
WLW02a	72.5 ± 3.3	12.5 ± 0.8	60.0 ± 3.4	27.3 ± 0.8	1572 ± 71	715 ± 22
WLW02b	52.2 ± 2.6	13.9 ± 0.6	38.3 ± 2.7	21.6 ± 0.6	1463 ± 72	824 ± 22
WLW02c	27.1 ± 2.0	13.9 ± 0.6	13.2 ± 2.1	4.7 ± 0.3	1026 ± 75	368 ± 22
WLW03a	67.9 ± 3.0	10.8 ± 0.7	57.1 ± 3.1	54.1 ± 1.0	1778 ± 79	1683 ± 31
WLW03b	33.2 ± 2.0	11.4 ± 0.6	21.8 ± 2.1	7.4 ± 0.4	1068 ± 66	364 ± 18
WLW03c	19.7 ± 1.8	11.7 ± 0.5	7.9 ± 1.9	2.0 ± 0.3	933 ± 84	236 ± 32
WLW04a	90.4 ± 3.5	12.4 ± 0.7	78.0 ± 3.6	64.5 ± 1.1	1853 ± 72	1533 ± 27
WLW04b	55.4 ± 2.6	12.2 ± 0.6	43.2 ± 2.7	29.5 ± 0.7	1737 ± 81	1184 ± 27
WLW04c	27.9 ± 2.0	13.1 ± 0.6	14.7 ± 2.1	5.1 ± 0.4	1046 ± 75	359 ± 26
WLW05a	85.8 ± 3.0	10.3 ± 0.6	75.5 ± 3.1	81.5 ± 1.1	1912 ± 68	2063 ± 27
WLW05b	29.9 ± 2.0	12.6 ± 0.6	17.4 ± 2.1	24.3 ± 0.6	678 ± 45	947 ± 24
WLW05c	25.7 ± 1.4	10.7 ± 0.4	15.0 ± 1.4	2.8 ± 0.2	1284 ± 68	241 ± 18
Mean ^{210}Pb and ^{137}Cs Inventory (Bq m^{-2})					3997 ± 390	2575 ± 567

Table B.5: *Soils from the Prestonfield Golf Course, Edinburgh.*

The ^{210}Pb and ^{137}Cs Specific Activities and Inventories in Soil Samples						
Sample Identity	^{210}Pb and ^{137}Cs (Bq kg^{-1})				^{210}Pb and ^{137}Cs (Bq m^{-2})	
	^{210}Pb$_{tot.}$	^{210}Pb$_{sup.}$	^{210}Pb$_{exs.}$	^{137}Cs	^{210}Pb	^{137}Cs
PRO01a	65.7 ± 6.3	34.8 ± 2.3	30.9 ± 6.7	25.4 ± 2.2	285 ± 27	234 ± 20
PRO01b	78.7 ± 7.0	42.5 ± 2.0	36.2 ± 7.3	29.8 ± 1.6	704 ± 63	565 ± 30
PRO01c	86.4 ± 6.9	46.4 ± 1.8	40.1 ± 7.2	14.0 ± 1.0	944 ± 76	329 ± 23
PRO01d	64.6 ± 6.4	52.5 ± 1.7	12.2 ± 6.6	6.1 ± 0.8	385 ± 38	194 ± 25
PRO02a	103.2 ± 7.5	36.0 ± 4.8	67.2 ± 9.0	23.9 ± 1.3	1064 ± 78	378 ± 20
PRO02b	93.0 ± 7.3	43.9 ± 1.7	49.1 ± 7.5	13.6 ± 0.9	933 ± 74	259 ± 18
PRO02c	80.6 ± 7.1	46.3 ± 2.0	34.3 ± 7.4	6.2 ± 1.0	866 ± 77	157 ± 26
PRO02d	51.7 ± 4.3	44.8 ± 1.3	6.9 ± 4.4	5.7 ± 0.6	173 ± 14	143 ± 24
PRO03a	107.5 ± 7.3	33.5 ± 2.3	74.0 ± 7.7	29.6 ± 1.4	1016 ± 69	407 ± 45
PRO03b	66.6 ± 5.9	41.0 ± 1.6	25.6 ± 6.1	17.8 ± 0.8	816 ± 72	566 ± 27
PRO03c	43.8 ± 4.0	35.8 ± 1.3	8.0 ± 4.2	5.9 ± 0.7	229 ± 21	167 ± 8
PRO03d	43.5 ± 6.4	39.6 ± 1.9	4.0 ± 2.5	3.7 ± 0.9	132 ± 19	124 ± 14
PRO04a	79.0 ± 6.4	27.6 ± 2.0	51.5 ± 6.7	29.8 ± 1.3	822 ± 67	476 ± 120
PRO04b	50.6 ± 5.9	33.5 ± 1.7	17.1 ± 6.1	12.7 ± 1.0	566 ± 66	418 ± 18

continued on next page

continued from previous page						
Sample	^{210}Pb and ^{137}Cs (Bq kg^{-1})				^{210}Pb and ^{137}Cs (Bq m^{-2})	
Identity	^{210}Pb$_{tot.}$	^{210}Pb$_{sup.}$	^{210}Pb$_{exs.}$	^{137}Cs	^{210}Pb	^{137}Cs
PRO04c	38.5 ± 6.1	36.0 ± 1.8	2.6 ± 2.5	8.2 ± 0.9	83 ± 13	265 ± 22
PRO04d	54.4 ± 6.0	35.8 ± 1.7	18.6 ± 6.3	3.0 ± 0.8	594 ± 66	95 ± 10
Mean ^{210}Pb and ^{137}Cs Inventory (Bq m^{-2})					2349 ± 480	1305 ± 58
PRW01a	93.8 ± 6.9	29.4 ± 1.9	64.3 ± 7.2	41.4 ± 1.1	1018 ± 75	656 ± 18
PRW01b	41.8 ± 4.1	30.4 ± 1.3	11.5 ± 4.3	10.8 ± 0.3	406 ± 40	360 ± 11
PRW01c	44.9 ± 5.7	34.4 ± 1.6	10.4 ± 5.9	1.1 ± 0.1	370 ± 47	37 ± 5
PRW01d	37.1 ± 3.8	35.0 ± 1.1	2.2 ± 4.0	1.5 ± 0.4	110.0 ± 11.0	75 ± 22
PRW02a	88.1 ± 7.0	27.9 ± 2.0	60.2 ± 7.3	40.6 ± 1.2	1077 ± 86	726 ± 21
PRW02b	65.1 ± 6.6	38.9 ± 1.7	26.1 ± 6.8	9.7 ± 0.8	962 ± 97	357 ± 31
PRW02c	53.1 ± 6.3	35.3 ± 1.8	17.8 ± 6.6	5.2 ± 0.7	731 ± 87	214 ± 29
PRW02d	38.2 ± 5.3	31.5 ± 1.5	6.7 ± 5.5	3.1 ± 0.6	299 ± 41	139 ± 27
PRW03a	97.0 ± 7.5	26.9 ± 2.3	70.1 ± 7.8	39.0 ± 1.3	1071 ± 83	595 ± 20
PRW03b	51.6 ± 6.0	35.1 ± 1.7	16.5 ± 6.2	18.0 ± 0.7	578 ± 67	631 ± 23
PRW03c	46.3 ± 4.4	36.9 ± 1.3	9.4 ± 4.6	4.6 ± 0.6	352 ± 33	172 ± 22
PRW03d	ND	ND	ND	ND	ND	ND
PRW04a	78.3 ± 6.2	29.7 ± 1.9	48.6 ± 6.5	39.5 ± 1.1	970 ± 77	789 ± 23
PRW04b	44.9 ± 5.5	37.4 ± 1.6	7.6 ± 5.8	11.5 ± 0.8	280 ± 34	426 ± 29
PRW04c	25.3 ± 3.5	38.4 ± 1.2	ND	2.8 ± 0.5	ND	98 ± 18
PRW04d	38.0 ± 3.9	38.8 ± 1.2	ND	ND	ND	ND
Mean ^{210}Pb and ^{137}Cs Inventory (Bq m^{-2})					2205 ± 1031	1318 ± 138

ND: Not Detected.

B.2 The Mid-Wales Sites

Table B.6: *Soils from the Ynys Hir, Mid-Wales.*

The ^{210}Pb and ^{137}Cs Specific Activities and Inventories in Soil Samples						
Sample Identity	^{210}Pb and ^{137}Cs (Bq kg^{-1})				^{210}Pb and ^{137}Cs (Bq m^{-2})	
	$^{210}Pb_{tot.}$	$^{210}Pb_{sup.}$	$^{210}Pb_{exs.}$	^{137}Cs	^{210}Pb	^{137}Cs
YHO01a	127.2 ± 6.0	26.6 ± 1.9	100.6 ± 6.3	30.2 ± 1.6	1575 ± 99	473 ± 25
YHO01b	80.1 ± 5.0	33.7 ± 1.4	46.4 ± 5.2	39.1 ± 1.2	1073 ± 120	903 ± 28
YHO01c	81.3 ± 4.0	34.2 ± 1.1	47.0 ± 4.1	20.4 ± 0.8	1344 ± 118	582 ± 24
YHO02a	90.5 ± 5.8	29.0 ± 1.7	61.6 ± 6.1	17.9 ± 1.2	1893 ± 187	550 ± 38
YHO02b	80.2 ± 6.0	35.3 ± 1.6	44.9 ± 6.2	19.7 ± 1.1	1925 ± 266	843 ± 49
YHO02c	41.9 ± 4.6	36.3 ± 1.4	5.6 ± 4.8	18.8 ± 1.0	194 ± 166	649 ± 34
YHO03a	86.4 ± 5.9	32.3 ± 2.0	54.1 ± 6.2	24.5 ± 1.5	1236 ± 142	559 ± 34
YHO03b	76.3 ± 5.2	36.8 ± 1.5	39.5 ± 5.4	26.3 ± 1.1	870 ± 119	580 ± 25
YHO03c	84.2 ± 6.4	33.8 ± 1.7	50.4 ± 6.6	23.6 ± 1.3	1742 ± 230	814 ± 44
YHO04a	366.6 ± 8.7	8.9 ± 2.2	357.7 ± 9.0	76.9 ± 2.4	2329 ± 59	501 ± 15
YHO04b	153.0 ± 6.8	17.0 ± 1.9	136.0 ± 7.1	101.5 ± 2.3	919 ± 48	686 ± 15
YHO04c	61.6 ± 4.1	12.1 ± 1.4	49.5 ± 4.4	35.7 ± 1.3	854 ± 75	616 ± 23
YHO05a	291.3 ± 11.1	ND	291.3 ± 11.1	52.4 ± 3.1	1692 ± 64	304 ± 18
YHO05b	93.3 ± 5.3	14.8 ± 1.7	78.4 ± 5.6	42.0 ± 1.7	508 ± 36	272 ± 11
YHO05c	57.8 ± 4.0	8.1 ± 1.5	49.7 ± 4.3	30.4 ± 1.3	976 ± 85	597 ± 25
Mean ^{210}Pb and ^{137}Cs Inventory (Bq m^{-2})					3826 ± 375	1786 ± 352
YHK01a	174.2 ± 7.0	25.2 ± 1.9	149.0 ± 7.3	75.3 ± 1.5	2088 ± 102	1055 ± 22
YHK01b	190.3 ± 7.9	25.8 ± 1.8	164.5 ± 8.1	109.0 ± 2.0	1485 ± 73	984 ± 18
YHK01c	100.3 ± 5.6	32.1 ± 1.3	68.3 ± 5.8	49.0 ± 1.1	2203 ± 186	1582 ± 35
YHK02a	243.5 ± 7.8	24.8 ± 1.8	218.6 ± 8.0	87.4 ± 2.0	2407 ± 88	962 ± 22
YHK02b	193.7 ± 6.9	29.8 ± 1.7	163.9 ± 7.1	122.3 ± 1.9	3035 ± 132	2266 ± 36
YHK02c	94.3 ± 4.1	35.4 ± 1.1	58.9 ± 4.2	89.1 ± 1.1	1430 ± 102	2163 ± 26
YHK03a	202.9 ± 7.5	19.1 ± 2.0	183.8 ± 7.7	61.1 ± 2.0	1785 ± 75	593 ± 19
YHK03b	150.5 ± 6.5	36.8 ± 1.6	113.7 ± 6.7	73.7 ± 1.6	1611 ± 95	1044 ± 23
YHK03c	93.5 ± 6.0	37.6 ± 1.5	56.0 ± 6.2	53.0 ± 1.4	1646 ± 183	1559 ± 41
YHK04a	195.0 ± 7.2	37.8 ± 1.7	157.2 ± 7.4	70.5 ± 1.6	3948 ± 185	1769 ± 39
YHK04b	98.6 ± 5.8	38.0 ± 1.6	60.6 ± 6.0	54.2 ± 1.4	1375 ± 137	1230 ± 31
YHK04c	59.9 ± 3.6	42.2 ± 1.1	17.7 ± 3.7	15.9 ± 0.7	562 ± 118	504 ± 23
YHK05a	210.9 ± 7.6	39.2 ± 1.7	171.7 ± 7.8	83.4 ± 1.7	4312 ± 197	2093 ± 44
YHK05b	87.8 ± 5.4	38.6 ± 1.4	49.2 ± 5.6	24.8 ± 1.1	1115 ± 128	563 ± 24
YHK05c	49.3 ± 5.6	45.4 ± 1.6	3.8 ± 5.9	3.7 ± 0.9	123 ± 187	119 ± 30
Mean ^{210}Pb and ^{137}Cs Inventory (Bq m^{-2})					5825 ± 669	3697 ± 1002
YHB01a	337.8 ± 8.4	ND	337.8 ± 8.4	114.4 ± 2.6	1657 ± 41	561 ± 13

continued on next page

continued from previous page

Sample Identity	^{210}Pb and ^{137}Cs (Bq kg^{-1})				^{210}Pb and ^{137}Cs (Bq m^{-2})	
	^{210}Pb$_{tot.}$	^{210}Pb$_{sup.}$	^{210}Pb$_{exs.}$	^{137}Cs	^{210}Pb	^{137}Cs
YHB01b	185.6 ± 7.5	5.5 ± 1.9	180.1 ± 7.7	88.6 ± 2.5	1068 ± 46	525 ± 15
YHB01c	119.2 ± 5.8	6.4 ± 1.9	112.8 ± 6.1	74.9 ± 2.2	440 ± 24	292 ± 9
YHB02a	339.9 ± 8.4	ND	339.9 ± 8.4	94.2 ± 2.5	1904 ± 47	527 ± 14
YHB02b	87.0 ± 5.6	ND	87.0 ± 5.6	58.7 ± 2.2	510 ± 33	344 ± 13
YHB02c	34.0 ± 2.1	4.6 ± 1.1	29.4 ± 2.4	35.9 ± 1.1	235 ± 19	287 ± 9
YHB03a	368.7 ± 11.8	10.3 ± 3.0	358.4 ± 12.2	95.6 ± 3.2	2119 ± 72	565 ± 19
YHB03b	212.0 ± 7.4	10.4 ± 2.4	201.6 ± 7.8	89.0 ± 2.6	1097 ± 42	484 ± 14
YHB03c	70.9 ± 4.4	ND	70.9 ± 4.4	60.2 ± 2.0	603 ± 37	512 ± 17
YHB04a	507.1 ± 11.9	ND	507.1 ± 11.9	91.9 ± 3.0	2438 ± 57	442 ± 14
YHB04b	147.6 ± 6.0	ND	147.6 ± 6.0	65.0 ± 1.9	794 ± 32	350 ± 10
YHB04c	64.3 ± 2.9	6.3 ± 1.1	58.0 ± 3.1	47.0 ± 1.2	540 ± 29	438 ± 11
YHB05a	409.6 ± 12.6	ND	409.6 ± 12.6	76.9 ± 3.2	2226 ± 69	418 ± 17
YHB05b	178.3 ± 6.6	6.8 ± 2.0	171.5 ± 6.9	99.3 ± 2.3	962 ± 39	557 ± 13
YHB05c	48.4 ± 3.6	8.8 ± 1.7	39.6 ± 4.0	55.0 ± 1.8	373 ± 37	518 ± 17
Mean ^{210}Pb and ^{137}Cs Inventory (Bq m^{-2})					3394 ± 439	1364 ± 153

ND: Not Detected.

Table B.7: *Soils from Bryn Maur, Mid-Wales.*

The ^{210}Pb and ^{137}Cs Specific Activities and Inventories in Soil Samples						
Sample Identity	^{210}Pb and ^{137}Cs (Bq kg^{-1})				^{210}Pb and ^{137}Cs (Bq m^{-2})	
	^{210}Pb$_{tot.}$	^{210}Pb$_{sup.}$	^{210}Pb$_{exs.}$	^{137}Cs	^{210}Pb	^{137}Cs
BMO01a	189.8 ± 8.0	23.4 ± 2.1	166.4 ± 166.4	80.8 ± 2.3	1234 ± 44	599 ± 17
BMO01b	111.5 ± 6.3	22.4 ± 1.6	89.2 ± 89.2	82.9 ± 1.8	1061 ± 56	987 ± 21
BMO01c	57.5 ± 4.4	33.2 ± 1.3	24.3 ± 24.3	20.8 ± 0.9	727 ± 93	622 ± 28
BMO02a	344.2 ± 10.8	24.7 ± 2.8	319.5 ± 319.5	96.2 ± 3.0	2340 ± 59	704 ± 22
BMO02b	54.6 ± 4.9	23.5 ± 1.6	31.1 ± 31.1	26.8 ± 1.2	870 ± 93	749 ± 33
BMO02c	48.8 ± 5.0	35.5 ± 1.5	13.3 ± 13.3	ND	617 ± 164	ND
BMO03a	303.1 ± 8.7	20.3 ± 1.8	282.8 ± 282.8	109.5 ± 2.5	2830 ± 69	1096 ± 25
BMO03b	105.0 ± 6.2	24.7 ± 1.6	80.4 ± 80.4	82.7 ± 1.7	946 ± 54	974 ± 21
BMO03c	64.0 ± 4.7	26.1 ± 1.3	37.9 ± 37.9	41.1 ± 1.1	992 ± 91	1077 ± 29
BMO04a	608.5 ± 9.0	11.0 ± 1.7	597.6 ± 597.6	404.6 ± 3.3	4558 ± 55	3086 ± 25
BMO04b	145.3 ± 5.9	13.4 ± 1.5	132.0 ± 132.0	115.2 ± 1.9	2082 ± 69	1816 ± 30

continued on next page

continued from previous page

Sample Identity	^{210}Pb and ^{137}Cs (Bq kg^{-1})				^{210}Pb and ^{137}Cs (Bq m^{-2})	
	^{210}Pb$_{tot.}$	^{210}Pb$_{sup.}$	^{210}Pb$_{exs.}$	^{137}Cs	^{210}Pb	^{137}Cs
BMO04c	58.7 ± 5.1	26.5 ± 1.5	32.1 ± 32.1	16.4 ± 1.2	1032 ± 116	527 ± 38
BMO05a	802.5 ± 14.7	13.7 ± 2.8	788.8 ± 788.8	316.7 ± 4.6	3696 ± 56	1484 ± 22
BMO05b	226.7 ± 6.8	16.7 ± 1.5	209.9 ± 209.9	268.0 ± 2.6	3072 ± 77	3922 ± 38
BMO05c	67.7 ± 4.6	24.1 ± 1.5	43.6 ± 43.6	28.2 ± 1.3	1387 ± 100	899 ± 41
BMO06a	643.4 ± 11.0	2.8 ± 2.3	640.6 ± 640.6	265.4 ± 3.6	2971 ± 40	1231 ± 17
BMO06b	208.7 ± 8.7	6.6 ± 2.0	202.1 ± 202.1	297.8 ± 3.5	2602 ± 85	3835 ± 45
BMO06c	80.3 ± 4.6	13.3 ± 1.2	67.1 ± 67.1	26.3 ± 1.1	2138 ± 109	840 ± 35
Mean ^{210}Pb and ^{137}Cs Inventory (Bq m^{-2})					5859 ± 2253	4075 ± 2068
BMW01a	860.4 ± 19.3	ND	860.4 ± 19.3	64.1 ± 3.5	5813 ± 130	433 ± 23
BMW01b	454.7 ± 8.3	9.7 ± 1.4	445.0 ± 8.4	212.3 ± 2.3	4028 ± 76	1922 ± 20
BMW01c	160.9 ± 5.7	8.1 ± 1.2	152.8 ± 5.8	67.8 ± 1.5	2578 ± 98	1144 ± 26
BMW02a	854.4 ± 24.9	14.6 ± 4.4	839.8 ± 25.3	80.0 ± 4.7	4201 ± 126	400 ± 23
BMW02b	231.0 ± 8.1	18.6 ± 1.7	212.4 ± 8.3	299.4 ± 2.7	2963 ± 116	4177 ± 38
BMW02c	95.2 ± 5.5	ND	95.2 ± 5.5	58.4 ± 1.8	1584 ± 92	972 ± 30
BMW03a	331.1 ± 11.0	ND	331.1 ± 11.0	59.4 ± 2.8	2771 ± 92	497 ± 24
BMW03b	258.0 ± 13.3	6.3 ± 0.5	251.7 ± 13.3	128.4 ± 3.1	2717 ± 143	1386 ± 34
BMW03c	86.0 ± 2.5	16.4 ± 4.1	69.6 ± 4.8	57.2 ± 1.0	1453 ± 100	1192 ± 20
BMW04a	356.5 ± 9.0	9.6 ± 2.1	346.9 ± 9.2	78.0 ± 2.3	4337 ± 115	975 ± 28
BMW04b	186.0 ± 7.8	9.7 ± 1.2	176.4 ± 7.9	133.9 ± 2.7	1927 ± 86	1462 ± 30
BMW04c	84.6 ± 3.3	8.5 ± 1.3	76.2 ± 3.6	55.1 ± 1.0	1302 ± 61	942 ± 16
BMW05a	569.3 ± 19.2	14.6 ± 2.7	554.7 ± 19.4	112.2 ± 3.4	3468 ± 121	701 ± 21
BMW05b	262.8 ± 7.1	19.8 ± 1.5	243.0 ± 7.3	139.3 ± 2.0	2077 ± 62	1190 ± 17
BMW05c	123.0 ± 5.3	14.9 ± 1.3	108.2 ± 5.5	45.1 ± 1.2	1478 ± 75	616 ± 17
BMW06a	549.3 ± 16.8	ND	549.3 ± 16.8	73.7 ± 3.5	2257 ± 69	303 ± 14
BMW06b	343.7 ± 9.0	10.9 ± 1.9	332.8 ± 9.2	122.0 ± 2.4	2899 ± 80	1063 ± 21
BMW06c	64.5 ± 4.8	26.5 ± 1.4	37.9 ± 5.0	18.1 ± 1.0	1562 ± 205	745 ± 43
BMW07a	490.0 ± 16.3	ND	490.0 ± 16.3	62.2 ± 3.7	2371 ± 79	301 ± 18
BMW07b	247.2 ± 6.2	12.9 ± 1.6	234.3 ± 6.4	149.0 ± 2.2	2504 ± 69	1592 ± 24
BMW07c	40.8 ± 3.7	30.1 ± 1.5	10.7 ± 4.0	18.0 ± 1.1	522 ± 192	874 ± 53
Mean ^{210}Pb and ^{137}Cs Inventory (Bq m^{-2})					7830 ± 2258	3270 ± 1116

ND: Not Detected.

Table B.8: *Soils from the Plynlimon Mountain, Mid-Wales.*

The ^{210}Pb and ^{137}Cs Specific Activities and Inventories in Soil Samples						
Sample	^{210}Pb and ^{137}Cs (Bq kg^{-1})				^{210}Pb and ^{137}Cs (Bq m^{-2})	
Identity	^{210}Pb$_{tot.}$	^{210}Pb$_{sup.}$	^{210}Pb$_{exs.}$	^{137}Cs	^{210}Pb	^{137}Cs
PLS01a	456.4 ± 7.5	25.2 ± 1.6	431.1 ± 7.7	247.4 ± 2.4	5364 ± 96	3078 ± 30
PLS01b	80.6 ± 5.0	29.1 ± 1.3	51.5 ± 5.2	65.6 ± 1.3	1487 ± 149	1894 ± 37
PLS01c	52.5 ± 3.7	32.9 ± 1.1	19.6 ± 3.8	18.1 ± 0.8	844 ± 166	781 ± 34
PLS02a	1165.4 ± 20.7	13.9 ± 3.6	1151.6 ± 21.1	302.8 ± 5.2	7727 ± 141	2032 ± 35
PLS02b	130.1 ± 5.7	28.5 ± 1.5	101.5 ± 5.8	86.9 ± 1.5	1306 ± 75	1118 ± 20
PLS02c	72.9 ± 5.5	37.3 ± 1.6	35.6 ± 5.7	17.0 ± 1.2	1259 ± 203	602 ± 42
PLS03a	723.5 ± 14.6	15.4 ± 3.3	708.1 ± 15.0	388.9 ± 5.1	6060 ± 128	3328 ± 44
PLS03b	109.1 ± 6.6	26.1 ± 1.8	83.1 ± 6.8	90.5 ± 1.9	2284 ± 188	2490 ± 53
PLS03c	47.7 ± 4.7	38.8 ± 1.7	8.9 ± 5.0	19.7 ± 1.2	328 ± 185	728 ± 44
PLS04a	1370.2 ± 27.4	ND	1370.2 ± 27.4	233.1 ± 5.6	7629 ± 153	1298 ± 31
PLS04b	177.8 ± 6.4	28.8 ± 1.5	149.0 ± 6.6	120.0 ± 1.7	2464 ± 109	1985 ± 29
PLS04c	44.1 ± 2.8	38.6 ± 0.9	5.6 ± 2.9	13.9 ± 0.6	229 ± 120	573 ± 24
Mean ^{210}Pb and ^{137}Cs Inventory (Bq m^{-2})					9246 ± 11290	4977 ± 1393
PLF01a	521.2 ± 11.5	20.7 ± 2.6	500.5 ± 11.8	543.4 ± 5.2	5974 ± 141	6486 ± 62
PLF01b	138.0 ± 5.9	18.7 ± 1.3	119.3 ± 6.0	101.0 ± 1.6	1408 ± 71	1193 ± 19
PLF01c	43.2 ± 4.1	21.2 ± 1.5	22.0 ± 4.4	9.2 ± 1.1	828 ± 164	345 ± 41
PLF02a	783.7 ± 16.1	12.1 ± 3.3	771.5 ± 16.5	411.0 ± 5.3	7111 ± 152	3789 ± 49
PLF02b	132.0 ± 6.3	22.3 ± 1.6	109.7 ± 6.5	85.0 ± 1.7	1292 ± 76	1001 ± 20
PLF02c	39.6 ± 3.8	24.7 ± 1.4	14.9 ± 4.0	8.1 ± 1.0	484 ± 130	263 ± 32
PLF03a	520.6 ± 8.3	12.9 ± 2.1	507.7 ± 8.6	600.9 ± 3.9	4704 ± 80	5567 ± 36
PLF03b	153.1 ± 6.6	15.9 ± 1.5	137.2 ± 6.7	115.1 ± 1.9	1582 ± 77	1328 ± 22
PLF03c	54.3 ± 4.2	18.5 ± 1.6	35.7 ± 4.5	7.5 ± 1.1	1220 ± 155	257 ± 36
PLF04a	376.0 ± 9.8	15.3 ± 2.5	360.7 ± 10.1	507.0 ± 4.4	4221 ± 118	5933 ± 52
PLF04b	139.1 ± 6.3	17.9 ± 1.6	121.3 ± 6.5	162.1 ± 2.1	1432 ± 77	1914 ± 25
PLF04c	37.6 ± 3.9	21.3 ± 1.5	16.3 ± 4.2	34.7 ± 1.4	458 ± 119	974 ± 39
PLF05a	887.1 ± 14.8	10.9 ± 2.9	876.2 ± 15.1	122.0 ± 3.0	4879 ± 84	679 ± 17
PLF05b	387.1 ± 11.0	17.1 ± 2.3	370.0 ± 11.2	236.1 ± 3.4	3454 ± 105	2204 ± 32
PLF05c	37.7 ± 4.2	15.6 ± 1.6	22.1 ± 4.5	42.6 ± 1.5	692 ± 141	1333 ± 47
Mean ^{210}Pb and ^{137}Cs Inventory (Bq m^{-2})					7948 ± 1192	6653 ± 1957
PLW01a	648.5 ± 14.7	11.8 ± 2.8	636.7 ± 14.9	116.2 ± 3.3	4129 ± 97	754 ± 22
PLW01b	266.6 ± 8.1	17.4 ± 1.7	249.2 ± 8.3	227.9 ± 2.6	2880 ± 96	2634 ± 30
PLW01c	92.9 ± 5.0	16.9 ± 1.2	76.0 ± 5.1	31.6 ± 1.0	947 ± 64	393 ± 13
PLW02a	933.0 ± 23.4	13.5 ± 4.7	919.6 ± 23.9	92.1 ± 4.2	5077 ± 132	509 ± 23
PLW02b	111.8 ± 5.8	25.7 ± 1.6	86.1 ± 6.0	89.3 ± 1.6	916 ± 64	950 ± 17
PLW02c	52.0 ± 5.2	23.4 ± 1.6	28.6 ± 5.4	64.8 ± 1.6	681 ± 129	1543 ± 38

continued on next page

continued from previous page						
Sample	^{210}Pb and ^{137}Cs (Bq kg^{-1})				^{210}Pb and ^{137}Cs (Bq m^{-2})	
Identity	^{210}Pb$_{tot.}$	^{210}Pb$_{sup.}$	^{210}Pb$_{exs.}$	^{137}Cs	^{210}Pb	^{137}Cs
PLW02d	172.6 ± 6.7	19.9 ± 1.5	152.7 ± 6.8	97.0 ± 1.8	3336 ± 149	2118 ± 38
PLW03a	658.4 ± 11.7	ND	658.4 ± 11.7	156.9 ± 2.9	3217 ± 57	767 ± 14
PLW03b	236.7 ± 8.3	18.6 ± 2.0	218.1 ± 8.5	216.3 ± 2.6	2576 ± 101	2553 ± 30
PLW03c	93.5 ± 5.5	19.4 ± 1.4	74.1 ± 5.7	34.0 ± 1.2	1376 ± 105	632 ± 22
PLW04a	759.5 ± 26.4	ND	759.5 ± 26.4	63.1 ± 5.1	4551 ± 158	378 ± 30
PLW04b	283.3 ± 7.6	16.1 ± 1.5	267.2 ± 7.8	152.0 ± 2.0	3262 ± 95	1856 ± 25
PLW04c	50.6 ± 4.4	23.4 ± 1.4	27.2 ± 4.6	13.8 ± 1.0	490 ± 83	248 ± 19
PLW05a	585.2 ± 9.6	8.9 ± 2.1	576.4 ± 9.8	174.6 ± 2.7	4512 ± 77	1367 ± 21
PLW05b	131.6 ± 6.8	28.5 ± 1.7	103.1 ± 7.0	130.4 ± 1.9	1332 ± 90	1684 ± 25
PLW05c	52.1 ± 5.2	37.3 ± 1.6	14.8 ± 5.5	9.0 ± 1.0	684 ± 253	419 ± 46
Mean ^{210}Pb and ^{137}Cs Inventory (Bq m^{-2})					7993 ± 1323	3761 ± 949

ND: Not Detected.

Table B.9: *Soils from the Tan Valley, Mid-Wales.*

The ^{210}Pb and ^{137}Cs Specific Activities and Inventories in Soil Samples						
Sample	^{210}Pb and ^{137}Cs (Bq kg^{-1})				^{210}Pb and ^{137}Cs (Bq m^{-2})	
Identity	^{210}Pb$_{tot.}$	^{210}Pb$_{sup.}$	^{210}Pb$_{exs.}$	^{137}Cs	^{210}Pb	^{137}Cs
TNO01a	844.3 ± 21.6	17.3 ± 4.0	827.0 ± 22.0	126.5 ± 4.7	2979 ± 79	456 ± 17
TNO01b	347.3 ± 9.9	12.5 ± 2.0	334.8 ± 10.1	163.9 ± 2.9	2097 ± 63	1026 ± 18
TNO01c	91.0 ± 4.6	8.7 ± 1.3	82.3 ± 4.8	44.8 ± 1.3	1428 ± 83	778 ± 23
TNO02a	1370.6 ± 32.6	ND	1370.6 ± 32.6	132.8 ± 5.6	2598 ± 62	252 ± 11
TNO02b	467.7 ± 6.6	6.3 ± 1.2	461.4 ± 6.7	160.2 ± 1.7	3471 ± 51	1205 ± 13
TNO02c	49.4 ± 4.5	27.1 ± 1.5	22.3 ± 4.8	42.3 ± 1.3	623 ± 133	1181 ± 35
TNO03a	774.9 ± 13.0	8.0 ± 2.5	766.9 ± 13.3	192.7 ± 3.4	4938 ± 85	1241 ± 22
TNO03b	90.1 ± 5.1	7.2 ± 1.5	82.9 ± 5.3	42.4 ± 1.6	747 ± 48	382 ± 14
TNO03c	38.2 ± 3.1	10.1 ± 1.3	28.1 ± 3.4	21.1 ± 1.3	401 ± 49	302 ± 18
TNO04a	1245.4 ± 61.3	ND	1245.4 ± 61.3	163.0 ± 11.8	4604 ± 226	602 ± 44
TNO04b	576.9 ± 8.2	9.4 ± 1.9	567.5 ± 8.5	220.1 ± 2.6	2712 ± 40	1052 ± 12
TNO04c	115.2 ± 5.3	10.3 ± 1.4	104.9 ± 5.5	53.6 ± 1.5	1594 ± 83	815 ± 23
TNO05a	837.9 ± 17.9	17.2 ± 3.4	820.6 ± 18.2	199.7 ± 4.9	5362 ± 119	1305 ± 32
TNO05b	153.2 ± 6.3	5.6 ± 1.7	147.6 ± 6.5	58.4 ± 1.9	940 ± 41	372 ± 12

continued on next page

continued from previous page						
Sample	^{210}Pb and ^{137}Cs (Bq kg^{-1})				^{210}Pb and ^{137}Cs (Bq m^{-2})	
Identity	^{210}Pb$_{tot.}$	^{210}Pb$_{sup.}$	^{210}Pb$_{exs.}$	^{137}Cs	^{210}Pb	^{137}Cs
TNO05c	20.5 ± 2.5	7.4 ± 1.5	13.0 ± 2.9	42.9 ± 1.7	195 ± 44	640 ± 25
Mean ^{210}Pb and ^{137}Cs Inventory (Bq m^{-2})					6937 ± 1125	2322 ± 266
TNW01a	613.7 ± 22.1	13.3 ± 4.9	600.3 ± 22.6	18.0 ± 3.9	2558 ± 96	77 ± 17
TNW01b	554.2 ± 15.4	10.3 ± 3.2	543.9 ± 15.7	39.2 ± 3.1	3048 ± 88	220 ± 17
TNW01c	108.4 ± 5.8	25.5 ± 1.5	83.0 ± 6.0	139.7 ± 1.8	3166 ± 228	5330 ± 70
TNW02a	840.7 ± 21.6	ND	840.7 ± 21.6	33.4 ± 4.0	6067 ± 156	241 ± 29
TNW02b	132.3 ± 5.7	22.2 ± 1.4	110.1 ± 5.9	41.6 ± 1.3	1712 ± 92	647 ± 20
TNW02c	52.9 ± 4.9	42.8 ± 1.9	10.0 ± 5.3	6.8 ± 1.2	709 ± 373	477 ± 82
TNW03a	645.8 ± 18.5	ND	645.8 ± 18.5	28.7 ± 3.2	3809 ± 109	169 ± 19
TNW03b	317.0 ± 7.8	10.4 ± 1.4	306.6 ± 7.9	100.7 ± 1.8	2974 ± 77	977 ± 18
TNW03c	54.0 ± 4.8	31.9 ± 1.4	22.1 ± 5.0	8.7 ± 0.9	1419 ± 320	562 ± 56
TNW04a	767.7 ± 17.0	11.8 ± 3.3	755.8 ± 17.3	77.8 ± 3.2	5009 ± 115	516 ± 21
TNW04b	128.7 ± 4.4	20.9 ± 1.1	107.8 ± 4.5	38.2 ± 1.0	1871 ± 79	662 ± 17
TNW04c	53.3 ± 4.9	30.9 ± 1.5	22.4 ± 5.2	4.4 ± 1.0	1276 ± 293	252 ± 57
TNW05a	783.9 ± 18.5	ND	783.9 ± 18.5	30.6 ± 3.2	3617 ± 85	141 ± 15
TNW05b	185.5 ± 9.3	18.4 ± 2.4	167.1 ± 9.6	189.8 ± 3.1	2778 ± 160	3154 ± 51
TNW05c	89.4 ± 5.2	29.4 ± 1.4	60.0 ± 5.4	35.3 ± 1.2	2402 ± 217	1411 ± 47
Mean ^{210}Pb and ^{137}Cs Inventory (Bq m^{-2})					8483 ± 304	2967 ± 2037

ND: Not Detected.

Appendix C

Precipitation Samples

C.1 Bulk and Throughfall Concentrations

Table C.1: *^{210}Pb and ^{7}Be concentrations in bulk precipitation and throughfall.*

^{210}Pb and ^{7}Be Concentrations in Precipitation						
Collection Dates	†Exp. (Days)	‡Ppt. (mm)	Bulk (mBq l^{-1})		Throughfall (mBq l^{-1})	
			^{210}Pb	^{7}Be	^{210}Pb	^{7}Be
18/05/01	Deployed					
04/06/01	17	41	5.5 ± 0.9	30.3 ± 0.5	NM	NM
27/06/01	23	66	12.4 ± 1.8	406.9 ± 24.1	14.5 ± 1.5	67.8 ± 22.9
31/07/01	34	75	4.8 ± 0.7	193.1 ± 18.3	5.1 ± 0.7	57.5 ± 19.8
14/08/01	14	100	10.0 ± 1.1	519.6 ± 14.9	3.0 ± 0.5	57.6 ± 14.7
21/08/01	7	100	8.8 ± 1.1	741.7 ± 20.9	5.4 ± 0.7	54.8 ± 18.3
17/09/01	28	44	55.1 ± 5.0	375.1 ± 27.2	20.8 ± 2.1	160.6 ± 17.5
03/10/01	16	49	26.2 ± 2.9	544.6 ± 27.5	8.7 ± 1.0	92.9 ± 15.6
23/10/01	20	95	22.3 ± 2.2	290.6 ± 14.4	4.9 ± 0.7	89.3 ± 18.1
21/11/01	29	70	19.7 ± 2.2	380.7 ± 17.6	17.1 ± 1.8	157.4 ± 37.9
16/01/02	56	85	9.1 ± 1.2	158.2 ± 17.5	6.6 ± 0.9	53.7 ± 5.9
12/02/02	27	189	13.5 ± 1.5	124.9 ± 10.8	NM	NM
04/03/02	20	132	0.9 ± 0.1	148.2 ± 21.2	5.4 ± 0.7	17.8 ± 4.1
25/03/02	21	72	23.0 ± 2.5	161.1 ± 22.1	17.4 ± 2.1	94.0 ± 14.2
10/05/02	46	66	79.2 ± 8.4	259.4 ± 23.7	31.4 ± 5.6	77.2 ± 18.3
§§Vol.-Wgtd. Avg. Conc. (mBq l^{-1})			53.8 ± 3.4	908.7 ± 47.1	¶12.7 ± 0.3	¶95.9 ± 4.4

†Period of Exposure.
‡Precipitation.
NM: Not Measured because collectors were overflowing.
§§Volume-Weighted Average Concentrations.
¶The Mean Values.

C.2 Bulk and Throughfall Fluxes

Table C.2: *^{210}Pb and ^{7}Be fluxes in bulk precipitation and throughfall.*

^{210}Pb and ^{7}Be fluxes						
Collection Dates	†Exp. (Days)	‡Ppt. (mm)	Bulk (Bq m^{-2})		Throughfall (Bq m^{-2})	
			^{210}Pb	^{7}Be	^{210}Pb	^{7}Be
18/05/01	Deployed					
04/06/01	17	41	0.68 ± 0.11	3.75 ± 0.06	NM	NM
27/06/01	23	66	2.52 ± 0.35	80.99 ± 4.79	0.48 ± 0.05	2.25 ± 0.76
31/07/01	34	75	1.08 ± 0.16	43.19 ± 4.09	0.18 ± 0.03	2.06 ± 0.71
14/08/01	14	100	3.01 ± 0.33	155.98 ± 4.48	0.14 ± 0.02	2.64 ± 2.03
21/08/01	7	100	2.65 ± 0.32	222.64 ± 6.28	0.21 ± 0.03	2.16 ± 0.72
17/09/01	28	44	7.28 ± 0.66	49.55 ± 3.60	0.32 ± 0.03	2.47 ± 0.27
03/10/01	16	49	3.85 ± 0.42	80.10 ± 4.04	0.18 ± 0.02	1.92 ± 0.32
23/10/01	20	95	6.35 ± 0.64	82.88 ± 4.09	0.21 ± 0.03	3.93 ± 0.80
21/11/01	29	70	4.14 ± 0.46	80.00 ± 3.70	0.48 ± 0.05	4.45 ± 1.07
16/01/02	56	85	2.32 ± 0.28	40.37 ± 4.45	0.20 ± 0.03	1.64 ± 0.18
12/02/02	27	189	7.64 ± 0.84	70.86 ± 6.14	NM	NM
04/03/02	20	132	0.34 ± 0.05	58.71 ± 8.41	0.25 ± 0.03	0.84 ± 0.19
25/03/02	21	72	4.97 ± 0.55	34.83 ± 4.77	0.60 ± 0.07	3.26 ± 1.19
10/05/02	46	66	15.69 ± 1.66	51.39 ± 4.70	0.72 ± 0.13	1.77 ± 0.42
Annual Flux (Bq m^{-2} y^{-1})			63.7 ± 2.4	1235 ± 21	4.8 ± 0.2	34.2 ± 8.8

†Period of Exposure.
‡Precipitation.
NM: Not Measured because collectors were overflowing.

C.3 Concentrations of ^{210}Pb and ^{7}Be in Foliage

Table C.3: *^{210}Pb and ^{7}Be concentrations and activities in sitka spruce needles.*

^{210}Pb and ^{7}Be Concentrations and Activities: June 2001					
Needle Class	†Age (Months)	Concentrations (Bq kg^{-1})		‡Activities (Bq m^{-2})	
		^{210}Pb	^{7}Be	^{210}Pb	^{7}Be
Cr.	2	19.3 ± 1.2	26.6 ± 8.4	4.0 ± 0.3	5.5 ± 1.7
1 yr	14	10.4 ± 1.3	63.6 ± 7.7	15.0 ± 0.3	16.6 ± 2.0
2 yr	26	51.0 ± 2.6	74.0 ± 9.8	16.0 ± 0.7	21.3 ± 2.8
3 yr	38	66.4 ± 3.9	80.0 ± 10.1	15.6 ± 1.3	23.0 ± 4.0
^{210}Pb and ^{7}Be Concentrations and Activities: July, 2002					
Cr.	3	19.3 ± 2.0	46.4 ± 7.8	5.8 ± 0.4	9.6 ± 1.6
1 yr	15	41.7 ± 2.7	63.3 ± 8.1	15.0 ± 0.7	16.5 ± 2.1
2 yr	27	41.3 ± 2.6	71.7 ± 7.9	15.8 ± 0.7	20.6 ± 2.3
3 yr	39	67.8 ± 3.1	79.3 ± 8.3	14.9 ± 1.1	26.8 ± 2.8

†Approximate age of needles after leafing.
‡Based on specific leaf area of the needles (in m^2 kg^{-1}).

Table C.4: *^{210}Pb and ^{7}Be concentrations and activities in oak, lime and sycamore.*

^{210}Pb and ^{7}Be Concentrations (in Bq kg^{-1})									
Collection Dates	Oak			Lime			Sycamore		
	^{210}Pb	^{7}Be	†^{7}Be	^{210}Pb	^{7}Be	†^{7}Be	^{210}Pb	^{7}Be	†^{7}Be
25/06/02	27.8 ± 2.5	69.8 ± 6.1	69.8	29.6 ± 2.5	53.8 ± 6.2	53.8	31.8 ± 2.6	174.3 ± 7.7	174.3
26/07/02	29.6 ± 2.2	127.3 ± 6.8	80.6	29.6 ± 2.0	71.6 ± 7.0	35.6	43.9 ± 2.5	274.9 ± 9.0	158.4
27/08/02	72.1 ± 3.5	192.6 ± 10.7	108.6	28.7 ± 2.8	156.7 ± 10.1	109.5	99.1 ± 4.5	455.1 ± 13.2	273.7
24/09/02	94.5 ± 4.2	210.2 ± 10.8	76.3	58.1 ± 3.5	175.5 ± 10.4	66.6	101.3 ± 4.4	461.7 ± 13.8	145.5
01/11/02	74.5 ± 3.0	277.3 ± 17.2	149.1	49.8 ± 3.4	183.8 ± 20.9	76.7	65.3 ± 3.4	338.1 ± 23.8	56.4
‡^{210}Pb and ^{7}Be Activities (in Bq m^{-2})									
25/06/02	2.2 ± 0.2	5.5 ± 0.5	5.5	1.7 ± 0.1	3.0 ± 0.4	3.0	2.0 ± 0.2	10.7 ± 0.5	10.7
26/07/02	2.3 ± 0.2	10.0 ± 0.5	6.4	1.7 ± 0.1	4.0 ± 0.4	2.0	2.7 ± 0.2	16.9 ± 0.6	9.7
27/08/02	5.7 ± 0.3	15.2 ± 0.8	8.6	1.6 ± 0.2	8.8 ± 0.6	6.1	6.1 ± 0.3	27.9 ± 0.8	16.8
24/09/02	7.4 ± 0.3	16.6 ± 0.9	6.0	3.3 ± 0.2	9.8 ± 0.6	3.7	6.2 ± 0.3	28.3 ± 0.9	8.9
01/11/02	5.9 ± 0.2	21.8 ± 1.4	11.7	2.8 ± 0.2	10.3 ± 1.2	4.3	4.0 ± 0.2	20.7 ± 1.5	3.5

†The difference between ^{7}Be concentration at time of sampling and previous concentrations (decay-corrected).
‡Based on specific leaf area of the leaves (in m^2 kg^{-1}).

Bibliography

[1] Sweden. Air pollution across national boundaries. The impact on the environment of sulphur in air and precipitation. Technical report, Sweden's Case Study for the United Nations Conference on the Human Environment., Stockholm, 1971.

[2] F. W. Oehme. *Toxicity of heavy metals in the environment: Part 1.* Marcel Dekker, New York, 1978.

[3] F. W. Oehme. *Toxicity of heavy metals in the environment: Part 2.* Marcel Dekker, New York, 1979.

[4] M. E. Jenkin and K. C. Clemitshaw. Ozone and other photochemical pollutants: chemical processes governing their formation in the planetary boundary layer. *Atmospheric Environment*, 34:2499–2527, 2000.

[5] PORG. Ozone in the United Kingdom. Fourth Report of the UK Photochemical Oxidants Review Group. Technical report, Department of the Environment, Transport and the Regions, London, UK, 1997.

[6] A. Volz and D. Kley. Evaluation of the Montsouris series of ozone measurements made in the nineteenth century. *Nature*, 332:240–242, 1988.

[7] PORG. Ozone in the United Kingdom. Third Report of the UK Photochemical Oxidants Review Group. Technical report, Department of the Environment, Transport and the Regions, London, UK, 1993.

[8] S. E. Poet, H. E. Moore, and E. A. Martell. Lead 210, bismuth 210, and polonium 210 in the atmosphere: accurate ratio measurement and application to aerosol residence time determination. *Journal of Geophysical Research*, 77(33):6515–6527, 1972.

[9] H. E. Moore, S. E. Poet, and E. A. Martell. ^{222}Rn, ^{210}Pb, and ^{210}Po profiles and aerosols residence times versus altitude. *Journal of Geophysical Research*, 78(30):7065–7074, 1973.

[10] H. E. Moore, S. E. Poet, and E. A. Martell. Size distribution and origin of lead-210, bismuth-210 and polonium-210 on airborne particles in the troposphere. In T. F. Gesell and W. M. Lowder, editors, *Natural Radiation Environment III*, volume 1, pages 415–429, Washington DC, 1980.

[11] G. Lambert, J. Sanak, and G. Polian. Mean residence time of the submicrometer aerosols in the global troposphere. *Precipitation Scavenging, Dry Deposition, and Resuspension*, pages 1353–1359, 1983.

[12] E. Wieland, P. H. Santschi, and J. Beer. A multitracer study of radionuclides in lake Zurich, Switzerland 2. Residence times, removal processes, and sediment focusing. *Journal of Geophysical Research*, 96(C9):17,067–17,080, 1991.

[13] T. Tokieda *et al.* Seasonal variations of residence time and upper atmospheric contribution of aerosols studied with Pb-210, Bi-210, Po-210 and Be-7. *Tellus*, 48B(5):690–702, 1996.

[14] P. H. McMurray. A review of atmospheric aerosol measurements. *Atmospheric Environment*, 34:1959–1999, 2000.

[15] S. Twomey. *Atmospheric Aerosols.* Elsevier Scientific Publishing Company, Elsevier Scientific Publishing Company 335 Jan van Galenstraat. P. O. Box 211, Amsterdam, The Netherlands, 1988.

[16] A. Wellburn. *Air Pollution and Acid rain: The Biological Impact.* Longman Scientific And Technical, Longman House, Essex CM20 2JE, England, 1988.

[17] C. E. Junge. *Air Chemistry and Radioactivity.* Academic Press, New York, 1963.

[18] D. Fowler, J. N. Cape, and M. H. Unsworth. Deposition of pollutants on forests. *Philosophical Transactions of the Royal Society of London Series B*, 324:247–265, 1989.

[19] K. T. Whitby. The physical characteristics of sulphur aerosols. *Atmospheric Environment*, 12:135–160, 1978.

[20] RGAR. Acid Rain in the United Kingdom 1992-1994: A Fourth Report of the United Kingdom Review Group on Acid Rain. Technical report, AEA Technology plc, Culham, UK, 1997.

[21] R. W. Mourne. *Lead-210 as a Tracer for Acidic Deposition in Areas of Complex Topography.* PhD thesis, University of Edinburgh, 1993.

[22] NEGTAP. Transboundary air pollution: acidification, eutrophication and ground-level ozone in the UK. In *National Expert Group on Transboundary Air Pollution*, Centre for Ecology and Hydrology, Edinburgh, 2001.

[23] J. F. Müller. Geographical distribution and seasonal variation of surface emissions and deposition velocities of atmospheric trace gases. *Journal of Geophysical Research*, 97:3787–3804, 1992.

[24] C. M. Benkovitz *et. al.* Global gridded inventories of anthropogenic emissions of sulphur and nitrogen. *Journal of Geophysical Research*, 101(29):29,239–29,253, 1996.

[25] D. S. Lee *et al.* Estimates of global NO_x emissions and their uncertainties. *Atmospheric Environment*, 31:1735–1749, 1997.

[26] A. Eliassen, O. Hov, and T. Iversen. Estimates of airborne transboundary transport of sulphur and nitrogen over Europe. EMEP/MSC-W 1/88. Technical report, Norwegian Meteorological Institute, Oslo, 1988.

[27] K. K. Turekian, Y. Nozaki, and L. K. Benninger. Geochemistry of atmospheric radon and radon products. *Annual Review of Earth and Planetary Sciences*, 5:227–255, 1977.

[28] F. Choubedar. *The Use of Radio-Nuclides (unsupported ^{210}Pb, ^{7}Be and ^{137}Cs) in Air, Rain and Undisturbed Soil as an Environmental tools.* PhD thesis, University of Edinburgh, 2000.

[29] J. A. Young and W. B. Silker. Aerosol deposition velocities on the Pacific and Atlantic oceans calculated from ^{7}Be measurements. *Earth and Planetary Science Letters*, 50(6):92–104, 1980.

[30] F. B. Smith. An overview of acid rain problem. *Meteorological Magazine*, 120(1426):77–91, 1991.

[31] D. Fowler. The transfer of air pollutants to the ground by wet and dry deposition. In Sandroni S., editor, *Regional and Long-range Transport of Air Pollutants*, pages 95–126, Ispra, Italy, 1986.

[32] J. W. Erisman *et al.* Review of deposition monitoring. *Tellus*, 46B(2):79–93, 1994.

[33] D. Fowler and J. N. Cape. The contamination of rain samples by dry deposition on rain collectors. *Atmospheric Environment*, 18:183–189, 1984.

[34] C. Beier and L. Rasmussen. Problems related to collection of rain and throughfall water. In Bresser, editor, *Proceedings on Monitoring Air Pollution and Forest Ecosystem Research*, pages 97–107. UK Conference, 1989.

[35] M. H. Unsworth J. C. and Wilshaw. Wet, occult and dry deposition of pollutants on forests. *Agricultural and Forest Meteorology*, 47:221–238, 1989.

[36] T. Begeron. On the low-level redistribution of atmospheric water caused by orography. In *Suppl. Proc. Int. Conf. Cloud Phys.*, pages 96–100. Tokyo, 1965.

[37] D. Fowler *et al.* The influence of altitude on rainfall composition at Great Dun Fell. *Atmospheric Environment*, 22(7):1355–1362, 1988.

[38] A. Jones and T. W. Choularton. A model of wet deposition on complex terrain. *Atmospheric Environment*, 22(11):2419–2430, 1988.

[39] A. J. Dore *et al.* Field measurements of wet deposition in an extended region of complex topography. *Quarterly Journal of Royal Meteorological Society*, 116:1193–1212, 1990.

[40] W. Ruijgrok, H. Tieben, and P. Eisinga. Dry deposition of particles to a forest Canopy: a comparison of model and experimental results. *Atmospheric Environment*, 31(3):399–415, 1997.

[41] D. Fowler, J. H. Duyzer, and D. D. Baldocchi. Inputs of trace gases, particles and cloud droplets to terrestrial surfaces. *Proceedings of the Royal Society of Edinburgh*, 97B:35–59, 1991.

[42] RGAR. Acid Rain in the United Kingdom 1992-1994: A Third Report of the United Kingdom Review Group on Acid rain. Technical report, Warren Spring Laboratory, Stevenage, UK, 1990.

[43] A. J. Dore, T. W. Choularton, and D. Fowler. An improved wet deposition map of the United Kingdom incorporating the seeder-feeder effect over mountainous terrain. *Atmospheric Environment*, 26A(8):1375–1385, 1992.

[44] N. Preiss *et al.* A compilation of data on lead 210 concentration in surface air and fluxes at the air-surface and water-sediment interfaces. *Journal of Geophysical Research*, 101(D22):28,847–28,862, 1998.

[45] A. J. Peters *et al.* Deposition of ^{210}Pb to the Agassiz ice cap, Canada. *Journal of Geophysical Research*, 102(D5):5971–5978, 1997.

[46] D. J. Jacob *et al.* Evaluation and intercomparison of global atmospheric transport models using ^{222}Rn and other short-lived tracers. *Journal of Geophysical Research*, 102(D5):5953–5970, 1997.

[47] Z. Jaworowski *et al.* Lead-210 from nuclear explosions in the environment. *Nuclear technology*, 37:159–166, 1978.

[48] D. H. Peirson, R. S. Cambray, and G. S. Spicer. Lead-210 and Polonium-210 in the atmosphere. *Tellus*, XVIII(2):427–433, 1966.

[49] W. E. Clements and M. H. Wilkening. Atmospheric pressure effects on ^{222}Rn transport across the east-air interface. *Journal of Geophysical Research*, 79(33):5025–5029, 1974.

[50] T. Kurata and S. Tsunogai. Exhalation rates of ^{222}Rn and deposition rates of ^{210}Pb at the earth's surface estimated from ^{226}Ra and ^{210}Pb profiles in soils. *Geochemical Journal*, 20:81–90, 1986.

[51] H. Dörr and K. O. Münnich. ^{222}Rn flux and soil air concentration profiles in west-Germany. Soil ^{222}Rn as a tracer for gas transport in the unsaturated soil zone. *Tellus*, 42B(1):20–28, 1990.

[52] Y. Nozaki *et al.* Atmospheric ^{210}Pb fluxes determined from soil profiles. *Journal of Geophysical Research*, 83(C8):4047–4051, 1978.

[53] W. C. Graustein and K. K. Turekian. Radon fluxes from the soil to the atmosphere measured by ^{210}Pb-^{226}Ra disequilibrium in soils. *Geophysical Research Letters*, 17(6):841–844, 1990.

[54] C. Dueñas *et al.* Release of ^{222}Rn from some soils. *Annales Geophysicae*, 15:124–133, 1997.

[55] P. M. C. Barretto, R. B. Clark, and J. A. S. Adams. Physical characteristics of radon-222 emanation from rocks, soils and minerals: its relation to temperature and alpha dose. *The Natural Radiation Environment 2*, USERDA Report Conference No. 720805-P2:731–740, 1972.

[56] T. Baltakmens. Profile of lead-210 and radium-226 in four New Zealand soils. *New Zealand Journal of Science*, 17:435–439, 1974.

[57] A. Tidjani. Study of the effects of atmospheric parameters on ground radon concentration by track technique. *Nuclear Tracks Radiation Measurements*, 14(4):457–460, 1988.

[58] J. E. Pearson and G. E. Jones. Emanation of radon 222 from soils and its use as a tracer. *Journal of Geophysical Research*, 70(20):5279–5290, 1965.

[59] D. Israël. Radioactivity of the atmosphere. In T. F. Malone, editor, *Compendium of meteorology*, pages 155–161, Boston, 1951.

[60] M. H. Wilkening, W. E. Clements, and D. Stanley. Radon-222 flux measurements in widely separated regions. In J. A. S. Adams, W. M. Lowder, and T. F. Gessel, editors, *The natural radiation environment II*, pages 717–730, Houston, Texas, 1975.

[61] G. Lambert, B. Ardouin, and J. Sanak. Atmospheric transport of trace elements toward Antarctica. *Tellus*, 42B(1):76–82, 1990.

[62] A. Marenco and J. Fontana. Comments on paper by S. E. Poet, H. E. Moore, and E. A. Martell, 'Lead 210, Bismuth 210, and Polonium 210 in the atmosphere: accurate ratio measurement and application to aerosol residence time determination'. *Journal of Geophysical Research*, 78(33):7149–7151, 1973.

[63] W. C. Graustein and K. K. Turekian. ^{210}Pb and ^{137}Cs in air and soils measure the rate and vertical profile of aerosol scavenging. *Journal of Geophysical Research*, 91(D13):14,355–14,366, 1986.

[64] Y. J. Balkanski *et al.* Transport and residence times of tropospheric aerosols inferred from a global three-dimensional simulation of ^{210}Pb. *Journal of Geophysical Research*, 98(D11):20,573–20,586, 1993.

[65] D. Lal and B. Peters. Cosmic ray produced radioactivity on the Earth. *Hanbuch der Physik*, 46:551–612, 1967.

[66] R. A. Brost, J. Feichter, and M. Heimann. Three-dimensional simulation of ^{7}Be in a global climate model. *Journal of Geophysical Research*, 96(D12):22,423–22,445, 1991.

[67] H. W. Feely, R. J. Larsen, and C. G. Sanderson. Factors that cause seasonal variations in beryllium-7 concentrations in surface air. *Journal of Environmental Radioactivity*, 9:223–249, 1989.

[68] V. A. Dutkiewicz and L. Husain. Stratospheric and tropospheric components of ^{7}Be in surface air. *Journal of Geophysical Research*, 90(D3):5783–5788, 1985.

[69] E. Gerasopoulos *et al.* A climatology of ^{7}Be at four high-altitude stations at the Alps and the northern Apennines. *Atmospheric Environment*, 35:6347–6360, 2001.

[70] D. H. Peirson. Beryllium 7 in air and rain. *Journal of Geophysical Research*, 68(13):3831–3832, 1963.

[71] M. H. Shapiro and J. L. Forbes-Resha. Mean residence time of ^{7}Be-Bearing aerosols in the troposphere. *Journal of Geophysical Research*, 18(15):2647–2649, 1976.

[72] E. A. Crecelius. Prediction of marine atmospheric deposition rates using total ^{7}Be deposition velocities. *Atmospheric Environment*, 15:579–582, 1981.

[73] H. Hötzl and R. Winkler. Activity concentrations of ^{226}Ra, ^{228}Ra, ^{210}Pb, ^{40}K and ^{7}Be and their temporal variations in surface air. *Journal of Environmental Radioactivity*, 5:445–458, 1987.

[74] P. F. Gustafson, M. A. Kerrigan, and S. S. Brar. Comparison of beryllium-7 and cesium-137 radioactivity in ground-level air. *Nature*, 191:454–456, 1961.

[75] J. F. Todd *et al.* Atmospheric depositional characteristics of beryllium 7 and lead 210 along the south-eastern Virginia coast. *Journal of Geophysical Research*, 94(D8):11,106–11,116, 1989.

[76] M. Baskaran, C. H. Coleman, and P. H. Santschi. Atmospheric depositional fuxes of ^{7}Be, ^{210}Pb at Galveston and college station, Texas. *Journal of Geophysical Research*, 98(D11):20,555–20,571, 1993.

[77] C. R. Olsen *et al.* Atmospheric fluxes and marsh-soil inventories of ^{7}Be and ^{210}Pb. *Journal of Geophysical Research*, 90(D6):10,487–10,495, 1985.

[78] D. M. Koch and M. E. Mann. Spatial and temporal variability of ^{7}Be surface concentrations. *Tellus*, 48B(3):387–396, 1996.

[79] E. R. Reiter. Stratosphere-troposphere exchange processes. *Review of Geophysical Space Physics*, 13:459–474, 1975.

[80] J. Sanak, G. Lambert, and B. Ardouin. Measurements of stratosphere-to-troposphere exchange in Antarctica by using short-lived cosmonuclides. *Tellus*, 37B(2):109–115, 1985.

[81] J. E. Dibb *et al.* Estimation of stratospheric input to the Arctic troposphere: ^{7}Be and ^{10}Be in aerosols at Alert, Canada. *Journal of Geophysical Research*, 99(D6):12,855–12,864, 1994.

[82] S. Rehfeld and M. Heimann. Three dimensional atmospheric transport simulation of the radioactive tracers ^{210}Pb, ^{7}Be, ^{10}Be, and ^{90}Sr. *Journal of Geophysical Research*, 100(D12):26,141–26,161, 1995.

[83] W. C. Graustein and K. K. Turekian. ^{7}Be and ^{210}Pb indicate an upper troposphere source for elevated ozone in the summertime subtropical free troposphere of the eastern North Atlantic. *Geophysical Research Letters*, 23(5):539–542, 1996.

[84] D. M. Koch, D. J. Jacob, and W. C. Graustein. Vertical transport of tropospheric aerosols as indicated by ^{7}Be and ^{210}Pb in a chemical tracer model. *Journal of Geophysical Research*, 101(D13):18,651–18,666, 1996.

[85] R. S. Cambray *et al.* Radionuclide fallout in air and rain: results to the end of 1988. *AERE - R 6556*, pages 1–10, 1989.

[86] R. S. Cambray *et al.* Observations on radioactivity from the Chernobyl accident. *Nuclear Energy*, 26(2):77–101, 1987.

[87] F. R. Livens and P. J. Loveland. The influence of soil properties on the environmental mobility of caesium in Cumbria. *Soil Use and Management*, 4(3):69–75, 1988.

[88] F. B. Smith. The deposition of Chernobyl cesium-137 in heavy rain and its persistent uptake by grazing sheep. *Agricultural and Forest Meteorology*, 47:163–177, 1989.

[89] W. C. Graustein and K. K. Turekian. ^{210}Pb as a tracer of the deposition of sub-micrometer aerosols. *Precipitation Scavenging, Dry Deposition, and Resuspension*, pages 1315–1324, 1983.

[90] W. C. Graustein and K. K. Turekian. The effects of forests and topography on the deposition of sub-micrometer aerosols measured by Lead-210 and Cesium-137 in soils. *Agricultural and Forest Meteorology*, 47:199–220, 1989.

[91] R. J. Clifton. The use of radionuclides (unsupported ^{210}Pb, ^{7}Be, and ^{137}Cs) in describing the mixing characteristics of estuarine sediments. In P. J. Kershaw and D. S. Woodhead, editors, *Radionuclides in the Study of Marine Processes*, pages 255–264. Elsevier Applied Science, 1991.

[92] J. D. Eakins. The ^{210}Pb technique for dating sediments, and some applications. *AERE - R 10831*, pages 1–22, 1983.

[93] L. K. Benninger, D. M. Lewis, and K. K. Turekian. The use of natural lead-210 as a heavy metal tracer in the river-estuarine system. In T. M. Church, editor, *Marine Chemistry in Coastal Environment*, volume 18, pages 202–210, Washington DC, 1975.

[94] D. M. Lewis. The use of ^{210}Pb as a heavy metal tracer in the Susquehanna River System. *Geochimica et Cosmochimica Acta*, 41(2):1557–1564, 1977.

[95] N. M. Cutshall, I. L. Larsen, and C. R. Olsen. Direct analysis of ^{210}Pb in sediment and samples: self-absorption corrections. *Nuclear Instruments and Methods*, 206:309–312, 1983.

[96] IAEA. Measurement of radionuclides in food and the environment. In *International Atomic Energy Agency: A Guide Book. Technical Report Series No. 295*, pages 33–69, Vienna, 1989.

[97] N. A. Hallden and J. H. Harley. Graphical resolving of gamma spectra. *Health Physics*, 10:265–269, 1964.

[98] L. Kokta. Determination of peak area. *Nuclear Instruments and Methods*, 112:245–251, 1973.

[99] L. B. Lockhart (Jr.), R. L. Patterson, and A. W. Saunders (Jr.). The size distribution of the radioactive atmospheric aerosols. *Journal of Geophysical Research*, 24:6033–6041, 1965.

[100] E. A. Bondietti, F. O. Hoffman, and I. L. Larsen. Air-to-vegetation transfer rates of natural submicron aerosols. *Journal of Environmental Radioactivity*, 1:5–27, 1984.

[101] M. C. Monaghan. Lead-210 in surface and soils from California: implications for the behaviour of trace constituents in the planetary boundary layer. *Journal of Geophysical Research*, 94(D5):6449–6456, 1989.

[102] N. Preiss and C. Genthon. The use of a new database of lead 210 for global aerosol model validation. *Journal of Geophysical Research*, 102(D21):25,347–25,357, 1997.

[103] S. K. Friedlander. *Smoke, Dust and Haze*. John Wiley and Sons, London, 1977.

[104] A. C. Chamberlain. The movement of particle in plant communities. In J. L. Monteith, editor, *Vegetation and the Atmosphere*, volume 1, pages 155–203, Academic Press, London, 1975.

[105] M. V. Moghaddam. *Study of Surface Roughness Effects on Deposition of Atmospheric Aerosols Using ^{210}Pb Soil Inventories*. PhD thesis, University of Edinburgh, 1998.

[106] C. Beier, P. Gundersen, and L. Rasmussen. A new method for estimation of the dry deposition of particles based on throughfall measurements in forest edge. *Atmospheric Environment*, 22(11):1553–1559, 1992.

[107] C. Beier and P. Gundersen. Atmospheric deposition to the edge of a Spruce forest in Denmark. *Environmental Pollution*, 60:257–271, 1989.

[108] R. Bobbink, G. W. Heil, and M. B. A. G. Raessen. Atmospheric deposition and canopy exchange processes in heathland ecosystems. *Environmental Pollution*, 75:29–37, 1992.

[109] R. K. Kolka *et al.* Atmospheric inputs of mercury and organic carbon into a forested upland/bog watershed. *Water, Air, and Soil Pollution*, 113(1/4):273–294, 1999.

[110] L. J. Sheppard *et al.* Early effects of acid mist on Sitka spruce planted on acid peat. *Phyton: Annales Rei Botanicae*, 39(1):1–184, 1999.

[111] L. J. Sheppard *et al.* Effects of simulated acid mist on Sitka spruce forest approaching canopy closure: significance of acidified versus non-Acidified nitrogen inputs. *Water, Air, and Soil Pollution*, 130:953–958, 2001.

[112] D. Purchas. Handbook of Filter Media. Technical report, Elsevier science ltd., Oxford, 1996.

[113] I. M. Fisenne. Distribution of ^{210}Pb and ^{226}Ra in soil. Technical Report 14, Health and Safety Laboratory Technical Memorandum 67-14, U. S. Atomic Energy Commission - HASL New York, New York, 1968.

[114] H. E. Moore and S. E. Poet. ^{210}Pb fluxes determined from ^{210}Pb and ^{226}Ra soil profiles. *Journal of Geophysical Research*, 81(6):1056–1058, 1976.

[115] Q. He and D. E. Walling. The Distribution of Fallout ^{137}Cs and ^{210}Pb in Undisturbed and Cultivated Soils. *Applied Radiation and Isotopes*, 48(5):677–690, 1997.

[116] H. Dörr and K. O. Münnich. Lead and cesium transport in European soils. *Water, Air, and Soil Pollution*, 57-58:809–818, 1991.

[117] I. D. Pulford *et al.* Mobility of ^{137}Cs and ^{210}Pb in organic soils. In Forester U. Wilken R. D. and Knockel A., editors, *Heavy Metals in the Environment*, volume 1, pages 137–140, Humburg, 1995.

[118] J. T. Smith *et al.* Inventories and fluxes of ^{210}Pb, ^{137}Cs and ^{241}Am determined from the soils of three small catchments in Cumbria, UK. *Journal of Environmental Radioactivity*, 37(2):127–142, 1997.

[119] K. Bunzl and W. Kracke. Cumulative deposition of ^{137}Cs, ^{238}Pu, $^{239+240}$Pu and ^{241}Am from global fallout in soils from forest, grassland and arable land in Bavaria (FRG). *Journal of Environmental Radioactivity*, 8:1–14, 1988.

[120] A. B. Mac Kenzie *et al.* Radionuclide and metal distributions in peat deposition in Scotland. In Forester U. Wilken R. D. and Knockel A., editors, *Heavy Metals in the Environment*, volume 1, pages 113–116, Humburg, 1995.

[121] Meteorological Office. *Annual average rainfall for (Northern and Southern) Britain: International Standard Period 1941-1970.* Meteorological Office: Met.0.886 (NB & SB), London Road, Bracknell, Berkshire. RG12 2SZ, 1977.

[122] I. J. Russell *et al.* Forest vegetation as a sink for atmospheric particulates: quantitative studies in rain and dry deposition. *Journal of Geophysical Research*, 86(C6):5347–5363, 1981.

[123] M. W. Ghallagher *et al.* Measurements of Aerosol Fluxes to Speulder Forest Using a Micrometeorological Technique. *Atmospheric Environment*, 31(3):359–373, 1997.

[124] P. B. Storebø. Small scale topographical influences on precipitation. *Tellus*, XXVIII(1):45–59, 1976.

[125] M. J. Bader and W. T. Roach. Orographic rainfall in warm sectors of depressions. *Quartely Journal of the Royal Meteorological Society*, 103:269–280, 1977.

[126] F. F. Hill, K. A. Browning, and M. J. Bader. Radar and raingauge observations of orographic rain over south Wales. *Quartely Journal of the Royal Meteorological Society*, 107:643–670, 1981.

[127] Ordnnace Survey. *Ordnance survey (Explorer 214 & OL23)*. Ordnance Survey, Southampton, United Kingdom, 1999.

[128] F. R. Livens, A. D. Horrill, and D. L. Singleton. Distribution of radiocesium in the soil-plant systems of upland areas of Europe. *Health Physics*, 60(4):539–545, 1991.

[129] P. J. Bonnett and R. S. Cambray. The record of deposition of radionuclides in the sediments of Ponsonby Tarn, Cumbria. *Hydrobiologia*, 214:63–70, 1991.

[130] D. Fowler *et al.* Measurement of cloud water deposition on vegetation using a lysimeter and flux gradient technique. *Tellus*, 42B(3):285–293, 1990.

[131] G. J. Leeks and G. Roberts. The effects of forestry on upland streams-with special reference to water quality and sediment transport. In Good J. E. G., editor, *Environmental Aspects of Plantation Forestry in Wales*, volume 22, pages 9–12, Institude of Terrestrial Ecology Symposium, Institute of Terrestrial Ecology, Grange-over-Sands, UK, 1987.

[132] J. Hudson, G. J. Leeks, and G. Roberts. The Hafren Forest clear-felling catchment study. In Roberts G., Reynolds B., and Talling A., editors, *Upland Management and Water Resources. TFS/NERC Report to Department of the Environment*, Institude of Hydrology, Wallinford, 1989.

[133] P. J. Bonnett and P. G. Appleby. Deposition and transport of radionuclides within an upland drainage basin in mid-Wales. *Hydrobiologia*, 214:71–76, 1991.

[134] G. J. Dollard *et al.* Pollutant transfer in upland regions by occult precipitation. *Nature*, 302:241–243, 1983.

[135] D. E. Pedgley. Heavy rainfalls over Snowdonia. *Weather*, 25:340–350, 1970.

[136] J. S. Sawyer. A study of rainfall of two synoptic situations. *Quartely Journal of the Royal Meteorological Society*, 78:231–246, 1952.

[137] M. J. Harvey and A. J. McArthur. Pollutant transfer to moor by occult deposition. *Atmospheric Environment*, 23:1073–1082, 2089.

[138] D. H. Peirson and R. S. Cambray. Fission product fallout from the nuclear explosions of 1961 and 1962. *Nature*, 205:433–440, 1965.

[139] D. H. Peirson and L. Salmon. Gamma-radiation from deposited fallout. *Nature*, 184:1678–1679, 1959.

[140] M. D. Newson. The erosion of drainage ditches and its effect on the bed-load yields in mid-Wales: reconnaissance case studies. *Earth Surface Processes*, 5:275–290, 1980.

[141] P. J. Bonnett, G. J. Leeks, and R. S. Cambray. Transport processes for Chernobyl-labelled sediments: preliminary evidence from upland mid-Wales. *Land Degradation and Rehabilitation*, 1:39–50, 1989.

[142] D. A. Barber. Influence of soil organic matter on the entry of caesium-137 into plants. *Nature*, 204, 1964.

[143] N. Preiss and M. Pourchet. Database on lead-210 concentrations in surface air, lead-210 atmospheric deposition and water-sediment flux. In N. Preiss and M. Pourchet, editors, *Laboratories de Glaciologie et Geophysique de l'Environnement*, http://www-lgge.obs.ujf-grenoble.fr/axes/radioactivite/Pb210_database/, 1998.

[144] P. H. Freer-Smith, S. Holloway, and A. Goodman. The uptake of particulates by an urban woodland: site description and particulate composition. *Environmental Pollution*, 95(1):27–35, 1997.